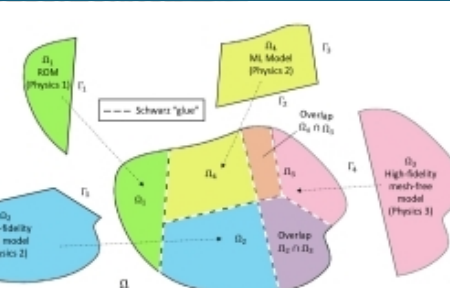
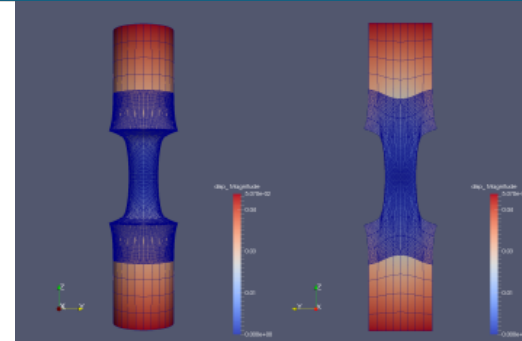
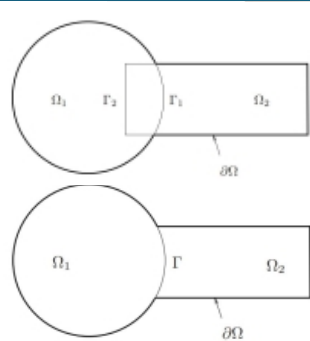




# Alternating Schwarz-based coupling of conventional and data-driven models



Irina Tezaur<sup>1</sup>, Joshua Barnett<sup>1,2</sup>, Alejandro Mota<sup>1</sup>, Chris Wentland<sup>1</sup>

<sup>1</sup>Sandia National Laboratories, <sup>2</sup>Stanford University



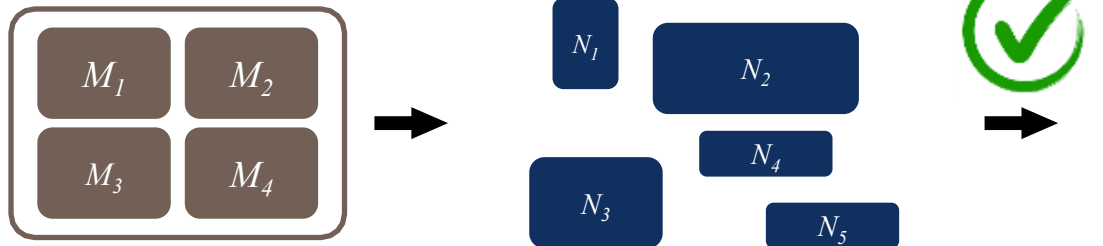
COUPLED 2023  
Chania, Greece, June 5-7, 2023

SAND2023-XXXX

# Motivation: multi-scale & multi-physics coupling



There exist established **rigorous mathematical theories** for coupling multi-scale and multi-physics components based on **traditional discretization methods** (“Full Order Models” or FOMs).



## Complex System Model

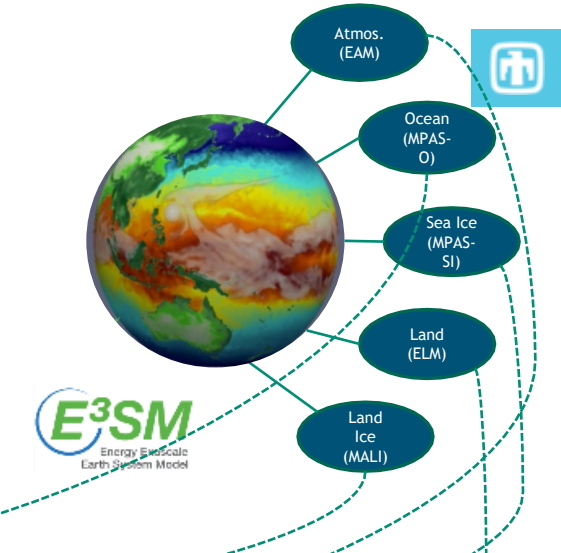
- PDEs, ODEs
- Nonlocal integral
- Classical DFT
- Atomistic, ...

## Traditional Methods

- Mesh-based (FE, FV, FD)
- Meshless (SPH, MLS)
- Implicit, explicit
- Eulerian, Lagrangian...

## Coupled Numerical Model

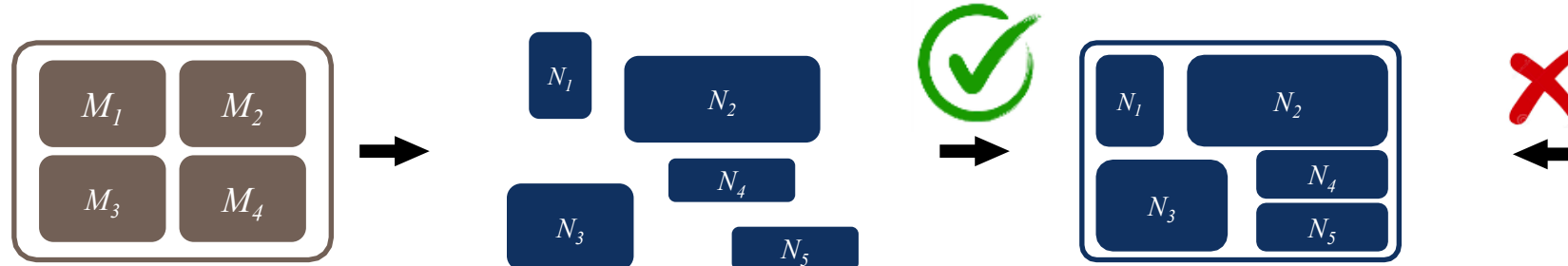
- Monolithic (Lagrange multipliers)
- Partitioned (loose) coupling
- Iterative (Schwarz, optimization)



# Motivation: multi-scale & multi-physics coupling



There exist established **rigorous mathematical theories** for coupling multi-scale and multi-physics components based on **traditional discretization methods** (“Full Order Models” or FOMs).



## Complex System Model

- PDEs, ODEs
- Nonlocal integral
- Classical DFT
- Atomistic, ...

## Traditional Methods

- Mesh-based (FE, FV, FD)
- Meshless (SPH, MLS)
- Implicit, explicit
- Eulerian, Lagrangian, ...

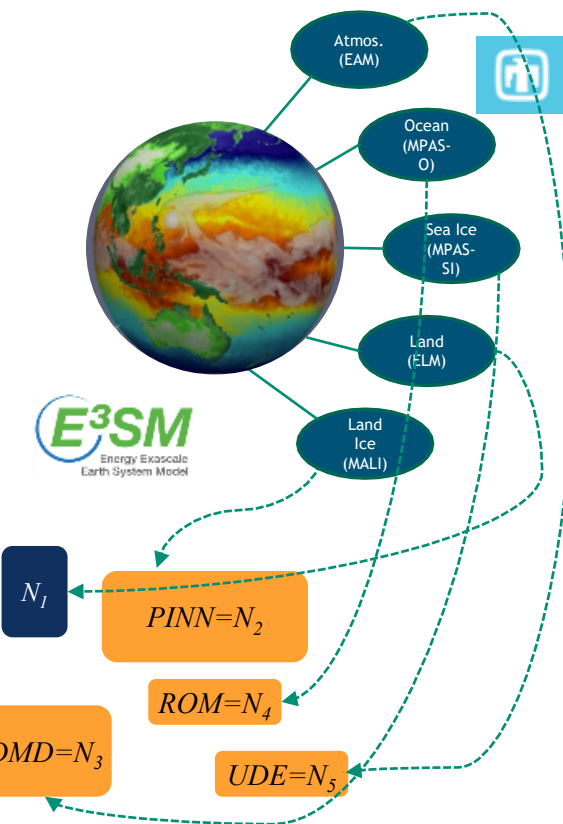
## Coupled Numerical Model

- Monolithic (Lagrange multipliers)
- Partitioned (loose) coupling
- Iterative (Schwarz, optimization)

## Traditional + Data-Driven Methods

- PINNs
- Neural ODEs
- Projection-based ROMs, ...

While there is currently a big push to integrate **data-driven methods** into modeling & simulation toolchains, existing algorithmic and software infrastructures are **ill-equipped** to handle **rigorous plug-and-play integration** of non-traditional, data-driven models!



# Coupling Project, Models and Methods



## fHNM (flexible Heterogeneous Numerical Methods) Project:

aims to discover the mathematical principles guiding the assembly of **standard** and **data-driven numerical models** in stable, accurate and physically consistent ways

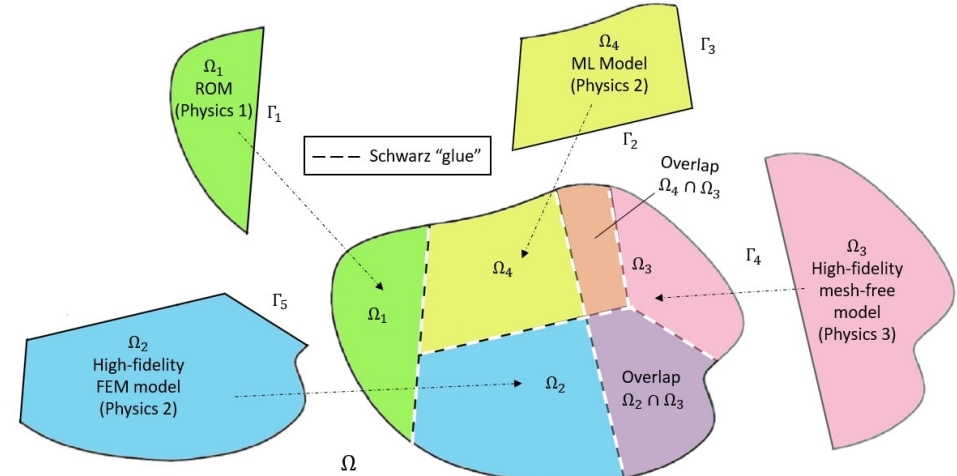
**Data-driven models:** to be “mixed-and-matched” with each other and first-principles models

- *Class A:* projection-based reduced order models (ROMs)
- *Class B:* machine-learned models, i.e., Physics-Informed Neural Networks (PINNs)
- *Class C:* flow map approximation models, i.e., dynamic model decomposition (DMD) models



**Coupling methods:**

- *Method 1:* Alternating Schwarz-based coupling
- *Method 2:* Optimization-based coupling
- *Method 3:* Coupling via generalized mortar methods (GMMs)



# Coupling Project, Models and Methods



## fHNM (flexible Heterogeneous Numerical Methods) Project:

aims to discover the mathematical principles guiding the assembly of **standard** and **data-driven numerical models** in stable, accurate and physically consistent ways

**Data-driven models:** to be “mixed-and-matched” with each other and first-principles models

- *Class A:* projection-based reduced order models (ROMs)

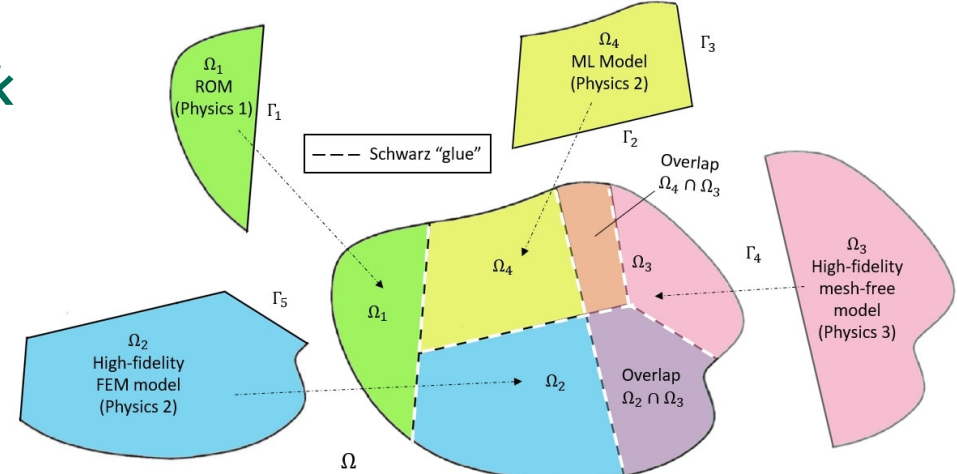
- *Class B:* machine-learned models, i.e., Physics-Informed Neural Networks (PINNs)
- *Class C:* flow map approximation models, i.e., dynamic model decomposition (DMD) models



## This talk

**Coupling methods:**

- *Method 1:* Alternating Schwarz-based coupling
- *Method 2:* Optimization-based coupling
- *Method 3:* Coupling via generalized mortar methods (GMMs)



# 6 Coupling Project, Models and Methods



## fHNM (flexible Heterogeneous Numerical Methods) Project:

aims to discover the mathematical principles guiding the assembly of **standard** and **data-driven numerical models** in stable, accurate and physically consistent ways

**Data-driven models:** to be “mixed-and-matched” with each other and first-principles models

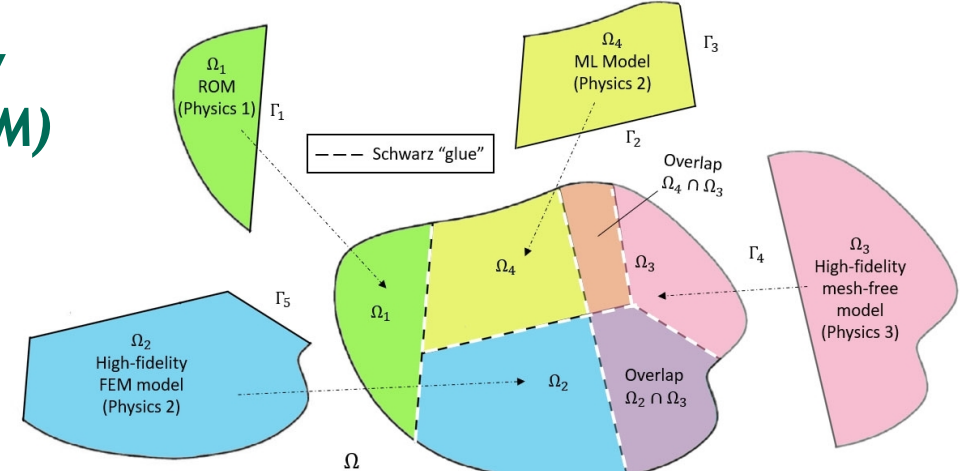
- *Class A:* projection-based reduced order models (ROMs)
- *Class B:* machine-learned models, i.e., Physics-Informed Neural Networks (PINNs)
- *Class C:* flow map approximation models, i.e., dynamic model decomposition (DMD) models



*Talk by Paul Kuberry  
(ISO3, Wed. June 6, 2PM)*

**Coupling methods:**

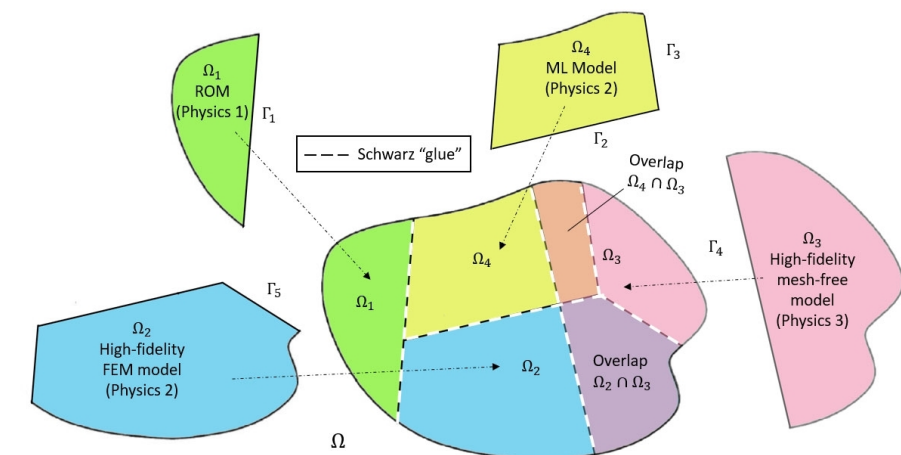
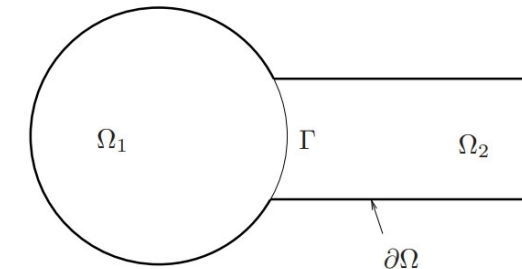
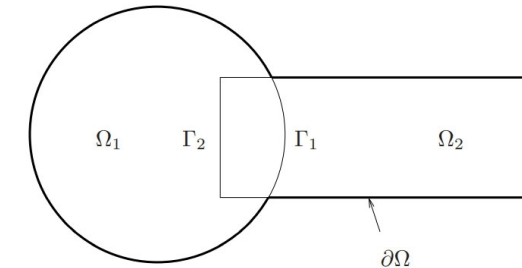
- *Method 1:* Alternating Schwarz-based coupling
- *Method 2:* Optimization-based coupling
- *Method 3:* Coupling via generalized mortar methods (GMMs)



# Outline

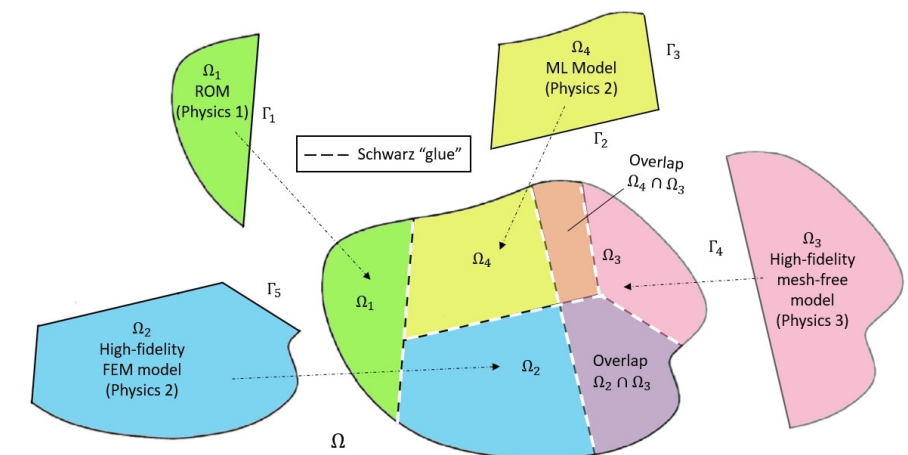
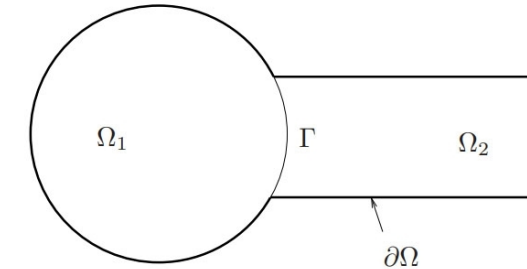
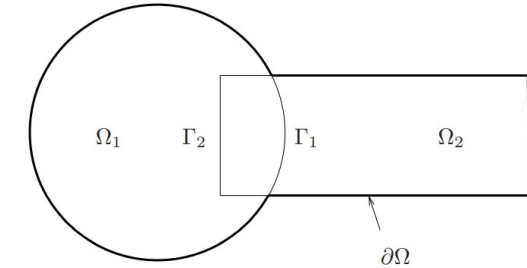


- The Schwarz Alternating Method for Domain Decomposition-Based Coupling
- Extension to FOM\*-ROM# and ROM-ROM Coupling
- Numerical Examples
  - 1D Dynamic Wave Propagation in Hyperelastic Bar
  - 2D Burgers Equation
- Summary & Future Work





- The Schwarz Alternating Method for Domain Decomposition-Based Coupling
- Extension to FOM\*-ROM<sup>#</sup> and ROM-ROM Coupling
- Numerical Examples
  - 1D Dynamic Wave Propagation in Hyperelastic Bar
  - 2D Burgers Equation
- Summary & Future Work

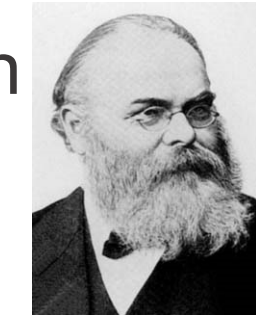


## 9 Schwarz Alternating Method for Domain Decomposition



- Proposed in 1870 by H. Schwarz for solving Laplace PDE on irregular domains.

**Crux of Method:** if the solution is known in regularly shaped domains, use those as pieces to iteratively build a solution for the more complex domain.



H. Schwarz (1843-1921)

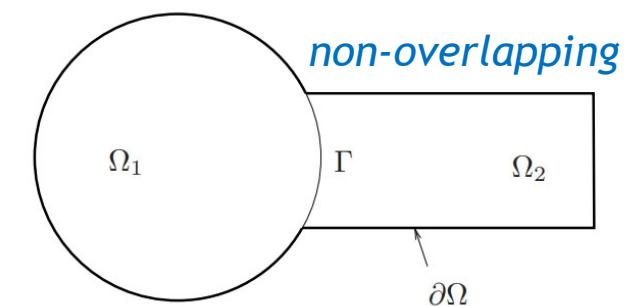
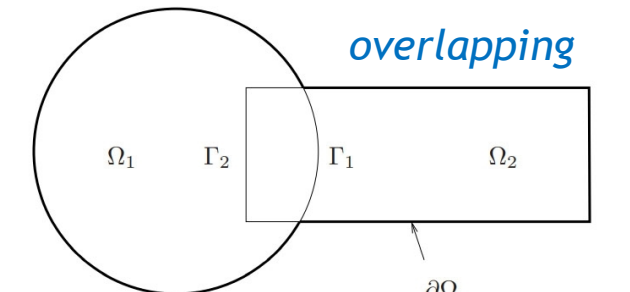
### Basic Schwarz Algorithm

#### Initialize:

- Solve PDE by any method on  $\Omega_1$  w/ initial guess for transmission BCs on  $\Gamma_1$ .

#### Iterate until convergence:

- Solve PDE by any method on  $\Omega_2$  w/ transmission BCs on  $\Gamma_2$  based on values just obtained for  $\Omega_1$ .
- Solve PDE by any method on  $\Omega_1$  w/ transmission BCs on  $\Gamma_1$  based on values just obtained for  $\Omega_2$ .



**Overlapping Schwarz:** convergent with all-Dirichlet transmission BCs<sup>1</sup> if  $\Omega_1 \cap \Omega_2 \neq \emptyset$ .

**Non-overlapping Schwarz:** convergent with Robin-Robin<sup>2</sup> or alternating Neumann-Dirichlet<sup>3</sup> transmission BCs.

<sup>1</sup>Schwarz, 1870; Lions, 1988. <sup>2</sup>Lions, 1990. <sup>3</sup>Zanolli *et al.*, 1987.

# How We Use the Schwarz Alternating Method

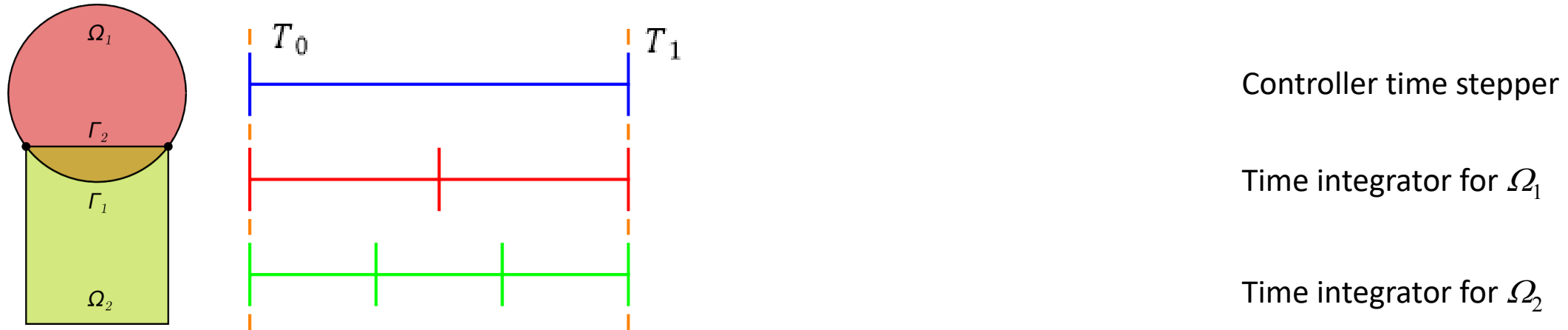


AS A ***PRECONDITIONER***  
FOR THE LINEARIZED  
SYSTEM



AS A ***SOLVER*** FOR THE  
COUPLED  
FULLY NONLINEAR  
PROBLEM

# Time-Advancement Within the Schwarz Framework

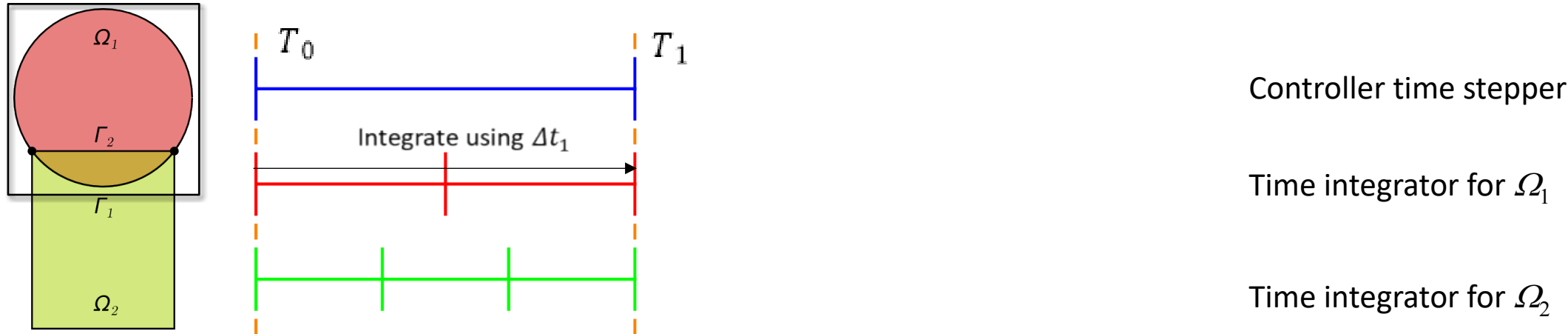


**Step 0:** Initialize  $i = 0$  (controller time index).

**Model PDE:**

$$\begin{cases} \dot{\mathbf{u}} + N(\mathbf{u}) = \mathbf{f}, & \text{in } \Omega \\ \mathbf{u}(x, t) = \mathbf{g}(t), & \text{on } \partial\Omega \\ \mathbf{u}(x, 0) = \mathbf{u}_0, & \text{in } \Omega \end{cases}$$

# Time-Advancement Within the Schwarz Framework

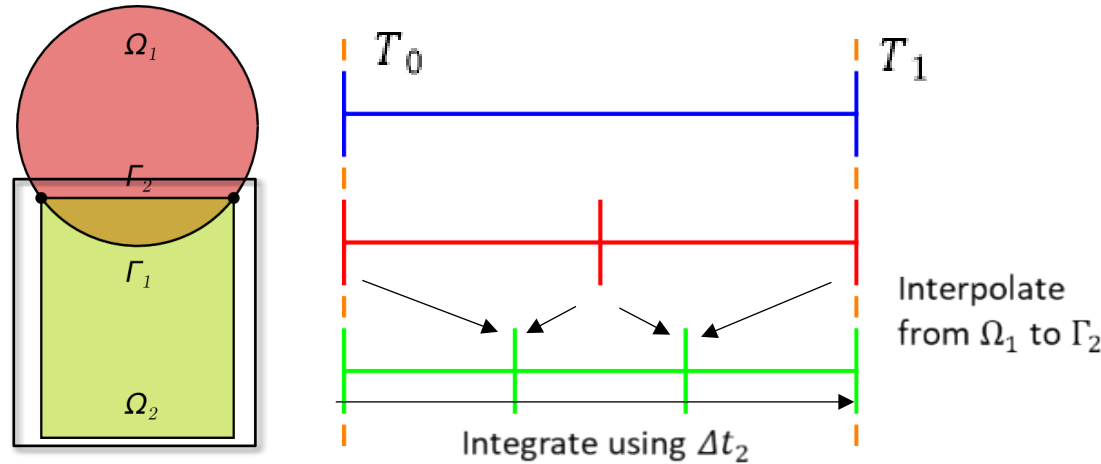


**Step 0:** Initialize  $i = 0$  (controller time index).

**Step 1:** Advance  $\Omega_1$  solution from time  $T_i$  to time  $T_{i+1}$  using time-stepper in  $\Omega_1$  with time-step  $\Delta t_1$ , using solution in  $\Omega_2$  interpolated to  $\Gamma_1$  at times  $T_i + n\Delta t_1$ .

**Model PDE:** 
$$\begin{cases} \dot{\mathbf{u}} + N(\mathbf{u}) = \mathbf{f}, & \text{in } \Omega \\ \mathbf{u}(x, t) = \mathbf{g}(t), & \text{on } \partial\Omega \\ \mathbf{u}(x, 0) = \mathbf{u}_0, & \text{in } \Omega \end{cases}$$

# Time-Advancement Within the Schwarz Framework



Controller time stepper

Time integrator for  $\Omega_1$

Time integrator for  $\Omega_2$

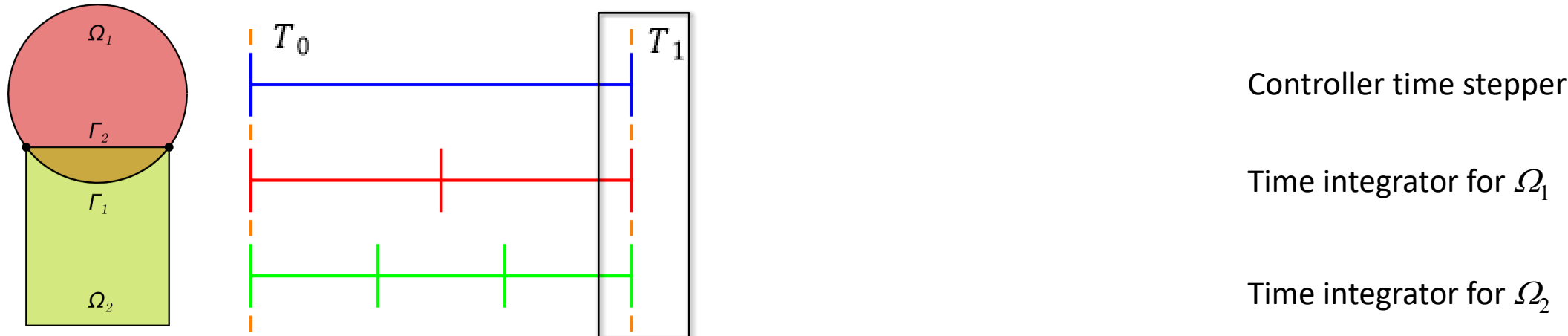
**Step 0:** Initialize  $i = 0$  (controller time index).

**Step 1:** Advance  $\Omega_1$  solution from time  $T_i$  to time  $T_{i+1}$  using time-stepper in  $\Omega_1$  with time-step  $\Delta t_1$ , using solution in  $\Omega_2$  interpolated to  $\Gamma_1$  at times  $T_i + n\Delta t_1$ .

**Step 2:** Advance  $\Omega_2$  solution from time  $T_i$  to time  $T_{i+1}$  using time-stepper in  $\Omega_2$  with time-step  $\Delta t_2$ , using solution in  $\Omega_1$  interpolated to  $\Gamma_2$  at times  $T_i + n\Delta t_2$ .

**Model PDE:** 
$$\begin{cases} \dot{\mathbf{u}} + N(\mathbf{u}) = \mathbf{f}, & \text{in } \Omega \\ \mathbf{u}(x, t) = \mathbf{g}(t), & \text{on } \partial\Omega \\ \mathbf{u}(x, 0) = \mathbf{u}_0, & \text{in } \Omega \end{cases}$$

# Time-Advancement Within the Schwarz Framework



**Step 0:** Initialize  $i = 0$  (controller time index).

**Step 1:** Advance  $\Omega_1$  solution from time  $T_i$  to time  $T_{i+1}$  using time-stepper in  $\Omega_1$  with time-step  $\Delta t_1$ , using solution in  $\Omega_2$  interpolated to  $\Gamma_1$  at times  $T_i + n\Delta t_1$ .

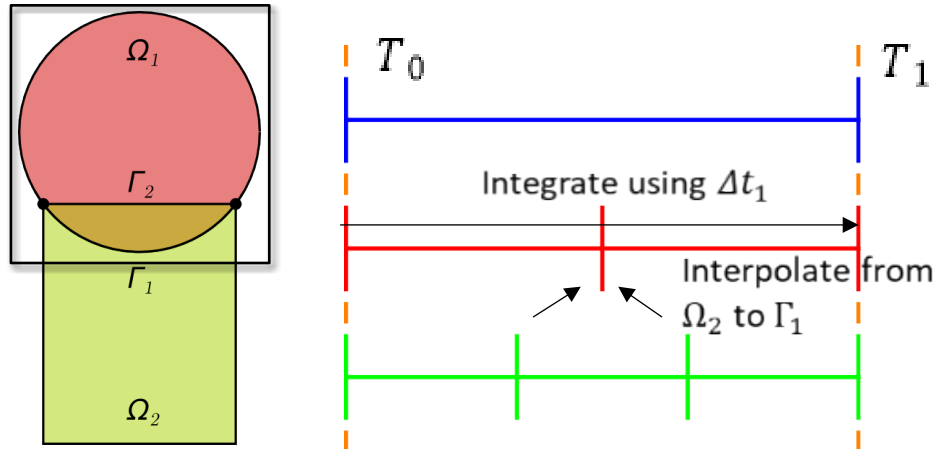
**Step 2:** Advance  $\Omega_2$  solution from time  $T_i$  to time  $T_{i+1}$  using time-stepper in  $\Omega_2$  with time-step  $\Delta t_2$ , using solution in  $\Omega_1$  interpolated to  $\Gamma_2$  at times  $T_i + n\Delta t_2$ .

**Step 3:** Check for convergence at time  $T_{i+1}$ .

**Model PDE:**

$$\begin{cases} \dot{\mathbf{u}} + N(\mathbf{u}) = \mathbf{f}, & \text{in } \Omega \\ \mathbf{u}(x, t) = \mathbf{g}(t), & \text{on } \partial\Omega \\ \mathbf{u}(x, 0) = \mathbf{u}_0, & \text{in } \Omega \end{cases}$$

# Time-Advancement Within the Schwarz Framework



Controller time stepper

Time integrator for  $\Omega_1$

Time integrator for  $\Omega_2$

**Step 0:** Initialize  $i = 0$  (controller time index).

**Step 1:** Advance  $\Omega_1$  solution from time  $T_i$  to time  $T_{i+1}$  using time-stepper in  $\Omega_1$  with time-step  $\Delta t_1$ , using solution in  $\Omega_2$  interpolated to  $\Gamma_1$  at times  $T_i + n\Delta t_1$ .

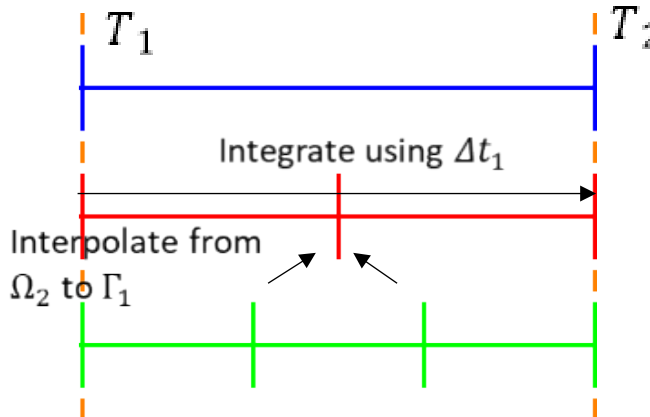
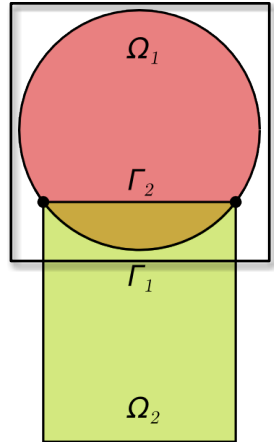
**Step 2:** Advance  $\Omega_2$  solution from time  $T_i$  to time  $T_{i+1}$  using time-stepper in  $\Omega_2$  with time-step  $\Delta t_2$ , using solution in  $\Omega_1$  interpolated to  $\Gamma_2$  at times  $T_i + n\Delta t_2$ .

**Step 3:** Check for convergence at time  $T_{i+1}$ .

➤ If unconverged, return to Step 1.

**Model PDE:** 
$$\begin{cases} \dot{\mathbf{u}} + N(\mathbf{u}) = \mathbf{f}, & \text{in } \Omega \\ \mathbf{u}(x, t) = \mathbf{g}(t), & \text{on } \partial\Omega \\ \mathbf{u}(x, 0) = \mathbf{u}_0, & \text{in } \Omega \end{cases}$$

# Time-Advancement Within the Schwarz Framework



Controller time stepper

Time integrator for  $\Omega_1$

Time integrator for  $\Omega_2$

Can use *different integrators* with *different time steps* within each domain!

**Step 0:** Initialize  $i = 0$  (controller time index).

**Step 1:** Advance  $\Omega_1$  solution from time  $T_i$  to time  $T_{i+1}$  using time-stepper in  $\Omega_1$  with time-step  $\Delta t_1$ , using solution in  $\Omega_2$  interpolated to  $\Gamma_1$  at times  $T_i + n\Delta t_1$ .

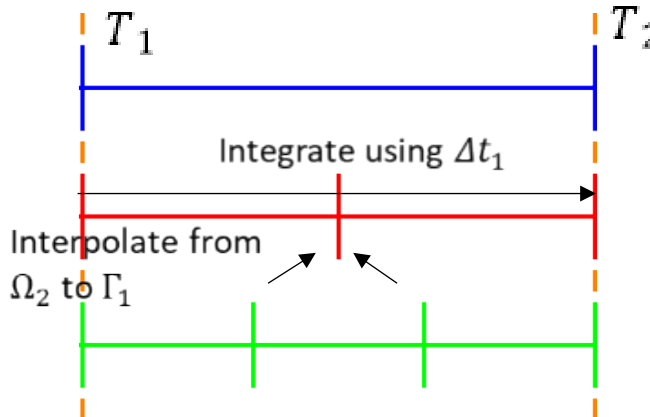
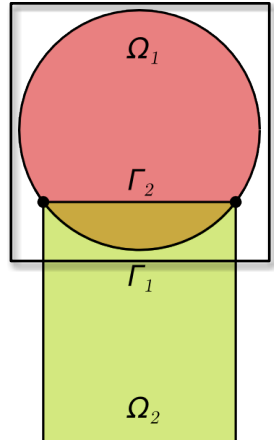
**Step 2:** Advance  $\Omega_2$  solution from time  $T_i$  to time  $T_{i+1}$  using time-stepper in  $\Omega_2$  with time-step  $\Delta t_2$ , using solution in  $\Omega_1$  interpolated to  $\Gamma_2$  at times  $T_i + n\Delta t_2$ .

**Step 3:** Check for convergence at time  $T_{i+1}$ .

- If unconverged, return to Step 1.
- If converged, set  $i = i + 1$  and return to Step 1.

**Model PDE:** 
$$\begin{cases} \dot{\mathbf{u}} + N(\mathbf{u}) = \mathbf{f}, & \text{in } \Omega \\ \mathbf{u}(x, t) = \mathbf{g}(t), & \text{on } \partial\Omega \\ \mathbf{u}(x, 0) = \mathbf{u}_0, & \text{in } \Omega \end{cases}$$

# Time-Advancement Within the Schwarz Framework



Controller time stepper

Time integrator for  $\Omega_1$

Time integrator for  $\Omega_2$

Time-stepping procedure is equivalent to doing Schwarz on space-time domain [Mota *et al.* 2022].

**Step 0:** Initialize  $i = 0$  (controller time index).

**Step 1:** Advance  $\Omega_1$  solution from time  $T_i$  to time  $T_{i+1}$  using time-stepper in  $\Omega_1$  with time-step  $\Delta t_1$ , using solution in  $\Omega_2$  interpolated to  $\Gamma_1$  at times  $T_i + n\Delta t_1$ .

**Step 2:** Advance  $\Omega_2$  solution from time  $T_i$  to time  $T_{i+1}$  using time-stepper in  $\Omega_2$  with time-step  $\Delta t_2$ , using solution in  $\Omega_1$  interpolated to  $\Gamma_2$  at times  $T_i + n\Delta t_2$ .

**Step 3:** Check for convergence at time  $T_{i+1}$ .

- If unconverged, return to Step 1.
- If converged, set  $i = i + 1$  and return to Step 1.

**Model PDE:** 
$$\begin{cases} \dot{\mathbf{u}} + N(\mathbf{u}) = \mathbf{f}, & \text{in } \Omega \\ \mathbf{u}(x, t) = \mathbf{g}(t), & \text{on } \partial\Omega \\ \mathbf{u}(x, 0) = \mathbf{u}_0, & \text{in } \Omega \end{cases}$$

# Schwarz for Multiscale FOM-FOM Coupling in Solid Mechanics<sup>1</sup>

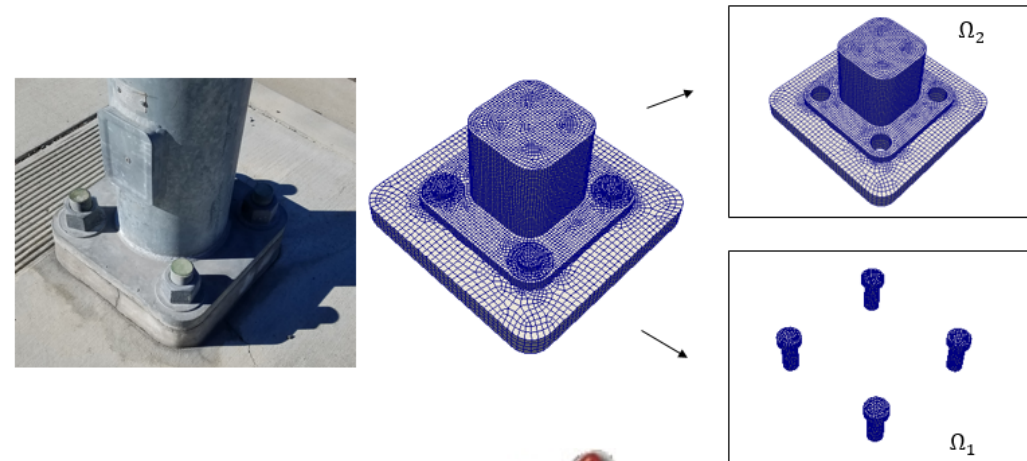


*Model Solid Mechanics PDEs:*

- Coupling is **concurrent** (two-way).
- **Ease of implementation** into existing massively-parallel HPC codes.
- **Scalable, fast, robust** (we target *real* engineering problems, e.g., analyses involving failure of bolted components!).
- Coupling does not introduce **nonphysical artifacts**.
- **Theoretical** convergence properties/guarantees<sup>1</sup>.
- **“Plug-and-play” framework:**

Quasistatic:  $\operatorname{Div} \mathbf{P} + \rho_0 \mathbf{B} = \mathbf{0}$  in  $\Omega$

Dynamic:  $\operatorname{Div} \mathbf{P} + \rho_0 \mathbf{B} = \rho_0 \ddot{\varphi}$  in  $\Omega \times I$



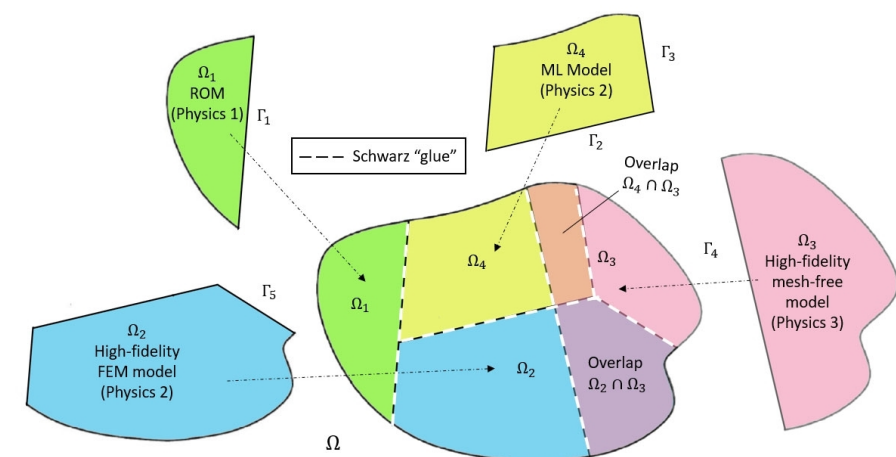
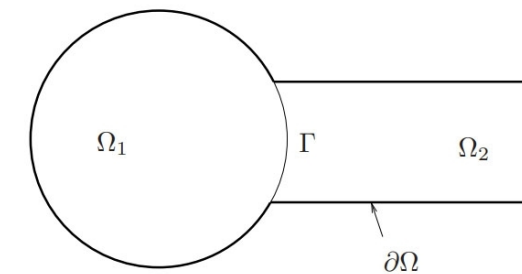
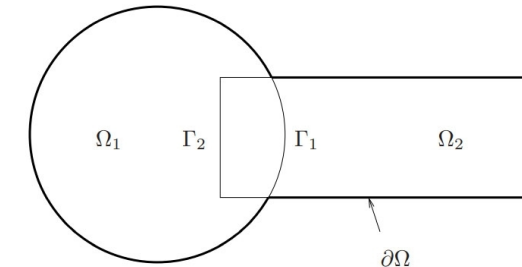
- Ability to couple regions with **different non-conformal meshes, different element types** and **different levels of refinement** to simplify task of **meshing complex geometries**.
- Ability to use **different solvers/time-integrators** in different regions.

<sup>1</sup> Mota *et al.* 2017; Mota *et al.* 2022. <sup>2</sup> <https://github.com/sandialabs/LCM>.

# Outline



- The Schwarz Alternating Method for Domain Decomposition-Based Coupling
- Extension to FOM\*-ROM# and ROM-ROM Coupling
- Numerical Examples
  - 1D Dynamic Wave Propagation in Hyperelastic Bar
  - 2D Burgers Equation
- Summary & Future Work

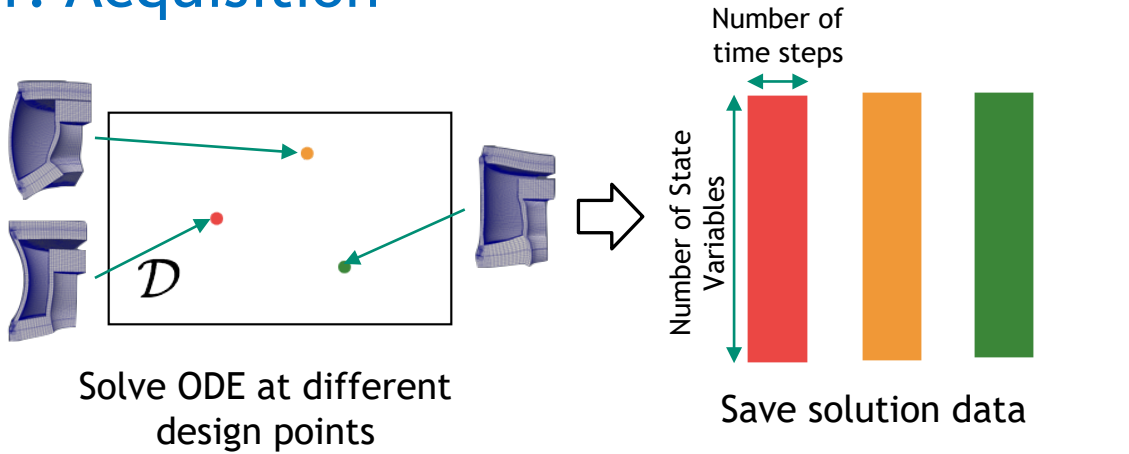


# Projection-Based Model Order Reduction via the POD/Galerkin Method



$$\text{Full Order Model (FOM): } \mathbf{M} \frac{d^2 \mathbf{u}}{dt^2} + \mathbf{f}_{\text{int}}(\mathbf{u}) = \mathbf{f}_{\text{ext}}$$

## 1. Acquisition



## 2. Learning

Proper Orthogonal Decomposition (POD):

$$\mathbf{X} = \begin{matrix} \text{Red Bar} \\ \text{Orange Bar} \\ \text{Green Bar} \end{matrix} = \begin{matrix} \text{Brown Bar} \\ \text{Blue Bar} \end{matrix} \Sigma \begin{matrix} \text{Blue Bar} \\ \text{V}^T \end{matrix}$$

ROM = projection-based Reduced Order Model

## 3. Projection-Based Reduction

Reduce the number of unknowns

$$\mathbf{u}(t) \approx \tilde{\mathbf{u}}(t) = \Phi \hat{\mathbf{u}}(t)$$

Perform Galerkin projection

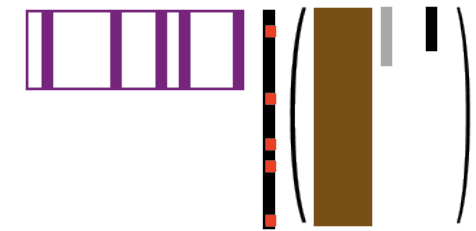
$$\Phi^T \mathbf{M} \Phi \frac{d^2 \hat{\mathbf{u}}}{dt^2} + \Phi^T \mathbf{f}_{\text{int}}(\Phi \hat{\mathbf{u}}) = \Phi^T \mathbf{f}_{\text{ext}}$$

Hyper-reduce nonlinear terms



Hyper-reduction/sample mesh

$$\mathbf{f}_{\text{int}}(\Phi \hat{\mathbf{u}}) \approx A \mathbf{f}_{\text{int}}(\Phi \hat{\mathbf{u}})$$



HROM = Hyper-reduced ROM

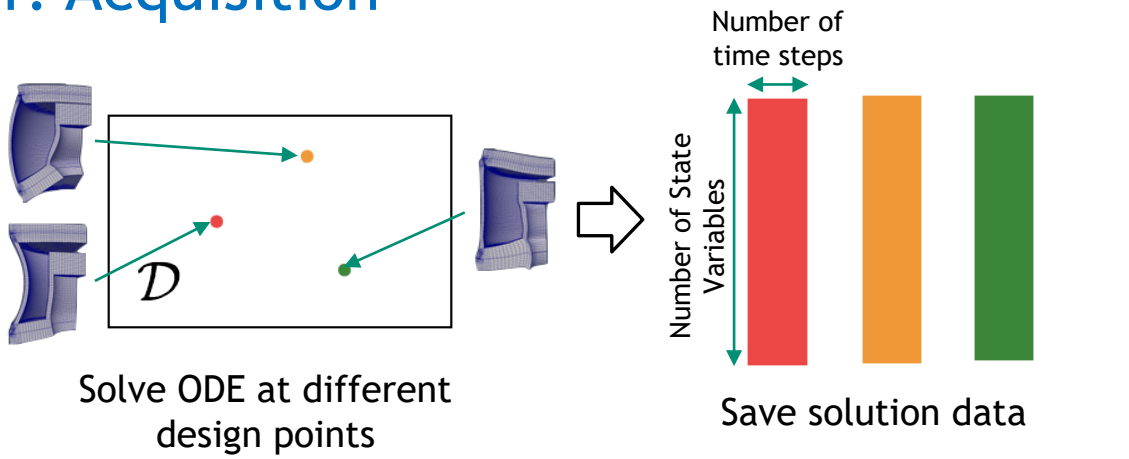
# Projection-Based Model Order Reduction via the POD/LSPG\* Method



Full Order Model (FOM):  $\frac{du}{dt} = f(u; t, \mu)$

\* Least-Squares Petrov-Galerkin

## 1. Acquisition



## 2. Learning

Proper Orthogonal Decomposition (POD):

$$\mathbf{X} = \begin{matrix} \text{Red Bar} \\ \text{Orange Bar} \\ \text{Green Bar} \end{matrix} = \begin{matrix} \text{Brown Matrix} \\ \text{Blue Matrix} \end{matrix} \Sigma \begin{matrix} \text{Blue Matrix} \\ \text{Light Blue Matrix} \end{matrix}$$

ROM = projection-based Reduced Order Model

## 3. Projection-Based Reduction

Choose ODE temporal discretization

$$\frac{du}{dt} = f(u; t, \mu) \downarrow r^n(u^n; \mu) = 0, n = 1, \dots, T$$

Reduce the number of unknowns

$$u(t) \approx \tilde{u}(t) = \Phi \hat{u}(t)$$

Minimize residual

$$\min_{\hat{v}} \| \mathbf{A} \begin{pmatrix} \text{Red Bar} \\ \text{Orange Bar} \\ \text{Green Bar} \end{pmatrix} - \mathbf{r}^n(\Phi \hat{v}; \mu) \|_2$$

Hyper-reduction/sample mesh

HROM = Hyper-reduced ROM

# Schwarz Extensions to FOM-ROM and ROM-ROM Couplings



## Enforcement of Dirichlet boundary conditions (DBC)s in ROM at indices $i_{\text{Dir}}$

- Method I in [Gunzburger *et al.* 2007] is employed

$$\mathbf{u}(t) \approx \bar{\mathbf{u}} + \Phi \hat{\mathbf{u}}(t), \quad \mathbf{v}(t) \approx \bar{\mathbf{v}} + \Phi \hat{\mathbf{v}}(t), \quad \mathbf{a}(t) \approx \bar{\mathbf{a}} + \Phi \hat{\mathbf{a}}(t)$$

- POD modes made to satisfy homogeneous DBCs:  $\Phi(i_{\text{Dir}}, :) = \mathbf{0}$
- BCs imposed by modifying  $\bar{\mathbf{u}}$ ,  $\bar{\mathbf{v}}$ ,  $\bar{\mathbf{a}}$ :  $\bar{\mathbf{u}}(i_{\text{Dir}}) \leftarrow \chi_u$ ,  $\bar{\mathbf{v}}(i_{\text{Dir}}) \leftarrow \chi_v$ ,  $\bar{\mathbf{a}}(i_{\text{Dir}}) \leftarrow \chi_a$

## Hyper-reduction considerations

- Boundary points must be included in sample mesh for DBC enforcement
- We employ the Energy-Conserving Sampling & Weighting Method (ECSW) [Farhat *et al.* 2015] → preserves Hamiltonian structure for solid mechanics problems

## Choice of domain decomposition

- Error-based indicators that help decide in what region of the domain a ROM can be viable should drive domain decomposition [Bergmann *et al.* 2018] (future work)

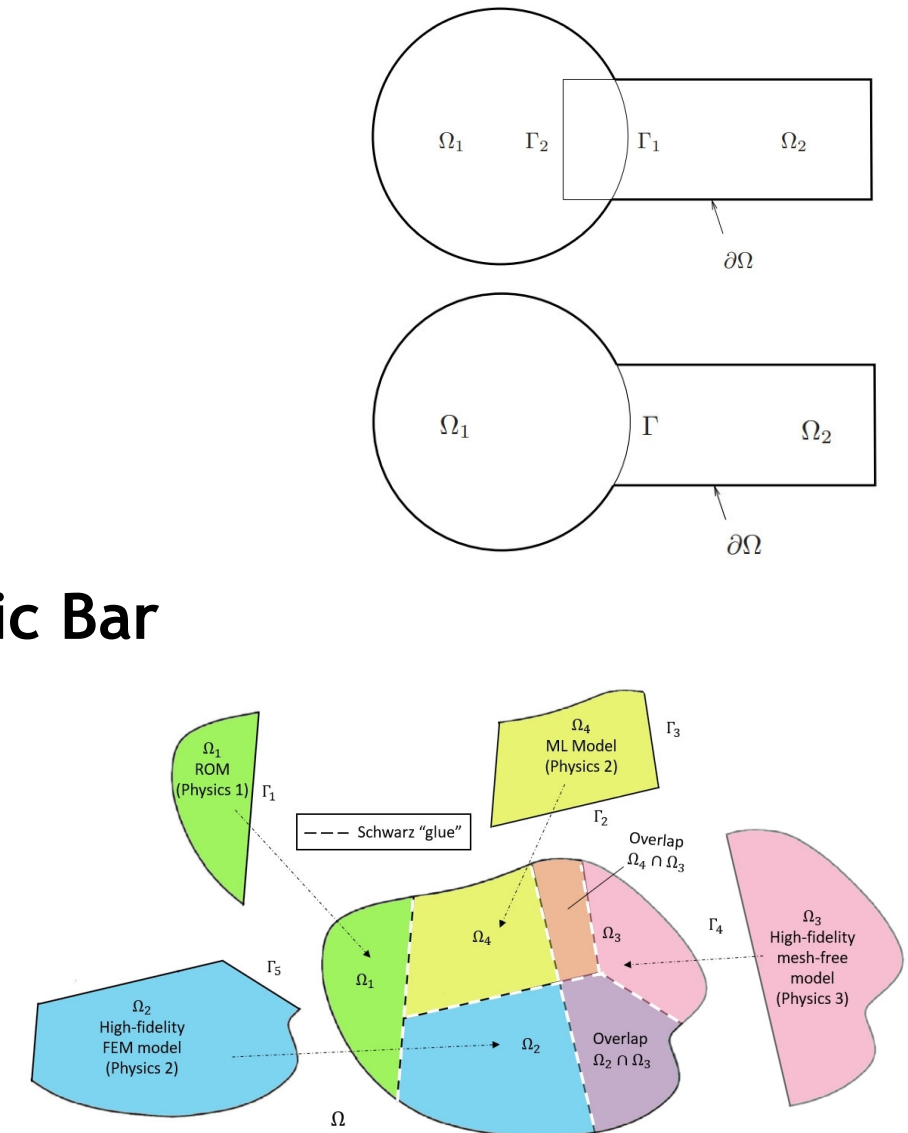
## Snapshot collection and reduced basis construction

- POD results presented herein use snapshots obtained via FOM-FOM coupling on  $\Omega = \bigcup_i \Omega_i$
- Future work: generate snapshots/bases separately in each  $\Omega_i$  [Hoang *et al.* 2021, Smetana *et al.* 2022]

# Outline



- The Schwarz Alternating Method for Domain Decomposition-Based Coupling
- Extension to FOM\*-ROM<sup>#</sup> and ROM-ROM Coupling
- Numerical Examples
  - 1D Dynamic Wave Propagation in Hyperelastic Bar
  - 2D Burgers Equation
- Summary & Future Work



# Numerical Example: 1D Dynamic Wave Propagation Problem



- **1D beam** geometry  $\Omega = (0,1)$ , clamped at both ends, with prescribed initial condition discretized using FEM + Newmark- $\beta$
- Simple problem but very **stringent test** for discretization/ coupling methods, and **difficult problem for ROMs**.
- Two **constitutive models** considered:
  - Linear elastic (problem has exact analytical solution)
  - Nonlinear hyperelastic Henky This talk
- ROMs results are **reproductive** and **predictive**, and are based on the **POD/Galerkin** method, with POD calculated from FOM-FOM coupled model.
  - 50 POD modes capture ~100% snapshot energy for linear variant of this problem.
  - 536 POD modes capture ~100% snapshot energy for Henky variant of this problem.
- Hyper-reduced ROMs (HROMs) perform **hyper-reduction** using ECSW [Farhat *et al.*, 2015]
  - Ensures that **Lagrangian structure** of problem is preserved in HROM.
- **Couplings tested:** overlapping, non-overlapping, FOM-FOM, FOM-ROM, ROM-ROM, FOM-HROM, HROM-HROM, implicit-explicit, implicit-implicit, explicit-explicit. This talk

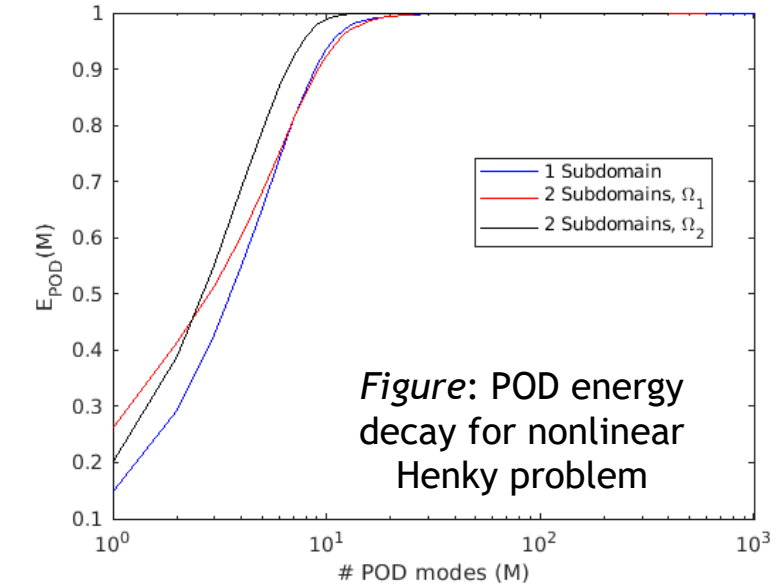


Figure: POD energy decay for nonlinear Henky problem

# Numerical Example: 1D Dynamic Wave Propagation



- Two variants of problem, with different initial conditions (ICs):
  - Symmetric Gaussian IC (top right)
  - Rounded Square IC (bottom right)
- Non-overlapping domain decomposition (DD) of  $\Omega = \Omega_1 \cup \Omega_2$ , where  $\Omega_1 = [0, 0.6]$  and  $\Omega_2 = [0.6, 1.0]$ 
  - DD is based on heuristics: during time-interval considered ( $0 \leq t \leq 1 \times 10^3$ ), sharper gradient forms in  $\Omega_1$ , suggesting FOM or larger ROM is needed there.
- Reproductive problem:
  - Displacement snapshots collected using FOM-FOM non-overlapping coupling with **Symmetric Gaussian IC**
  - FOM-ROM, FOM-HROM, ROM-ROM and HROM-HROM run with **Symmetric Gaussian IC**
- Predictive problem:
  - Displacement snapshots collected using FOM-FOM non-overlapping coupling with **Symmetric Gaussian IC**
  - FOM-ROM, FOM-HROM, ROM-ROM and HROM-HROM run with **Rounded Square IC**

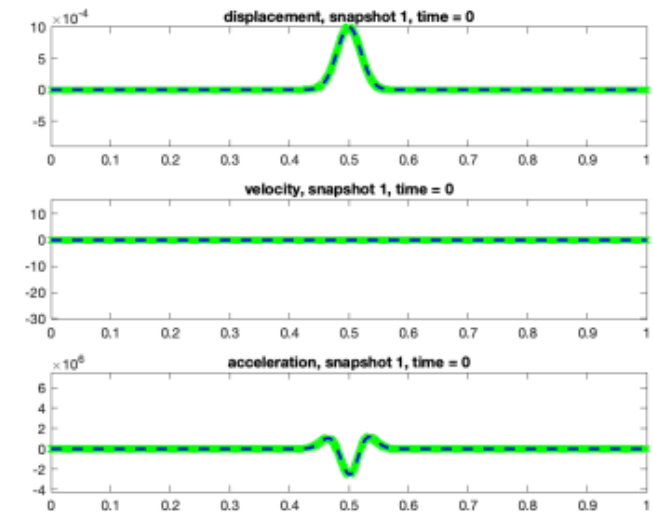
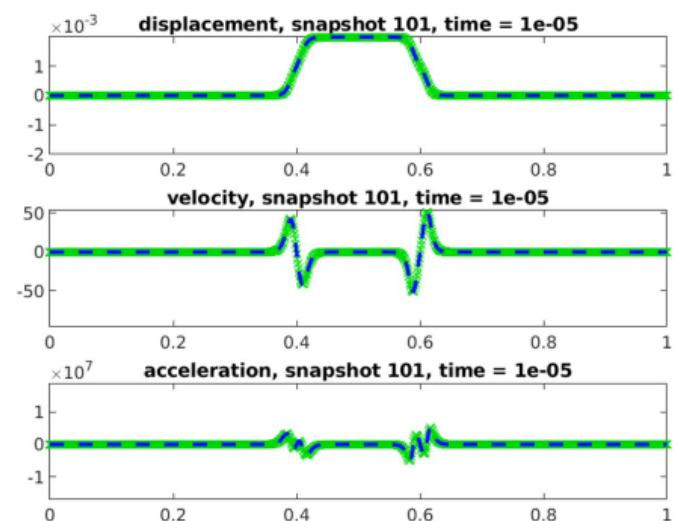
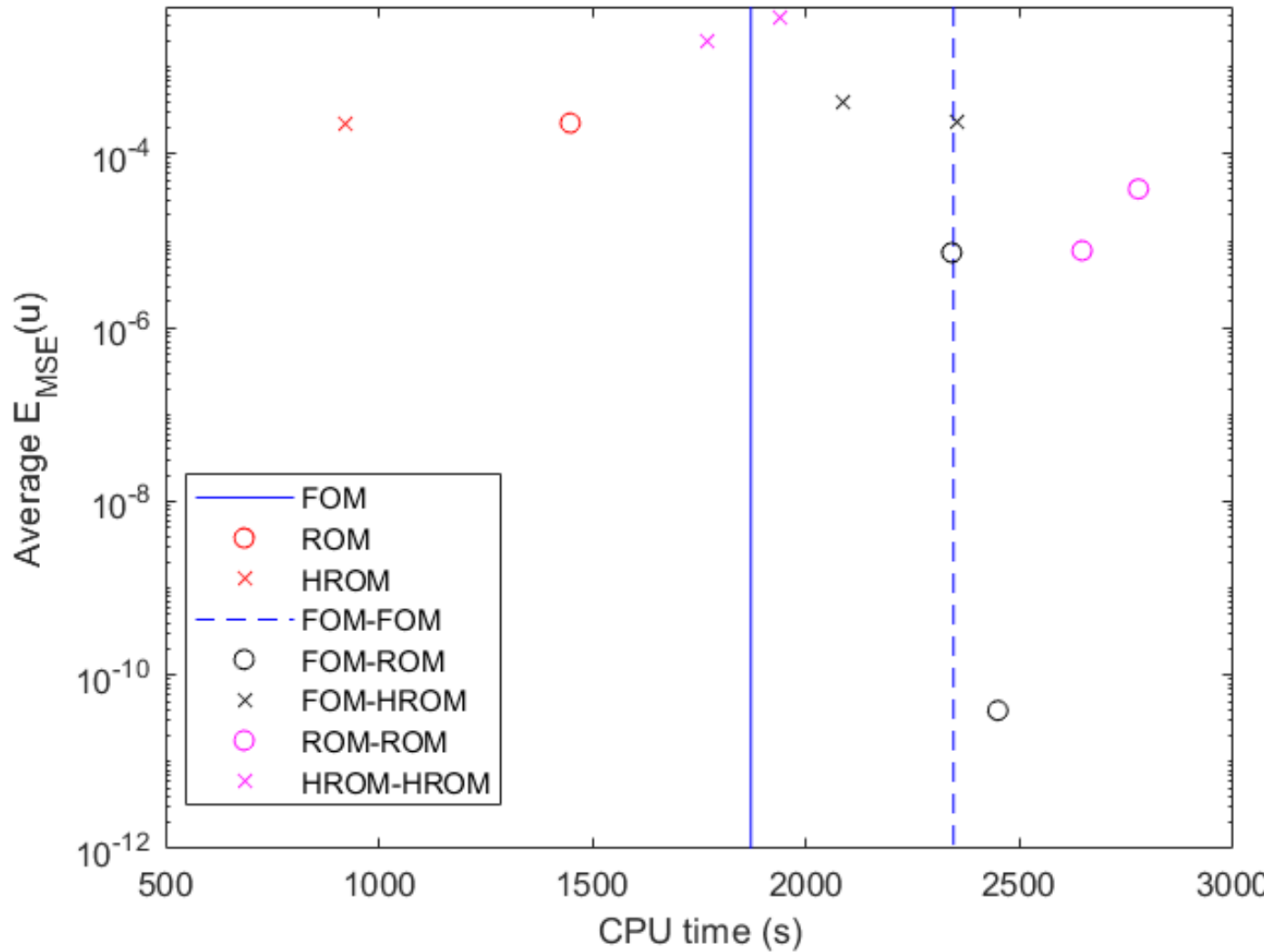


Figure above: Symmetric Gaussian IC problem solution

Figure below: Rounded Square IC problem solution



# Numerical Example: Reproductive Problem Results



- Single-domain ROM and HROM are most efficient
- Couplings involving ROMs and HROMs enable one to achieve smaller errors
- Benefits of hyper-reduction are limited on 1D problem
- FOM-HROM and HROM-HROM couplings outperform the FOM-FOM coupling in terms of CPU time by 12.5-32.6%

# Numerical Example: Reproductive Problem Results

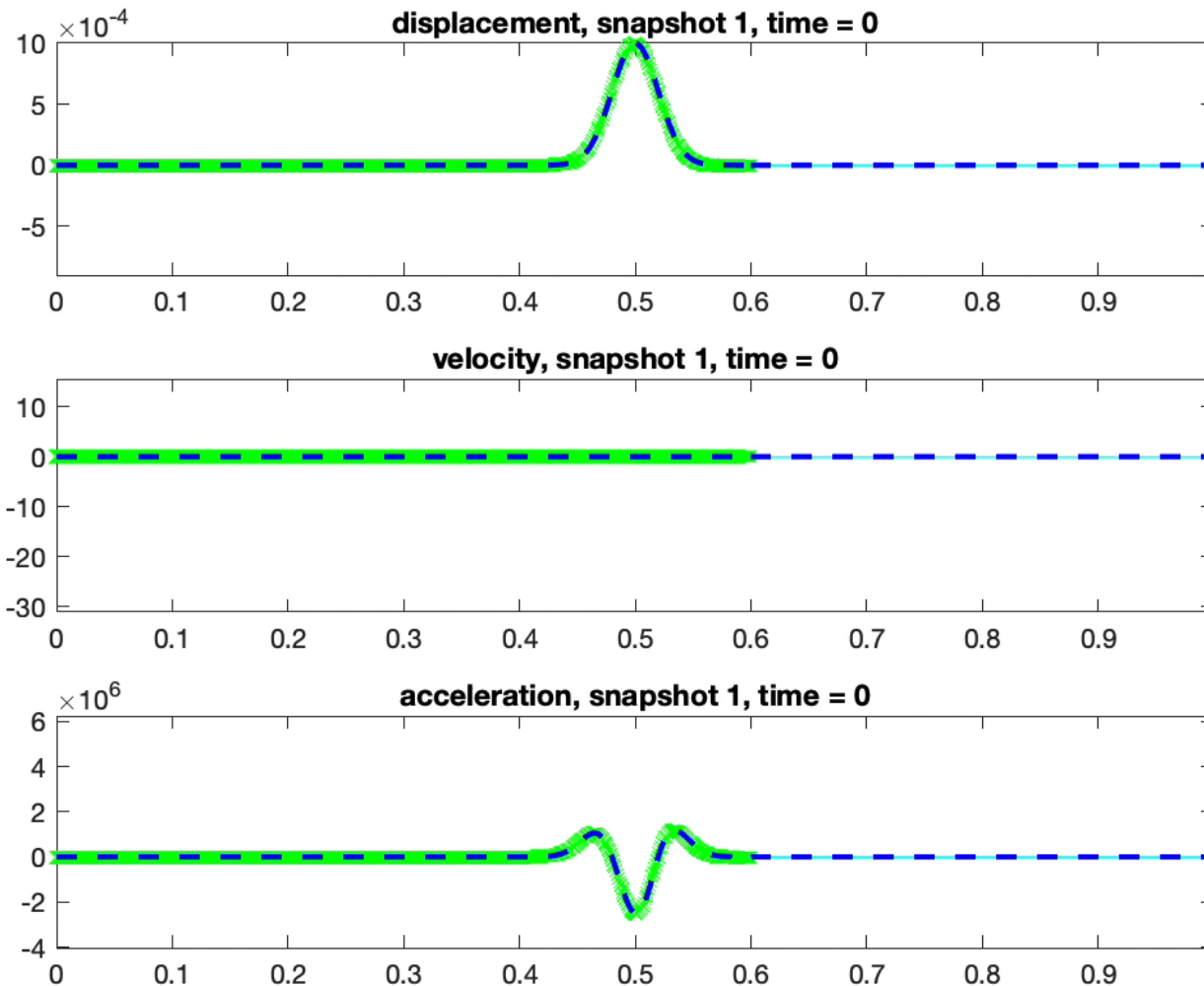
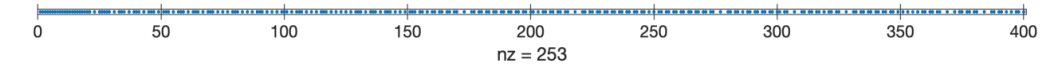


*Figure left:* FOM (green) - HROM (cyan) coupling compared with single-domain FOM solution (blue). HROM has 200 modes.

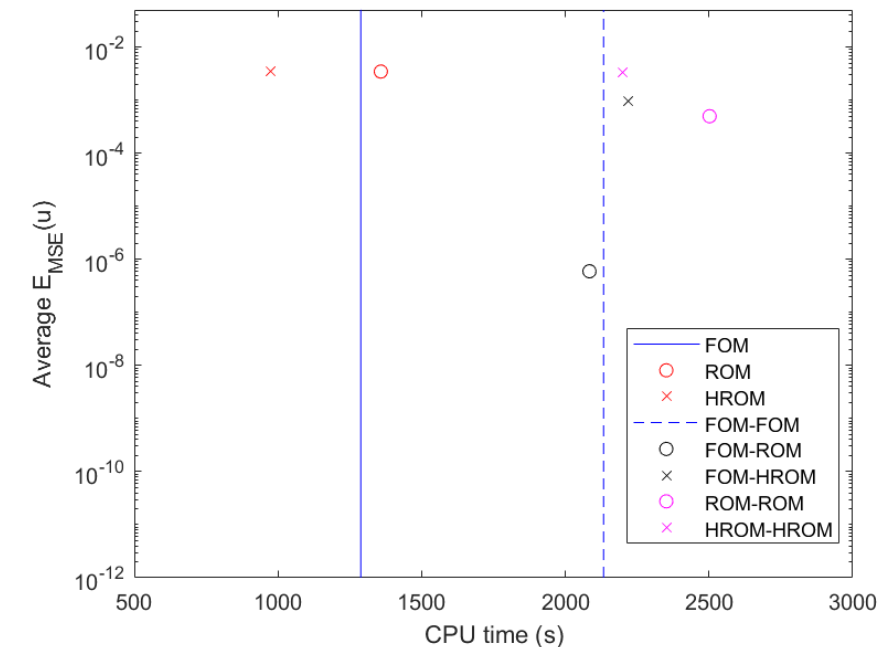
*Figure below:* ECSW algorithm samples 253/400 elements



# Numerical Example: Predictive Problem Results

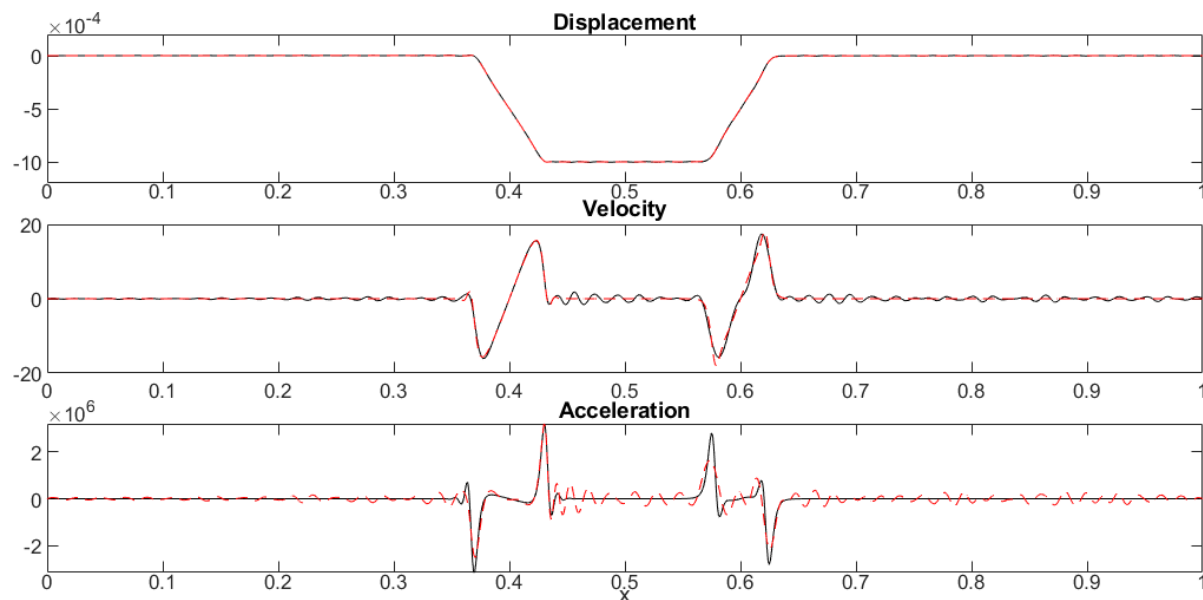


Model	CPU time (s)	$N_{e,1}/N_{e,2}$	$\mathcal{E}_{\text{MSE}}(\tilde{\mathbf{u}}_1)/\mathcal{E}_{\text{MSE}}(\tilde{\mathbf{u}}_2)$	$\mathcal{E}_{\text{MSE}}(\tilde{\mathbf{v}}_1)/\mathcal{E}_{\text{MSE}}(\tilde{\mathbf{v}}_2)$	$\mathcal{E}_{\text{MSE}}(\tilde{\mathbf{a}}_1)/\mathcal{E}_{\text{MSE}}(\tilde{\mathbf{a}}_2)$	$N_S$
FOM	$1.288 \times 10^3$	—/—	—/—	—/—	—/—	—
ROM	$1.358 \times 10^3$	—/—	$3.451 \times 10^{-3}$ /—	$6.750 \times 10^{-2}$ /—	$3.021 \times 10^{-1}$ /—	—
HROM	$9.759 \times 10^2$	614/—	$3.463 \times 10^{-3}$ /—	$6.750 \times 10^{-2}$ /—	$3.021 \times 10^{-1}$ /—	—
FOM-FOM	$2.133 \times 10^3$	—/—	—/—	—/—	—/—	23,280
FOM-ROM	$2.084 \times 10^3$	—/—	$1.907 \times 10^{-8}$ / $1.170 \times 10^{-6}$	$1.461 \times 10^{-6}$ / $9.882 \times 10^{-5}$	$3.973 \times 10^{-5}$ / $1.757 \times 10^{-3}$	23,288
FOM-HROM	$2.219 \times 10^3$	—/253	$1.967 \times 10^{-4}$ / $1.720 \times 10^{-3}$	$4.986 \times 10^{-3}$ / $4.185 \times 10^{-2}$	$2.768 \times 10^{-2}$ / $2.388 \times 10^{-1}$	29,700
ROM-ROM	$2.502 \times 10^3$	—/—	$5.592 \times 10^{-4}$ / $4.346 \times 10^{-4}$	$1.575 \times 10^{-2}$ / $1.001 \times 10^{-2}$	$9.197 \times 10^{-2}$ / $5.304 \times 10^{-2}$	26,220
HROM-HROM	$2.200 \times 10^3$	405/253	$4.802 \times 10^{-3}$ / $1.960 \times 10^{-3}$	$8.500 \times 10^{-2}$ / $4.630 \times 10^{-2}$	$3.744 \times 10^{-1}$ / $2.580 \times 10^{-1}$	30,067

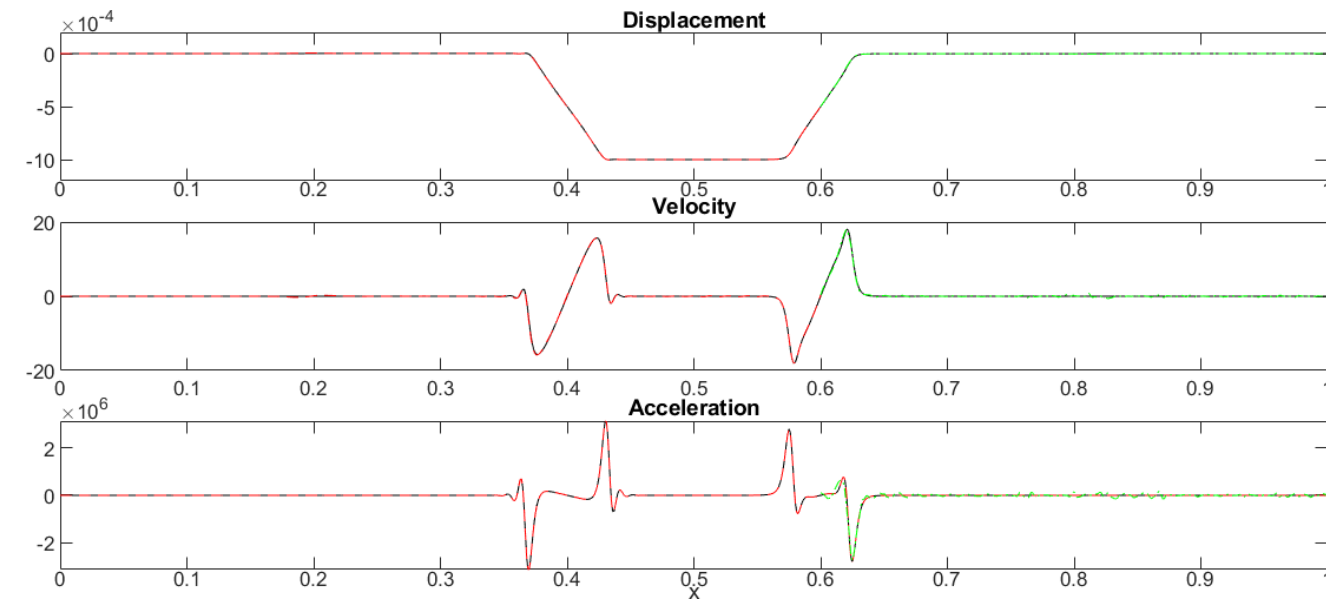


- Results indicate that **predictive accuracy/robustness** can be **improved** by **coupling ROM or HROM to FOM**
  - FOM-ROM coupling is **remarkably accurate**, achieving displacement error  $O(1 \times 10^{-8})$
  - FOM-HROM and ROM-ROM couplings are **more accurate** than single-domain ROMs
  - HROM-HROM **on par** with single-domain HROM in terms of accuracy
- **Wall-clock times** of coupled models can be improved
  - FOM-HROM, ROM-ROM and HROM-HROM models are **slower** than FOM-FOM model as **more Schwarz iterations** required to achieve convergence
  - **Hyper-reduction** samples ~60% of total mesh points for this 1D traveling wave problem
    - ❖ Greater gains from hyper-reduction anticipated for 2D/3D problems

# Numerical Example: Predictive Problem Results



Predictive single-domain ROM ( $M_1 = 300$ )  
solution at final time



Predictive FOM-HROM ( $M_2 = 200$ )  
solution at final time

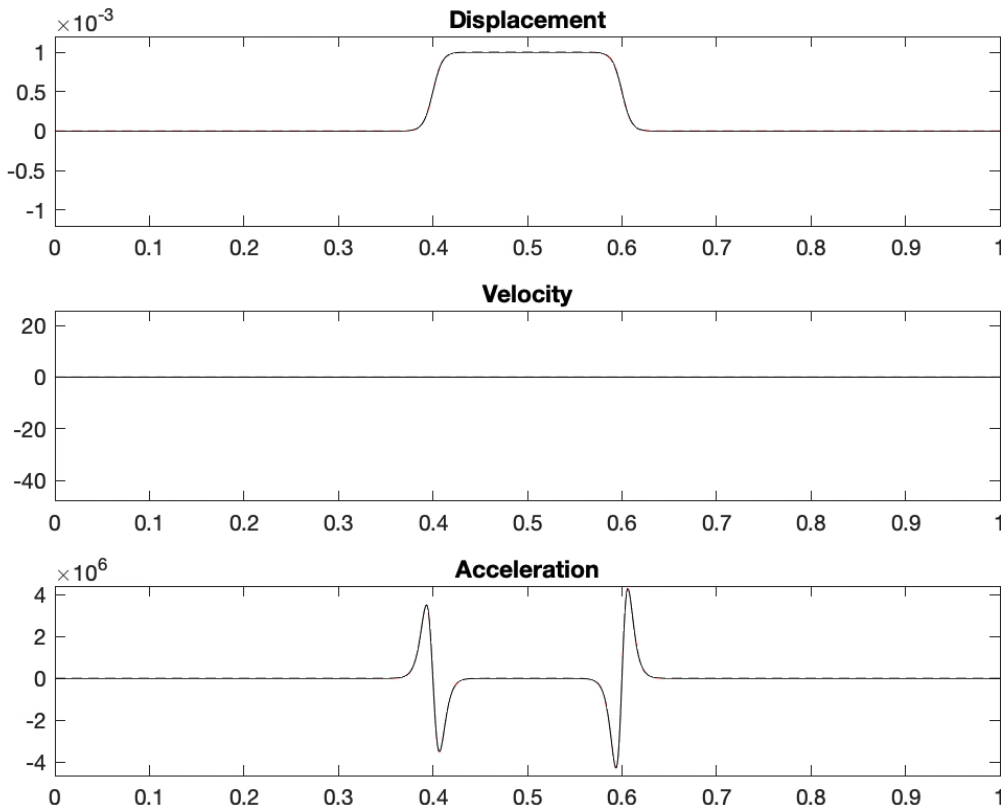
— Single-domain FOM solution

— Solution in  $\Omega_1$

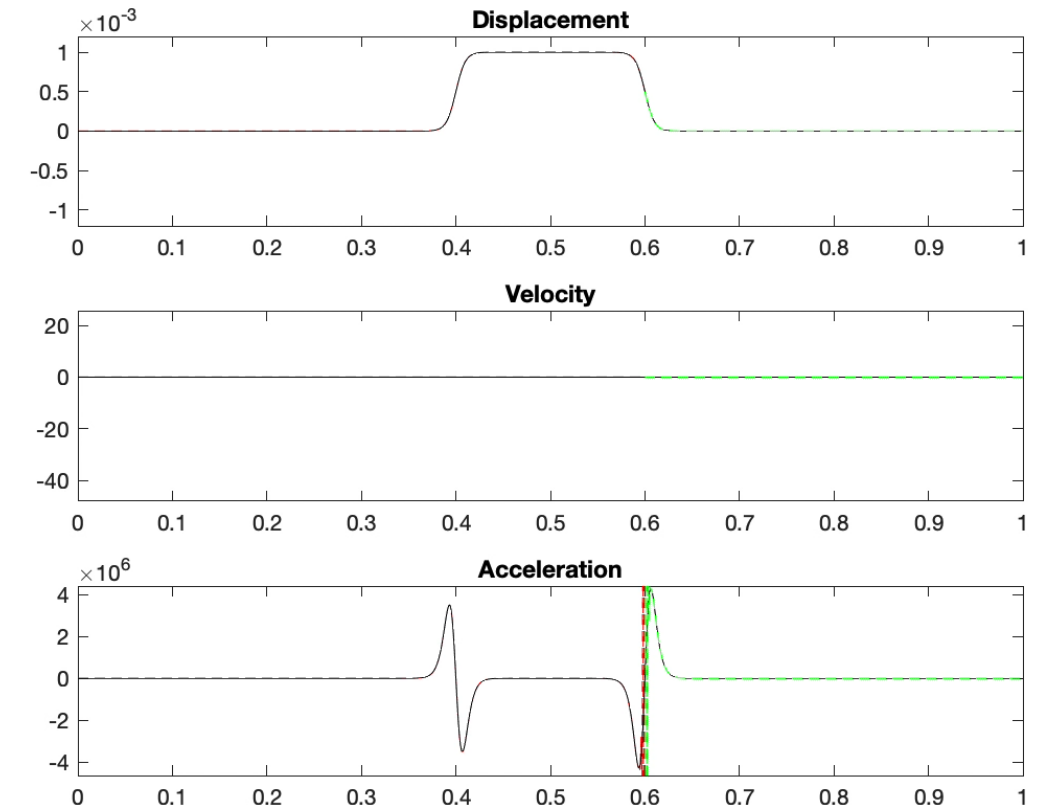
— Solution in  $\Omega_2$

- Predictive **single-domain ROM** solution exhibits **spurious oscillations** in velocity and acceleration
- Predictive **FOM-HROM** solution is **smooth** and **oscillation-free**
  - Highlights coupling method's ability to improve ROM predictive accuracy

# Numerical Example: Predictive Problem Results



Predictive single-domain ROM ( $M_1 = 300$ )



Predictive FOM-HROM ( $M_2 = 200$ )

— Single-domain FOM solution

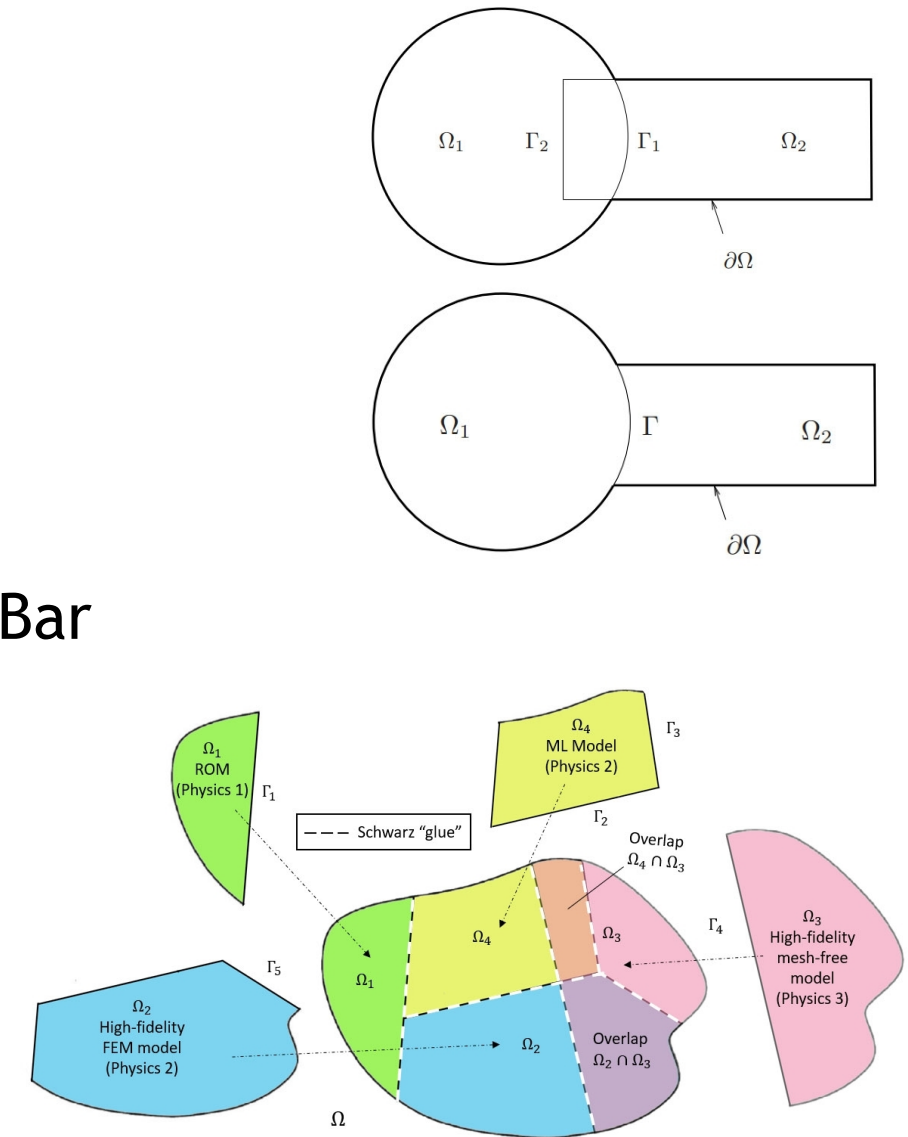
— Solution in  $\Omega_1$

— Solution in  $\Omega_2$

# Outline



- The Schwarz Alternating Method for Domain Decomposition-Based Coupling
- Extension to FOM\*-ROM# and ROM-ROM Coupling
- Numerical Examples
  - 1D Dynamic Wave Propagation in Hyperelastic Bar
  - 2D Burgers Equation
- Summary & Future Work



# Numerical Example: 2D Inviscid Burgers Problem



$$\frac{\partial u}{\partial t} + \frac{1}{2} \left( \frac{\partial u^2}{\partial x} + \frac{\partial uv}{\partial y} \right) = 0.02 \exp(\mu_2 x)$$

$$\frac{\partial v}{\partial t} + \frac{1}{2} \left( \frac{\partial vu}{\partial x} + \frac{\partial v^2}{\partial y} \right) = 0$$

$$u(x=0, y, t; \mu) = \mu_1$$

$$u(x, y, t=0) = v(x, y, t=0) = 1$$

$$x, y \in [0, 100], t \in [0, T_f]$$

## FOM discretization:

- Spatial discretization given by a **Godunov-type scheme** with  $N = 250$  elements in each dimension
- Implicit temporal discretization: **trapezoidal method** with fixed  $\Delta t = 0.05$ ; Choose  $T_f = 25.0$

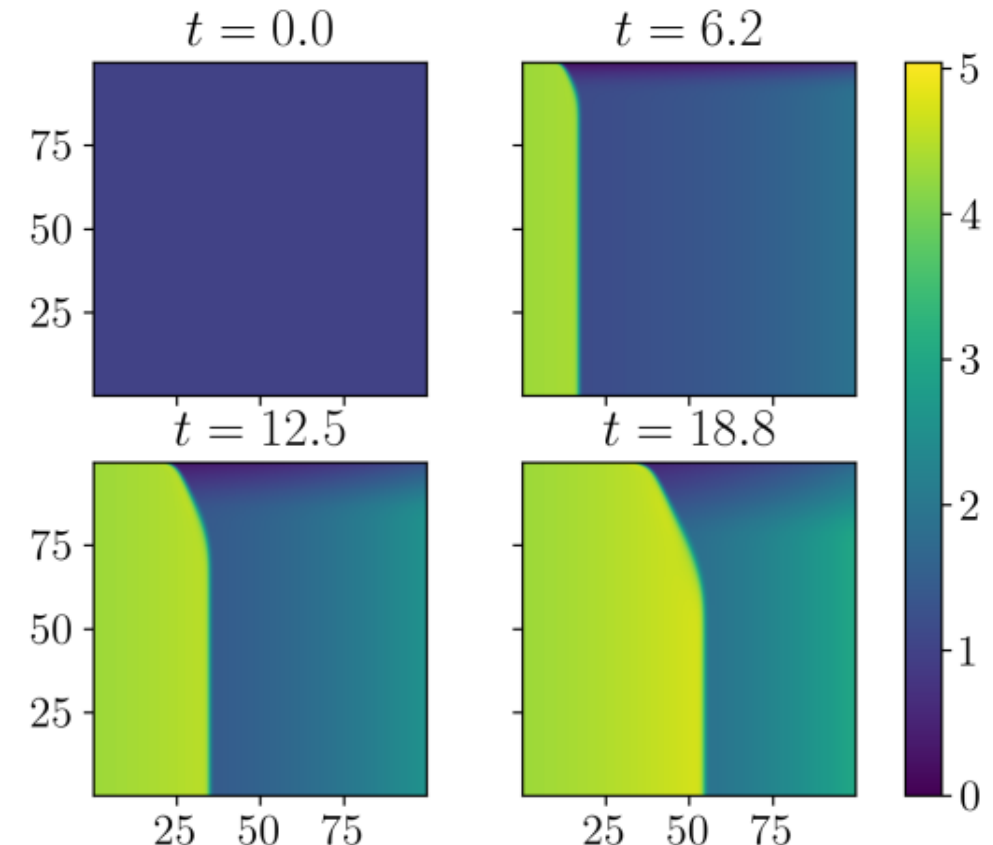
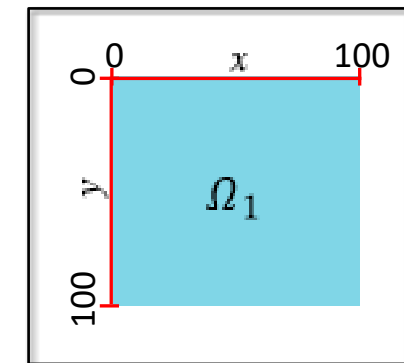


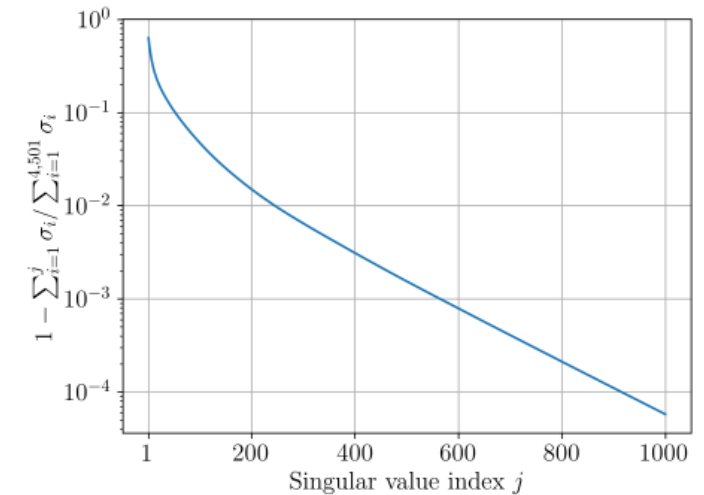
Figure above: solution of  $u$  component at various times



# Numerical Example: 2D Inviscid Burgers Problem



- **2D** makes for a more appropriate testing of potential speedups from coupling subdomains to ROMs
- The **inviscid Burgers' equation** is a popular analog for fluid problems where shocks are possible, and is particularly difficult for conventional projection-based ROMs
- Two **parameters** considered:
  - Dirichlet BC parameterization  $\mu_1$
  - Source term parameterization  $\mu_2$
- ROMs results are ***predictive*** and are based on the ***Least-Squares Petrov-Galerkin (LSPG)*** method, with POD calculated from FOM coupling models.
  - Greater than 200 POD modes required to capture 99% snapshot energy for when sampling 9  $\mu = [\mu_1, \mu_2]$  values
- Hyper-reduced ROMs (HROMs) perform ***hyper-reduction*** using ECSW [Farhat *et al.*, 2015]
- **Couplings tested:** overlapping, FOM-FOM, FOM-ROM, ROM-ROM, FOM-HROM, HROM-HROM, implicit-explicit, implicit-implicit, explicit-explicit.



*This talk*

# Single Domain ROM



- **Uniform sampling** of  $\mathcal{D} = [4.25, 5.50] \times [0.015, 0.03]$  by a  $3 \times 3$  grid  $\Rightarrow 9$  training parameter points characterized by  $\Delta\mu_1 = 0.625$  and  $\Delta\mu_2 = 0.0075$
- Queried but **unsampled parameter point**  $\mu = [4.75, 0.02]$  with reduced dimension of  $n = 95$
- **Reduced mesh** resulting from solving non-negative least squares problem formulate by ECSW gives  $n_e = 5,689$  elements (9.1% of  $N_e = 62,500$  elements).

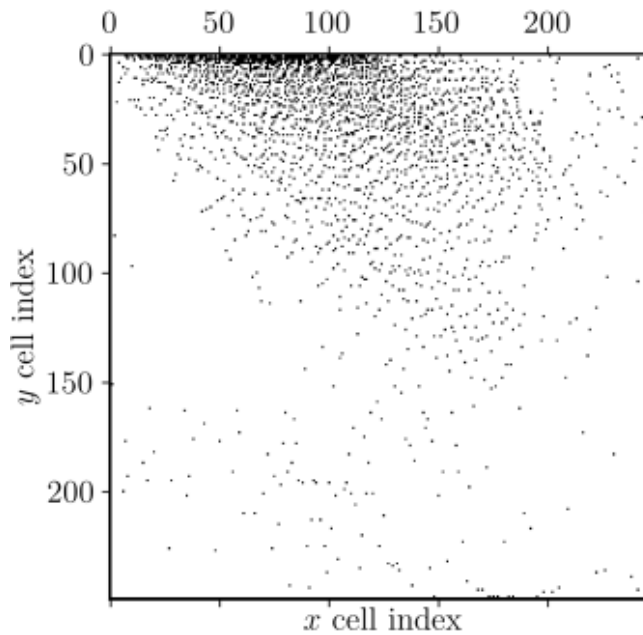


Figure above: Reduced mesh of single domain HROM

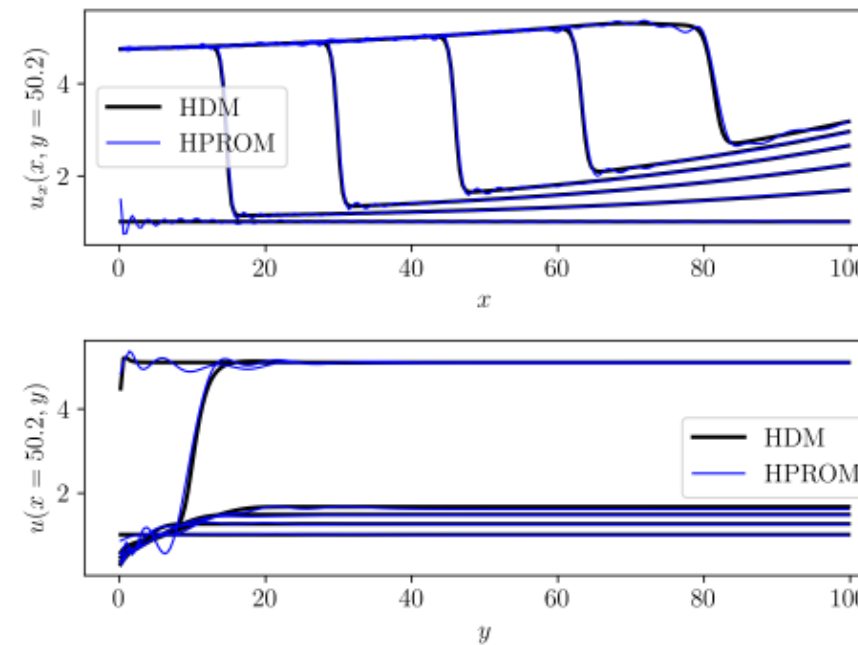
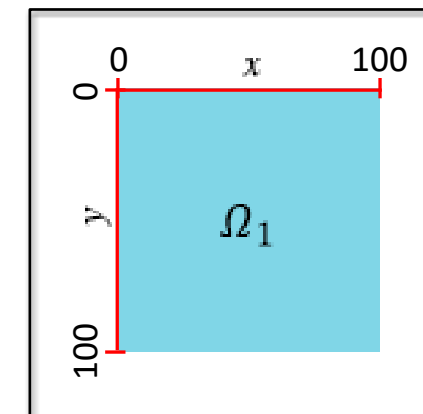


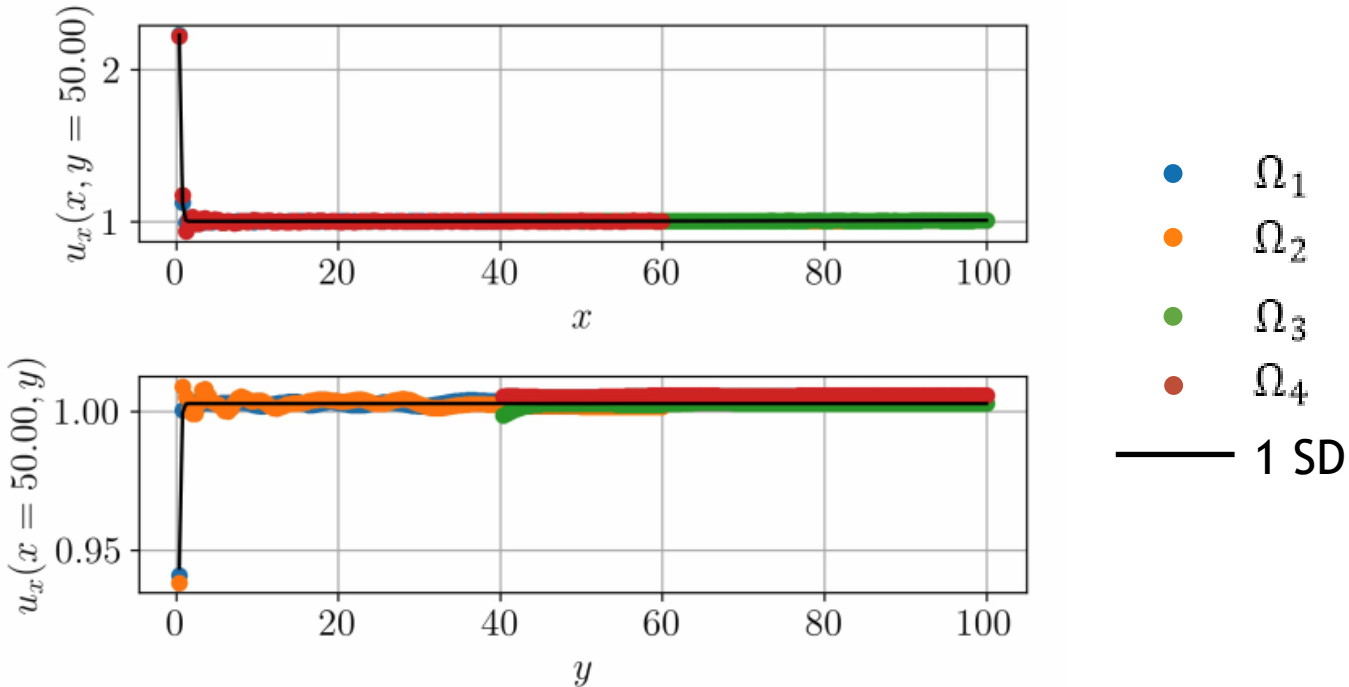
Figure above: HROM and FOM results at various time steps



# ROM-ROM-ROM-ROM Coupling



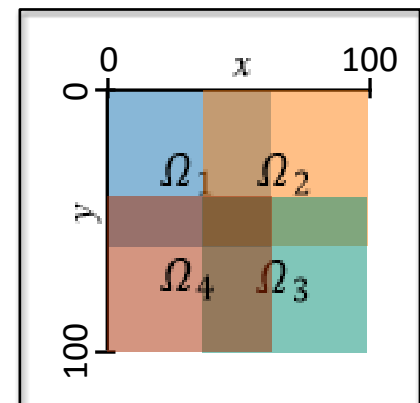
$t = 0.00$



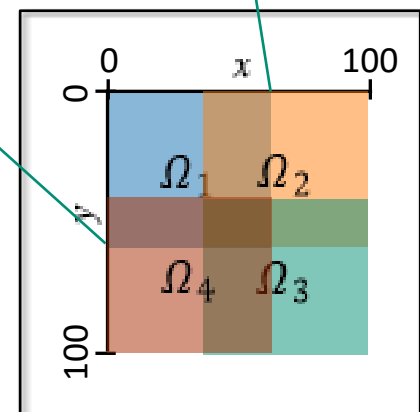
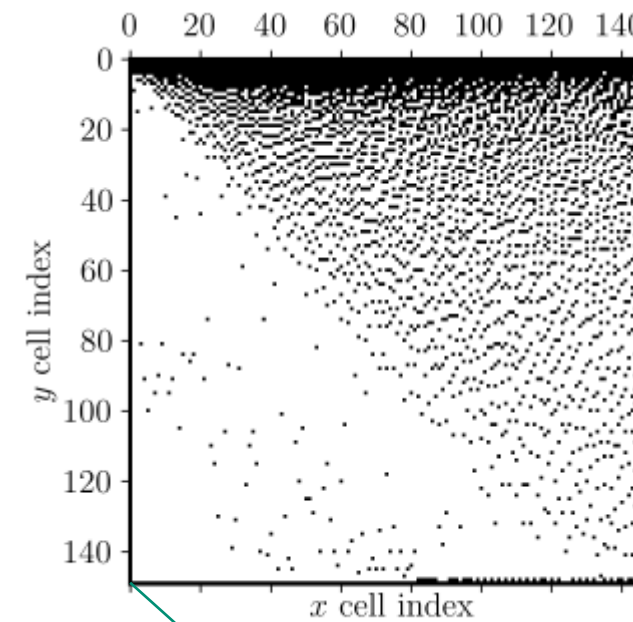
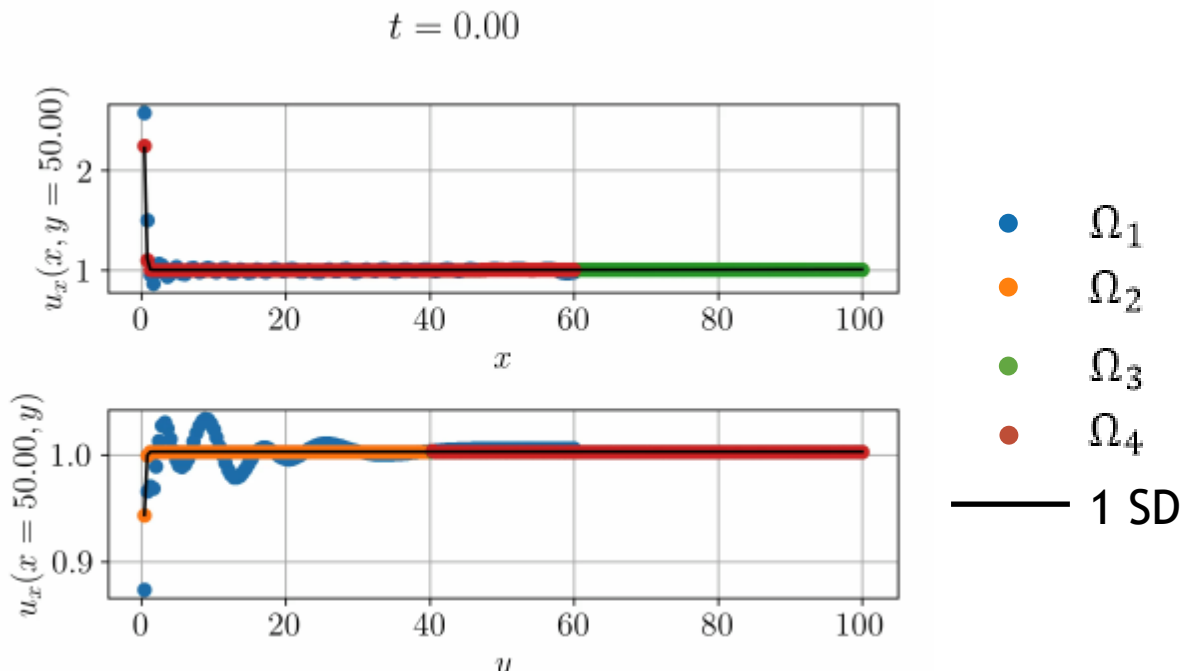
Subdomains	$M$	MSE (%)	Wall Clock Time (s)
$\Omega_1$	197	0.16	323
$\Omega_2$	197	0.17	379
$\Omega_3$	102	0.13	200
$\Omega_4$	87	0.21	117
<b>Total</b>			<b>1019</b>

- Spatial/temporal resolution:**  $\Delta x_1 = \Delta x_4 = 0.4, \Delta x_2 = \Delta x_3 = 0.3, \Delta y_i = 0.4, \Delta t_i = 0.05$
- Basis size calculated to retain **99% of snapshot energy**
- Domains traversed in **counterclockwise fashion** for Schwarz BC transfer.
- Method converges in **only 3 Schwarz iterations** per controller time-step
- Solution exhibits **some spurious oscillations** due to under-resolved solution.

Spurious oscillations *do not* impact coupled solution.



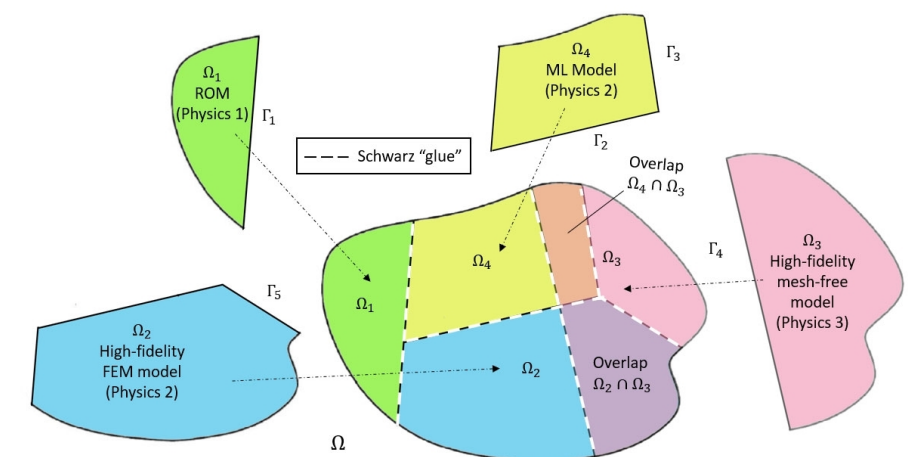
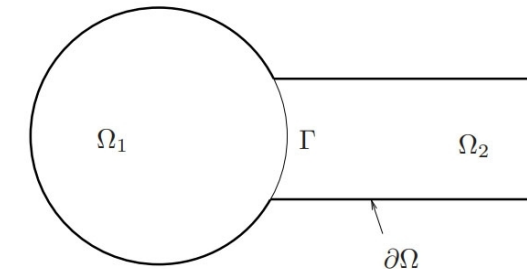
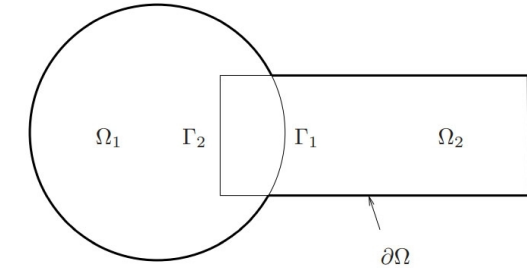
# HROM-FOM-FOM-FOM Coupling



- Same mesh and time-step resolutions as ROM-ROM-ROM-ROM coupling
- HROM is in  $\Omega_1$  and retains **95% of snapshot energy**  $\Rightarrow$  76 modes
  - HROM assignment is “worst-case-scenario”
- **Reduced mesh** trained only using a single parameter instance of  $\mu = [4.25, 0.0225]$
- Method converges in **3 Schwarz iterations** per controller time-step.
- **1.1x speedup** w.r.t. corresponding FOM-FOM-FOM-FOM coupling.
- Significant **spurious oscillations** in first/last time steps due to under-resolved solution

Spurious oscillations *do not* impact Schwarz coupling.

- The Schwarz Alternating Method for Domain Decomposition-Based Coupling
- Extension to FOM\*-ROM<sup>#</sup> and ROM-ROM Coupling
- Numerical Examples
  - 1D Dynamic Wave Propagation in Hyperelastic Bar
  - 2D Burgers Equation
- Summary & Future Work



# Summary and Future Work

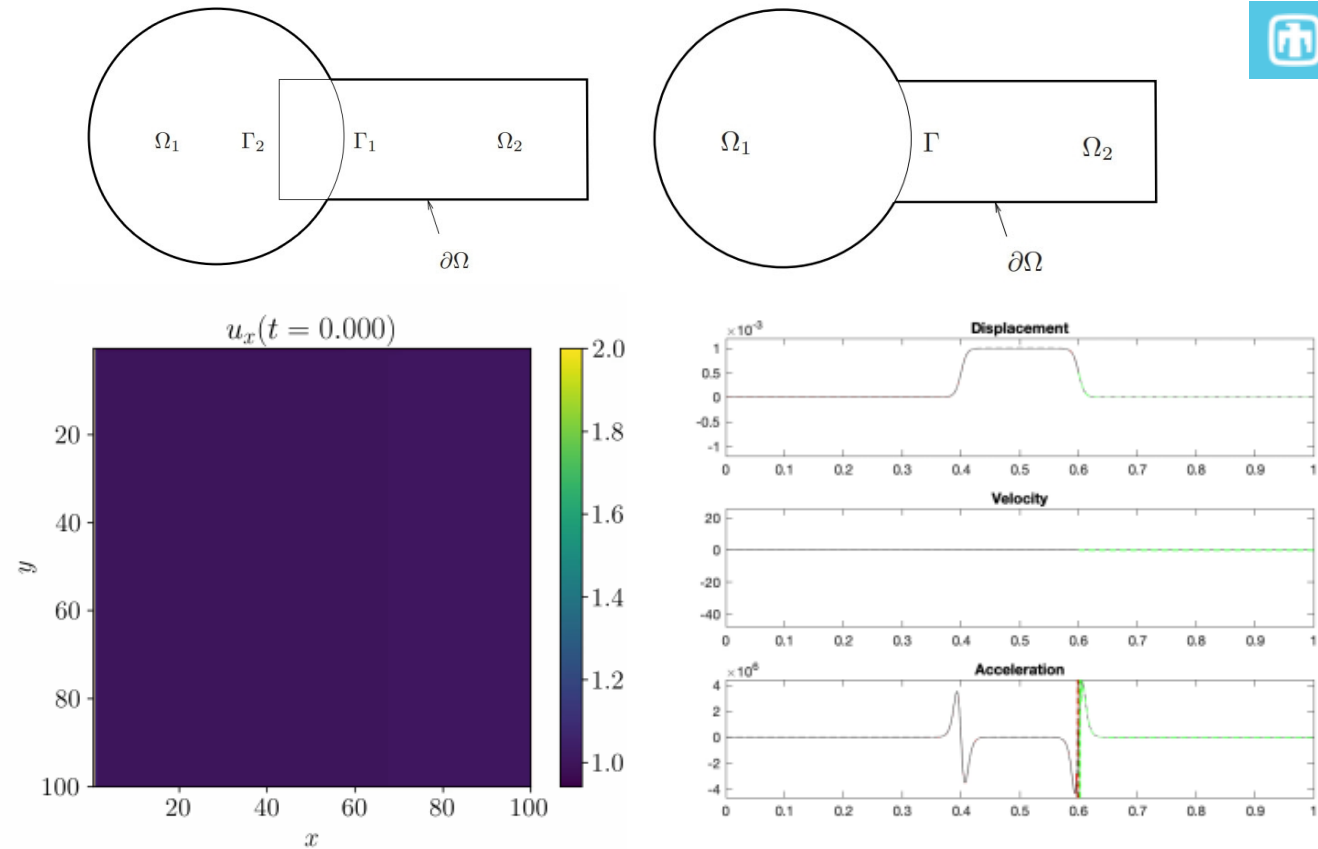


## Summary:

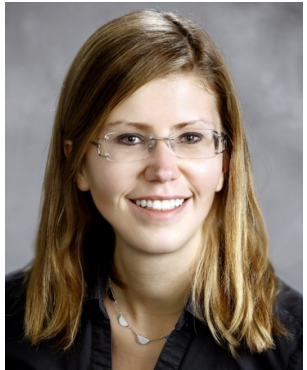
- In a 1D solid mechanics and a 2D hyperbolic PDE setting, Schwarz has been demonstrated for coupling subdomains using both FOMs and (H)ROMs
- In both cases, computational gains can be obtained using HROMs, although the monolithic compute times are not bested
  - Mitigation: additive Schwarz

## Ongoing & future work:

- Improving efficiency of coupling implementation
- Dynamically adapting domain partitioning and “on-the-fly” ROM-FOM switching
- Coupling nonlinear approximation manifold methods (quadratic, general nonlinear)
- Learning of “optimal” transmission conditions to ensure structure preservation
- Extension of coupling methods to coupling of Physics Informed Neural Networks (PINNs) (WIP)
- Journal paper in preparation.



# Team & Acknowledgments



Irina Tezaur



Joshua Barnett  
*Year-Round Intern*



Alejandro Mota



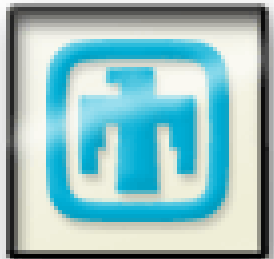
Chris Wentland  
*Postdoc*



Sandia  
National  
Laboratories



LABORATORY DIRECTED  
RESEARCH & DEVELOPMENT



Photo

Will Snyder  
*Summer Intern*

***Thank you! Questions?***



- [1] A. Salinger, *et al.* "Albany: Using Agile Components to Develop a Flexible, Generic Multiphysics Analysis Code", *Int. J. Multiscale Comput. Engng.* 14(4) (2016) 415-438.
- [2] H. Schwarz. "Über einen Grenzübergang durch alternierendes Verfahren". In: *Vierteljahrsschrift der Naturforschenden Gesellschaft in Zurich* 15 (1870), pp. 272-286.
- [3] S.L. Sobolev. "Schwarz's Algorithm in Elasticity Theory". In: *Selected Works of S.L Sobolev. Volume I: equations of mathematical physics, computational mathematics and cubature formulats*. Ed. By G.V. Demidenko and V.L. Vaskevich. New York: Springer, 2006.
- [4] S. Mikhlin. "On the Schwarz algorithm". In: *Proceedings of the USSR Academy of Sciences* 77 (1951), pp. 569-571.
- [5] P.L. Lions. "On the Schwarz alternating method I." In: *1988, First International Symposium on Domain Decomposition methods for Partial Differential Equations*, SIAM, Philadelphia.
- [6] SIERRA Solid Mechanics Team. *Sierra/SM 4.48 User's Guide*. Tech. rep. SAND2018-2961. SNL Report, Oct. 2018.
- [7] M. Gunzburger, J. Peterson, J. Shadid. "Reduced-order modeling of time-dependent PDEs with multiple parameters in the boundary data". *CMAME* 196 (2007) 1030-1047.
- [8] C. Hoang, Y. Choi, K. Carlberg. "Domain-decomposition least-squares Petrov-Galerkin (DD-LSPG) nonlinear model reduction". *CMAME* 384 (2021) 113997.
- [9] K. Smetana, T. Taddei. "Localized model reduction for nonlinear elliptic partial differential equations: localized training, partition of unity, and adaptive enrichment", *ArXiV pre-print*, 2022.
- [10] C. Farhat, T. Chapman, P. Avery. "Structure-preserving, stability & accuracy properties of the energy-conserving sampling and weighting method for the hyper reduction of nonlinear FE dynamic models", *IJNME* 102 (2015) 1077-1110.
- [11] M. Bergmann, A. Ferrero, A. Iollo, E. Lombardi, A. Scardigli, H. Telib. "A zonal Galerkin-free POD model for incompressible flows." *JCP* 352 (2018) 301-325.

## References (cont'd)

Email: [ikalash@sandia.gov](mailto:ikalash@sandia.gov)  
URL: [www.sandia.gov/~ikalash](http://www.sandia.gov/~ikalash)



- [12] A. Iollo, G. Sambataro, T. Taddei. "A one-shot overlapping Schwarz method for component-based model reduction: application to nonlinear elasticity", *CMAME* 404 (2023) 115786.
- [13] A. Mota, I. Tezaur, C. Alleman. "The Schwarz Alternating Method in Solid Mechanics", *Comput. Meth. Appl. Mech. Engng.* 319 (2017), 19-51.
- [14] A. Mota, I. Tezaur, G. Phlipot. "The Schwarz Alternating Method for Dynamic Solid Mechanics", *Comput. Meth. Appl. Mech. Engng.* 121 (21) (2022) 5036-5071.
- [15] J. Hoy, I. Tezaur, A. Mota. "The Schwarz alternating method for multiscale contact mechanics". in *Computer Science Research Institute Summer Proceedings 2021*, J.D. Smith and E. Galvan, eds., Technical Report SAND2021-0653R, Sandia National Labs, 360-378, 2021.
- [16] J. Barnett, I. Tezaur, A. Mota. "The Schwarz alternating method for the seamless coupling of nonlinear reduced order models and full order models", in *Computer Science Research Institute Summer Proceedings 2022*, S.K. Seritan and J.D. Smith, eds., Technical Report SAND2022-10280R, Sandia National Laboratories, 2022, pp. 31-55. ***This talk***

***Journal article on ROM-FOM/ROM-ROM  
coupling using Schwarz is in preparation.***

## References (cont'd)



- [20] J.M. Connors, K. Sockwell, A Multirate Discontinuous-Galerkin-in-Time Framework for Interface-Coupled Problems, *SIAM Journal on Numerical Analysis*, 5(60), 2373-2404, 2022.
- [21] K. Sockwell, K. Peterson, P. Kuberry, P. Bochev, Interface Flux Recovery Framework for Constructing Partitioned Heterogeneous Time-Integration Methods, to appear.



# Start of Backup Slides

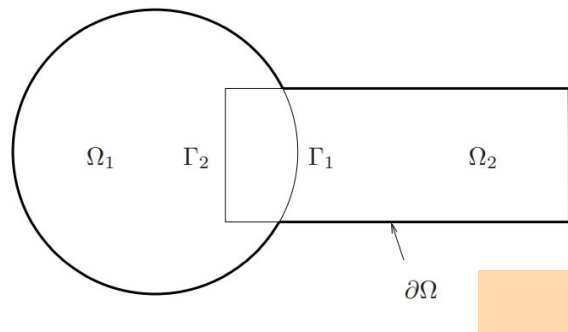
# Spatial Coupling via Alternating Schwarz



## Overlapping Domain Decomposition

$$\begin{cases} N(\mathbf{u}_1^{(n+1)}) = f, \text{ in } \Omega_1 \\ \mathbf{u}_1^{(n+1)} = \mathbf{g}, \text{ on } \partial\Omega_1 \setminus \Gamma_1 \\ \mathbf{u}_1^{(n+1)} = \mathbf{u}_2^{(n)} \quad \text{on } \Gamma_1 \end{cases}$$

$$\begin{cases} N(\mathbf{u}_2^{(n+1)}) = f, \text{ in } \Omega_2 \\ \mathbf{u}_2^{(n+1)} = \mathbf{g}, \text{ on } \partial\Omega_2 \setminus \Gamma_2 \\ \mathbf{u}_2^{(n+1)} = \mathbf{u}_1^{(n+1)} \quad \text{on } \Gamma_2 \end{cases}$$



**Model PDE:**  $\begin{cases} N(\mathbf{u}) = f, \text{ in } \Omega \\ \mathbf{u} = \mathbf{g}, \text{ on } \partial\Omega \end{cases}$

- Dirichlet-Dirichlet transmission BCs [Schwarz 1870; Lions 1988; Mota *et al.* 2017; Mota *et al.* 2022]

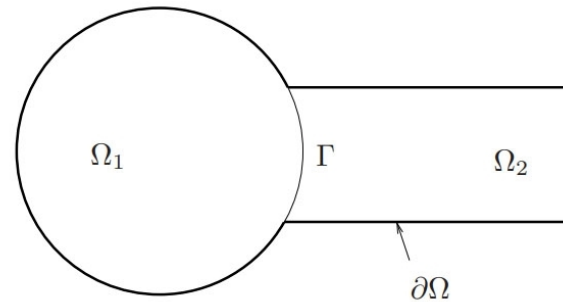
**This talk:** sequential subdomain solves (**multiplicative Schwarz**). Parallel subdomain solves (**additive Schwarz**) also possible.

## Non-overlapping Domain Decomposition

$$\begin{cases} N(\mathbf{u}_1^{(n+1)}) = f, \quad \text{in } \Omega_1 \\ \mathbf{u}_1^{(n+1)} = \mathbf{g}, \quad \text{on } \partial\Omega_1 \setminus \Gamma \\ \mathbf{u}_1^{(n+1)} = \lambda_{n+1}, \quad \text{on } \Gamma \end{cases}$$

$$\begin{cases} N(\mathbf{u}_2^{(n+1)}) = f, \quad \text{in } \Omega_2 \\ \mathbf{u}_2^{(n+1)} = \mathbf{g}, \quad \text{on } \partial\Omega_2 \setminus \Gamma \\ \nabla \mathbf{u}_2^{(n+1)} \cdot \mathbf{n} = \nabla \mathbf{u}_1^{(n+1)} \cdot \mathbf{n}, \text{ on } \Gamma \end{cases}$$

$$\lambda_{n+1} = \theta \varphi_2^{(n)} + (1 - \theta) \lambda_n \text{ on } \Gamma, \text{ for } n \geq 1$$



- Relevant for multi-material and multi-physics coupling
- Alternating Dirichlet-Neumann transmission BCs [Zanolli *et al.* 1987]
- Robin-Robin transmission BCs also lead to convergence [Lions 1990]
- $\theta \in [0,1]$ : relaxation parameter (can help convergence)

# Numerical Example: 1D Dynamic Wave Propagation Problem

- Basis sizes  $M_1$  and  $M_2$  vary from 60 to 300
  - Larger ROM used in  $\Omega_1$ , since solution has **steeper gradient** here
- For couplings involving FOM and ROM/HROM, **FOM** is placed in  $\Omega_1$ , since solution has steeper gradient here
- **Non-negative least-squares optimization problem** for ECSW weights solved using MATLAB's `lsqnonneg` function with early termination criterion (solution step-size tolerance =  $10^{-4}$ )
  - Ensures all HROMs have **consistent termination criterion** w.r.t. MATLAB implementation
  - However, **relative error tolerance** of selected reduced elements will differ
    - ❖ Switching to termination criterion based on relative error is work in progress and expected to improve HROM results
  - Convergence tolerance determines **size of sample mesh**  $N_{e,i}$
  - **Boundary points** must be in sample mesh for application of Schwarz BC

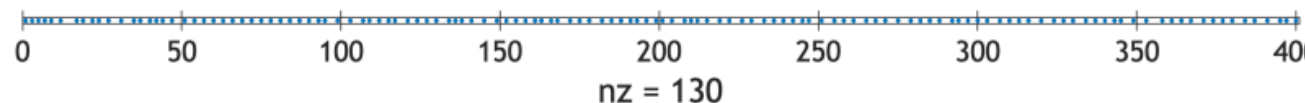


Figure left: sample sample mesh for 1D wave propagation problem

J. Barnett, I. Tezaur, A. Mota. "The Schwarz alternating method for the seamless coupling of nonlinear reduced order models and full order models", in [Computer Science Research Institute Summer Proceedings 2022](#), S.K. Seritan and J.D. Smith, eds., Technical Report SAND2022-10280R, Sandia National Laboratories, 2022, pp. 31-55. (<https://arxiv.org/abs/2210.12551>)

# Numerical Example: Reproductive Problem Results



Model	$M_1/M_2$	$N_{e,1}/N_{e,2}$	CPU time (s)	$\mathcal{E}_{\text{MSE}}(\tilde{\mathbf{u}}_1)/\mathcal{E}_{\text{MSE}}(\tilde{\mathbf{u}}_2)$	$\mathcal{E}_{\text{MSE}}(\tilde{\mathbf{v}}_1)/\mathcal{E}_{\text{MSE}}(\tilde{\mathbf{v}}_2)$	$\mathcal{E}_{\text{MSE}}(\tilde{\mathbf{a}}_1)/\mathcal{E}_{\text{MSE}}(\tilde{\mathbf{a}}_2)$	$N_S$
FOM	-/-	-/-	$1.871 \times 10^3$	-/-	-/-	-/-	-
ROM	60/-	-/-	$1.398 \times 10^3$	$1.659 \times 10^{-2} / -$	$1.037 \times 10^{-1}$	$4.681 \times 10^{-1} / -$	-
HROM	60/-	155/-	$5.878 \times 10^2$	$1.730 \times 10^{-2} / -$	$1.063 \times 10^{-1} / -$	$4.741 \times 10^{-1} / -$	-
ROM	200/-	-/-	$1.448 \times 10^3$	$2.287 \times 10^{-4} / -$	$4.038 \times 10^{-3} / -$	$4.542 \times 10^{-2} / -$	-
HROM	200/-	428/-	$9.229 \times 10^2$	$8.396 \times 10^{-4} / -$	$8.947 \times 10^{-3} / -$	$7.462 \times 10^{-2} / -$	-
FOM-FOM	-/-	-/-	$2.345 \times 10^3$	-	-	-	24,630
FOM-ROM	-/80	-/-	$2.341 \times 10^3$	$2.171 \times 10^{-6} / 1.253 \times 10^{-5}$	$3.884 \times 10^{-5} / 2.401 \times 10^{-4}$	$2.982 \times 10^{-4} / 2.805 \times 10^{-3}$	25,227
FOM-HROM	-/80	-/130	$2.085 \times 10^3$	$2.022 \times 10^{-4} / 5.734 \times 10^{-4}$	$1.723e \times 10^{-3} / 5.776 \times 10^{-3}$	$7.421 \times 10^{-3} / 3.791 \times 10^{-2}$	29,678
FOM-ROM	-/200	-/-	$2.449 \times 10^3$	$4.754 \times 10^{-12} / 7.357 \times 10^{-11}$	$1.835 \times 10^{-10} / 4.027 \times 10^{-9}$	$5.550 \times 10^{-9} / 1.401 \times 10^{-7}$	24,630
FOM-HROM	-/200	-/252	$2.352 \times 10^3$	$1.421 \times 10^{-5} / 4.563 \times 10^{-4}$	$1.724 \times 10^{-4} / 2.243 \times 10^{-3}$	$9.567 \times 10^{-4} / 1.364 \times 10^{-2}$	27,156
ROM-ROM	200/80	-/-	$2.778 \times 10^3$	$4.861 \times 10^{-5} / 3.093 \times 10^{-5}$	$1.219 \times 10^{-3} / 4.177 \times 10^{-4}$	$1.586 \times 10^{-2} / 3.936 \times 10^{-3}$	27,810
HROM-HROM	200/80	315/130	$1.769 \times 10^3$	$3.410 \times 10^{-3} / 6.662 \times 10^{-4}$	$4.110 \times 10^{-2} / 6.432 \times 10^{-3}$	$2.485 \times 10^{-1} / 4.307 \times 10^{-2}$	29,860
ROM-ROM	300/80	-/-	$2.646 \times 10^3$	$2.580 \times 10^{-6} / 1.292 \times 10^{-5}$	$6.226 \times 10^{-5} / 2.483 \times 10^{-4}$	$9.470 \times 10^{-4} / 2.906 \times 10^{-3}$	25,059
HROM-HROM	300/80	405/130	$1.938 \times 10^3$	$6.960 \times 10^{-3} / 7.230 \times 10^{-4}$	$6.328 \times 10^{-2} / 7.403 \times 10^{-3}$	$3.137 \times 10^{-1} / 4.960 \times 10^{-2}$	29,896

Green shading highlights most competitive coupled models

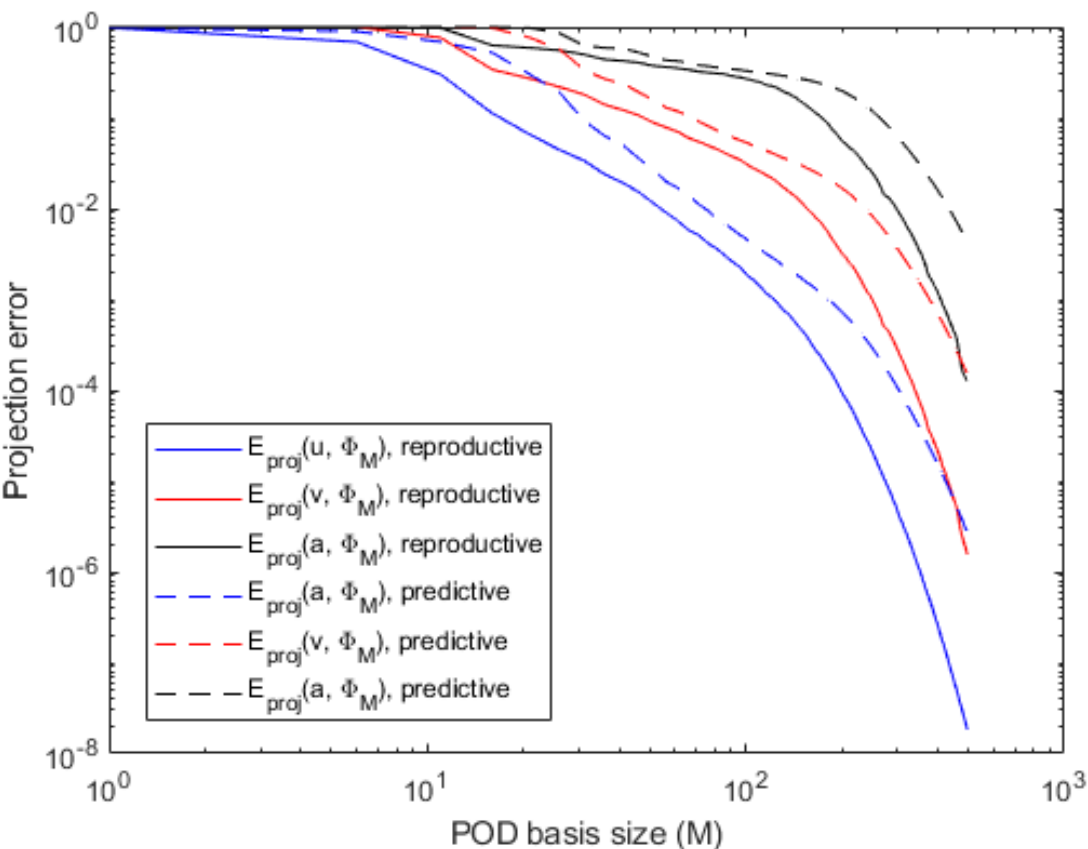
- All coupled models evaluated converged on average in **<3 Schwarz iterations** per time-step
- Larger FOM-ROM coupling has **same total # Schwarz iters** ( $N_S$ ) as FOM-FOM coupling
- Other couplings require more Schwarz iters than FOM-FOM coupling to converge
  - **More Schwarz iters** required when coupling **less accurate models**
  - Larger 300/80 mode ROM-ROM takes less wall-clock time than smaller 200/80 mode ROM-ROM
- **FOM-HROM** and **HROM-HROM** couplings **outperform** the **FOM-FOM** coupling in terms of CPU time by 12.5-32.6%
- All couplings involving ROMs/HROMs are **at least as accurate** as single-domain ROMs/HROMs

# Numerical Example: Predictive Problem Results



- Start by calculating **projection error** for reproductive and predictive version of the Rounded Square IC problem:

$$\mathcal{E}_{\text{proj}}(\mathbf{u}, \Phi_M) := \frac{\|\mathbf{u} - \Phi_M(\Phi_M^T \Phi_M)^{-1} \Phi_M^T \mathbf{u}\|_2}{\|\mathbf{u}\|_2}$$



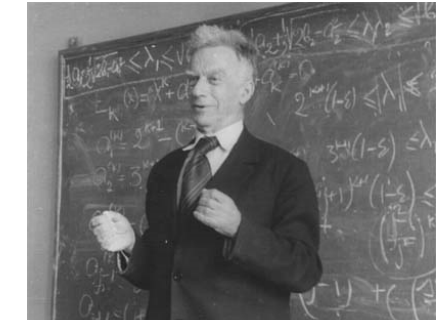
- Projection error suggests **predictive ROM** can achieve **accuracy and convergence with basis refinement**
- O(100) modes** are needed to achieve sufficiently accurate ROM
  - Larger ROMs containing O(100) modes considered in our coupling experiments:  $M_1 = 300$ ,  $M_2 = 200$

# Theoretical Foundation

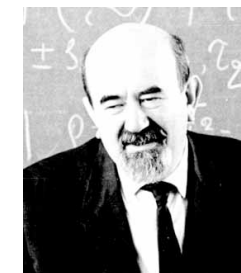


Using the Schwarz alternating as a *discretization method* for PDEs is natural idea with a sound *theoretical foundation*.

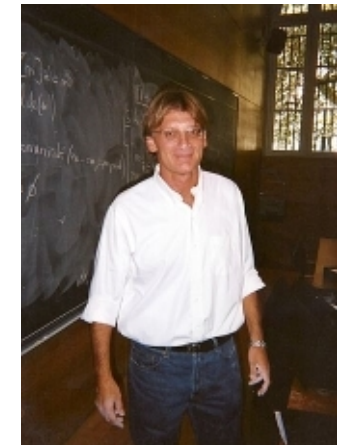
- **S.L. Sobolev (1936):** posed Schwarz method for *linear elasticity* in variational form and *proved method's convergence* by proposing a convergent sequence of energy functionals.
- **S.G. Mikhlin (1951):** *proved convergence* of Schwarz method for general linear elliptic PDEs.
- **P.-L. Lions (1988):** studied convergence of Schwarz for *nonlinear monotone elliptic problems* using max principle.
- **A. Mota, I. Tezaur, C. Alleman (2017):** proved *convergence* of the alternating Schwarz method for *finite deformation quasi-static nonlinear PDEs* (with energy functional  $\Phi[\varphi]$ ) with a *geometric convergence rate*.



S.L. Sobolev (1908 – 1989)



S.G. Mikhlin  
(1908 – 1990)



P.-L. Lions (1956-)



A. Mota, I. Tezaur, C. Alleman

$$\Phi[\varphi] = \int_B A(F, Z) dV - \int_B B \cdot \varphi dV$$

$$\nabla \cdot P + B = 0$$

# Convergence Proof\*



A. Mota, I. Tezaur, C. Alleman  
Schwarz Alternating Method in Solid Mechanics

## 2 Formulation of the Schwarz Alternating Method

We start by defining the standard finite-difference variational formulation to establish notation before presenting the formulation of the coupling method.

### 2.1 Variational Formulation on a Single Domain

Consider a body in the open set  $\Omega \subset \mathbb{R}^2$  undergoing a motion described by the mapping  $x = \varphi(X)$ ,  $\Omega \subset \mathbb{R}^2$ ,  $X \in \mathbb{R}^2$ . Assume that the boundary of  $\Omega$  is  $\partial\Omega = \partial\Omega_1 \cup \partial\Omega_2$  with unit normal  $\mathbf{n}$ , where  $\partial\Omega_1$  is the boundary of the subdomain  $\Omega_1$  and  $\partial\Omega_2$  is the boundary of the subdomain  $\Omega_2$ . The prescribed boundary tractions or Neumann boundary conditions are  $\mathbf{q} = \mathbf{q}(\varphi) \in \mathbb{R}^2$ . The prescribed boundary tractions or Neumann boundary conditions are  $\mathbf{q}^* = \mathbf{q}^*(\varphi) \in \mathbb{R}^2$ . Let  $\mathbf{P} = \mathbf{P}(\varphi)$  be the deformation gradient. Let  $\mathbf{F} = \mathbf{F}(\varphi)$  be the stress tensor, with  $\mathbf{F}(\varphi)$  the stress tensor in the reference configuration. Furthermore, we denote the initial material

$$\mathbf{F}_0 = \int_{\Omega} \mathbf{F}(\mathbf{x}) \, d\mathbf{x} = \int_{\Omega} \mathbf{F}(\varphi) \, d\mathbf{x} = \int_{\Omega} \mathbf{F}(\varphi) \, d\mathbf{X} \quad (1)$$

in which  $\mathbf{F}(\varphi)$  is the reference boundary density and  $\mathbf{F}$  is the density of internal rotations. The weak form of the problem is obtained by minimizing the energy functional  $\Phi[\varphi]$  over the Sobolev space  $W_1^1(\Omega)$  that is composed of functions that are square-integrable and have square-integrable first derivatives. Define

$$S = \{\varphi \in W_1^1(\Omega) : \mathbf{q}^* - \mathbf{q}(\varphi) = 0\} \quad (2)$$

and

$$V = \{\varphi \in W_1^1(\Omega) : \mathbf{q}^* - \mathbf{q}(\varphi) = 0\} \quad (3)$$

where  $\mathbf{q}^* \in V$  is a function. The potential energy is minimized if and only if  $\Phi[\varphi] \leq \Phi[\varphi']$  for all  $\varphi' \in V$  and  $\varphi \in S$ . It is straightforward to show that the solution of  $\Phi[\varphi]$  in the mapping  $\varphi = \varphi^*$  that satisfies

$$\partial\Phi(\varphi^*) = \int_{\Omega} \mathbf{F}_0 : \mathbf{D}\varphi^* \, d\mathbf{X} = \int_{\Omega} \mathbf{F}(\varphi^*) : \mathbf{D}\varphi^* \, d\mathbf{X} = 0 \quad (4)$$

where  $\mathbf{F}_0 = \mathbf{F}(\varphi^*)$  denotes the first Piola-Kirchhoff stress. The Euler-Lagrange equation corresponding to the variational statement (3) is

A. Mota, I. Tezaur, C. Alleman  
Schwarz Alternating Method in Solid Mechanics



Figure 1: Two subdomains  $\Omega_1$  and  $\Omega_2$  and the corresponding boundaries  $T_1$  and  $T_2$  used by the Schwarz alternating method.

A. Mota, I. Tezaur, C. Alleman  
Schwarz Alternating Method in Solid Mechanics

$$\begin{aligned} 1. & \mathbf{u}_1^{(0)} \in \mathbf{X}_1^{(0)} \text{ in } \Omega_1, \mathbf{u}_2^{(0)} \in \mathbf{X}_2^{(0)} \text{ in } \Omega_2, \\ 2. & \text{restr. } \mathbf{u}_1^{(0)} \text{ in } \Omega_1 \cap \Omega_2 = \mathbf{q}(\mathbf{u}_1^{(0)}), \\ 3. & \text{restr. } \mathbf{u}_2^{(0)} \text{ in } \Omega_1 \cap \Omega_2 = \mathbf{q}^*(\mathbf{u}_2^{(0)}), \\ 4. & \left\{ \begin{array}{l} \mathbf{u}_1^{(1)} = \mathbf{u}_1^{(0)} + \mathbf{K}_1^{-1} \mathbf{F}_1(\mathbf{u}_2^{(0)}) \\ \mathbf{u}_2^{(1)} = \mathbf{u}_2^{(0)} + \mathbf{K}_2^{-1} \mathbf{F}_2(\mathbf{u}_1^{(0)}) \end{array} \right\} \left[ \begin{array}{l} \mathbf{u}_1^{(0)} \\ \mathbf{u}_2^{(0)} \end{array} \right] \\ & \text{+ iteration loop} \\ & \vdots \\ & \text{+ linear system} \end{aligned}$$

Appendix 1: Schwarz-Schmidt Method

A. Mota, I. Tezaur, C. Alleman  
Schwarz Alternating Method in Solid Mechanics

$$\begin{aligned} \text{Research that } & \mathbf{S}_0 = \mathbf{q}^{(n-1)} + V_1 \quad \text{or} \quad \mathbf{p}^{(n-1)} \in \mathcal{S}_{n-1} \rightarrow \mathbf{p}^{(n-1)} \in \mathcal{S}_n \\ \text{presenting the formulation of the coupling method.} \\ \text{Theorem 1.} & \text{ Assume that the energy functional } \Phi[\varphi] \text{ satisfies properties 1-5 above. Consider the Schwarz alternating method of Section 2 defined by (9)-(13) and its equivalent form (39). Then} \\ \text{(a)} & \Phi[\tilde{\varphi}^{(0)}] \geq \Phi[\tilde{\varphi}^{(1)}] \geq \dots \geq \Phi[\tilde{\varphi}^{(n-1)}] \geq \Phi[\varphi], \text{ where } \varphi \text{ is the minimizer of } \Phi[\varphi] \text{ over } S. \\ \text{(b)} & \text{The sequence } \{\tilde{\varphi}^{(n)}\} \text{ defined in (39) converges to the minimizer } \varphi \text{ of } \Phi[\varphi] \text{ in } S. \\ \text{(c)} & \text{The Schwarz minimum values } \Phi[\tilde{\varphi}^{(n)}] \text{ converge monotonically to the minimum value } \Phi[\varphi] \text{ in } S \text{ starting from any initial guess } \tilde{\varphi}^{(0)}. \end{aligned}$$

Proof. See Appendix 1.  $\square$

Finally, we present a series of results and their relation. Our analysis for the specific case of two subdomains, although not fully established in a general framework, can be extended to multiple subdomains, specifically to Lemaire [35], Belytschko [4], and Li-Shen and Dvornic [34].

## 4 Numerical Examples

In this section, we present two examples of the behavior of the Schwarz alternating method for different input data. First, we briefly describe the two implementations, one in MATLAB and the other in the open-source ABAQUS finite element code [33]. Next, we discuss the error measures used throughout the examples. Finally, we present the convergence of the Schwarz alternating method, the Schwarz-Schmidt method, and our implementation. The following example is a standard academic one used to demonstrate the behavior of the first Schwarz variant of Section 2.1. The second example, a cutout hole specimen, is used to demonstrate the convergence of the overlapping regions in the overlapping Schwarz variant. The observation of the error measure is a standard criterion to measure the accuracy in the results.

**Theorem 1.** Assume that the energy functional  $\Phi[\varphi]$  satisfies properties 1–5 above. Consider the Schwarz alternating method of Section 2 defined by (9)–(13) and its equivalent form (39). Then

- $\Phi[\tilde{\varphi}^{(0)}] \geq \Phi[\tilde{\varphi}^{(1)}] \geq \dots \geq \Phi[\tilde{\varphi}^{(n-1)}] \geq \Phi[\varphi]$ , where  $\varphi$  is the minimizer of  $\Phi[\varphi]$  over  $S$ .
- The sequence  $\{\tilde{\varphi}^{(n)}\}$  defined in (39) converges to the minimizer  $\varphi$  of  $\Phi[\varphi]$  in  $S$ .
- The Schwarz minimum values  $\Phi[\tilde{\varphi}^{(n)}]$  converge monotonically to the minimum value  $\Phi[\varphi]$  in  $S$  starting from any initial guess  $\tilde{\varphi}^{(0)}$ .

**Remark 1.** By the properties of  $\Phi[\varphi]$ , the minimization of  $\Phi[\varphi]$  is equivalent to

$$(\mathbf{F}[\varphi], \mathbf{q}) \geq (\mathbf{F}[\varphi], \mathbf{q}^*) \quad (5)$$

for all  $\mathbf{q} \in S$ .

**Remark 2.** Recall that the strict continuity property of  $\Phi[\varphi]$  can be written as

$$\Phi(\mathbf{q}_1) - \Phi(\mathbf{q}_2) = (\mathbf{F}[\mathbf{q}_1], \mathbf{q}_1) - (\mathbf{F}[\mathbf{q}_2], \mathbf{q}_2) \quad (5)$$

where  $\mathbf{q}_1, \mathbf{q}_2 \in S$ . From (5), we know that if  $\mathbf{q}_1$  is strictly convex over  $S$ , then for each  $R > 0$ , we can find an  $\epsilon > 0$  such that if  $\mathbf{q}_2 \in S$ , we have

$$|\Phi(\mathbf{q}_1) - \Phi(\mathbf{q}_2)| = |\Phi(\mathbf{q}_1, \mathbf{q}_2) - \Phi(\mathbf{q}_2, \mathbf{q}_1)| \geq \epsilon R \quad (5)$$

**Remark 3.** By property 5, the uniform continuity of  $\Phi[\varphi]$ . There exists a modulus of continuity  $\omega > 0$ , with  $\omega = \omega_R > 0$ , such that

$$|\Phi(\mathbf{q}_1) - \Phi(\mathbf{q}_2)| \leq \omega_R |\mathbf{q}_1 - \mathbf{q}_2| \quad (5)$$

forall  $\mathbf{q}_1, \mathbf{q}_2 \in S$ . By definition,  $\omega_R \rightarrow 0$  as  $R \rightarrow \infty$ .

**Remark 4.** It was shown in [34] that in the case  $\Omega_1 \cap \Omega_2 \neq \emptyset$ , there exist  $\mathbf{q}_1 \in \Omega_1$  and  $\mathbf{q}_2 \in \Omega_2$  such that

$$\mathbf{q}^* = \mathbf{q}_1 = \mathbf{q}_2 \quad (5)$$

and

$$|\Phi(\mathbf{q}_1) - \Phi(\mathbf{q}_2)| \leq C_0 |\mathbf{q}_1 - \mathbf{q}_2| \quad (5)$$

for some  $C_0 > 0$  independent of  $\varphi$ .

**Remark 5.** Note that the  $\Phi[\varphi]$  can be written as

$$|\Phi(\mathbf{q}^{(n+1)}) - \Phi(\mathbf{q}^{(n)})| = 0 \quad (5)$$

for  $n \in \{1, 2, \dots\}$ . Recall from (5) the definition between  $\mathbf{q}^{(n)}$  and  $\mathbf{q}^{(n+1)}$ . This is due to the uniqueness of the solution to each individual problem over  $\Omega_1$  and the definition of  $\mathbf{q}^{(n)}$  as the minimizer of  $\Phi[\varphi]$  over  $\Omega_1$ .

**Remark 6.** Note that  $\Phi[\varphi]$  is the minimizer of  $\Phi[\varphi]$  over  $S$ . Since the problem is well-posed,  $\Phi[\varphi]$  is unique. Hence  $\Phi[\varphi] \leq \Phi[\varphi^{(n)}]$  for all  $n \in \{1, 2, \dots\}$ .

**Remark 7.** Let  $\mathbf{q}^{(n)} \subset \Omega_1$  and  $\mathbf{q} \in S$ . By Remark 5, there exist  $\mathbf{q}_1 \in \Omega_1$  and  $\mathbf{q}_2 \in \Omega_2$  such that

$$|\Phi(\mathbf{q}^{(n+1)}) - \Phi(\mathbf{q}^{(n)})| = 0 \quad (5)$$

for  $n \in \{1, 2, \dots\}$ . Note that  $\varphi$  is the minimizer of  $\Phi[\varphi]$  over  $S$ . Since the problem is well-posed,  $\Phi[\varphi]$  is unique. Hence  $\Phi[\varphi] \leq \Phi[\varphi^{(n)}]$  for all  $n \in \{1, 2, \dots\}$ .

Again using (5) and also (5) leads to

$$(\mathbf{F}[\mathbf{q}^{(n)}], \mathbf{q}_1 - \mathbf{q}^{(n)}) \leq (\mathbf{F}[\mathbf{q}^{(n)}], \mathbf{q}^*) - (\mathbf{F}[\mathbf{q}^{(n+1)}], \mathbf{q}_1 - \mathbf{q}^{(n)}) \quad (5)$$

and substituting (5) into (5) we readily obtain

$$(\mathbf{F}[\mathbf{q}^{(n+1)}], \mathbf{q}_1 - \mathbf{q}^{(n)}) \leq (\mathbf{F}[\mathbf{q}^{(n)}], \mathbf{q}^*) - (\mathbf{F}[\mathbf{q}^{(n+1)}], \mathbf{q}_1 - \mathbf{q}^{(n)}) \quad (5)$$

for all  $\mathbf{q}_1 \in \Omega_1$ .

**Remark 8.** For part (a) of Theorem 1, recall the definition of geometric convergence:

$$E_{n+1} := \frac{1}{n+1} \left( \Phi(\mathbf{q}^{(n)}) - \Phi(\mathbf{q}^{(n+1)}) \right) \quad (5)$$

where  $n \in \{0, 1, 2, \dots\}$ . For some  $C > 0$ , where

$$E_n := \frac{1}{n} \left( \Phi(\mathbf{q}^{(n)}) - \Phi(\mathbf{q}^{(n-1)}) \right) \quad (5)$$

Now  $\Phi(\mathbf{q}^{(n+1)}) - \Phi(\mathbf{q}^{(n)}) \geq 0$  since  $\mathbf{q}^{(n+1)}$  is the minimizer of  $\Phi[\mathbf{q}^{(n+1)}]$  over  $\Omega_1$ .

Combining (5) and (5) leads to

$$\frac{1}{n+1} \left( \Phi(\mathbf{q}^{(n+1)}) - \Phi(\mathbf{q}^{(n)}) \right) \leq \frac{1}{n} \left( \Phi(\mathbf{q}^{(n)}) - \Phi(\mathbf{q}^{(n-1)}) \right) \quad (5)$$

Substituting (5) into (5) we have

$$|\Phi(\mathbf{q}^{(n+1)}) - \Phi(\mathbf{q}^{(n)})| \leq \frac{1}{n+1} \left( \Phi(\mathbf{q}^{(n)}) - \Phi(\mathbf{q}^{(n-1)}) \right) \quad (5)$$

Now by (5) (Remark 7),

$$|\Phi(\mathbf{q}^{(n+1)}) - \Phi(\mathbf{q}^{(n)})| \leq \frac{1}{n+1} \left( \Phi(\mathbf{q}^{(n)}) - \Phi(\mathbf{q}^{(n-1)}) \right) \leq \frac{1}{n+1} \left( \Phi(\mathbf{q}^{(n)}) - \Phi(\mathbf{q}^{(0)}) \right) \quad (5)$$

Substituting (5) into (5) we have

$$|\Phi(\mathbf{q}^{(n+1)}) - \Phi(\mathbf{q}^{(n)})| \leq \frac{1}{n+1} \left( \Phi(\mathbf{q}^{(n)}) - \Phi(\mathbf{q}^{(0)}) \right) \quad (5)$$

Combining (5) and (5) leads to

$$\frac{1}{n+1} \left( \Phi(\mathbf{q}^{(n+1)}) - \Phi(\mathbf{q}^{(n)}) \right) \leq \frac{1}{n} \left( \Phi(\mathbf{q}^{(n)}) - \Phi(\mathbf{q}^{(0)}) \right) \quad (5)$$

Applying the uniform continuity assumption (5), we obtain

$$|\Phi(\mathbf{q}^{(n+1)}) - \Phi(\mathbf{q}^{(n)})| \leq \frac{C_0}{n+1} |\mathbf{q}^{(n)} - \mathbf{q}^{(0)}| \quad (5)$$

By (5),  $|\mathbf{q}^{(n+1)} - \mathbf{q}^{(n)}| \rightarrow 0$  as  $n \rightarrow \infty$ . From this we obtain the result, namely that  $\mathbf{q}^{(n)} \rightarrow \mathbf{q}^*$  as  $n \rightarrow \infty$ .

**Proof of (a).** This follows immediately from (5).

**Proof of (b).** By (5), for large enough  $n$ , we can write  $\mathbf{q}^{(n)} \subset \Omega_1$  and  $\mathbf{q}^{(n+1)} \subset \Omega_2$ .

**Proof of (c).** Let  $\mathbf{q}^{(n+1)} \subset \Omega_1$  and  $\mathbf{q}^{(n)} \subset \Omega_2$ . By (5),  $|\mathbf{q}^{(n+1)} - \mathbf{q}^{(n)}| \leq \frac{C_0}{n+1} |\mathbf{q}^{(n)} - \mathbf{q}^{(0)}|$ .

Let us choose  $C_1$  such that  $C_1 > C_0/R$ , where  $R$  is the Lipschitz continuity constant in (5). Combining (5) with (5) leads to

$$\frac{1}{n+1} \left( \Phi(\mathbf{q}^{(n+1)}) - \Phi(\mathbf{q}^{(n)}) \right) \geq \frac{1}{n+1} |\mathbf{q}^{(n+1)} - \mathbf{q}^{(n)}| \geq \frac{1}{n+1} \frac{C_0}{n+1} |\mathbf{q}^{(n)} - \mathbf{q}^{(0)}| \geq \frac{C_0}{n+1} |\mathbf{q}^{(n)} - \mathbf{q}^{(0)}| \quad (5)$$

and

$$|\mathbf{q}^{(n+1)} - \mathbf{q}^{(n)}| \leq \frac{C_0}{n+1} |\mathbf{q}^{(n)} - \mathbf{q}^{(0)}| \quad (5)$$

which implies the claim.  $\square$

\*A. Mota, I. Tezaur, C. Alleman. "The Schwarz Alternating Method in Solid Mechanics", CMAME 319 (2017), 19-51.



- Like for quasistatics, dynamic alternating Schwarz method converges provided each single-domain problem is ***well-posed*** and ***overlap region*** is ***non-empty***, under some ***conditions*** on  $\Delta t$ .
- ***Well-posedness*** for the dynamic problem requires that action functional  $S[\varphi] := \int_I \int_{\Omega} L(\varphi, \dot{\varphi}) dV dt$  be ***strictly convex*** or ***strictly concave***, where  $L(\varphi, \dot{\varphi}) := T(\dot{\varphi}) + V(\varphi)$  is the Lagrangian.
  - This is studied by looking at its second variation  $\delta^2 S[\varphi_h]$
- We can show assuming a ***Newmark*** time-integration scheme that for the ***fully-discrete*** problem:

$$\delta^2 S[\varphi_h] = \mathbf{x}^T \left[ \frac{\gamma^2}{(\beta \Delta t)^2} \mathbf{M} - \mathbf{K} \right] \mathbf{x}$$

- $\delta^2 S[\varphi_h]$  can always be made positive by choosing a ***sufficiently small***  $\Delta t$
- Numerical experiments reveal that  $\Delta t$  requirements for ***stability/accuracy*** typically lead to automatic satisfaction of this bound.

# Schwarz for Multiscale FOM-FOM Coupling in Solid Mechanics<sup>1</sup>

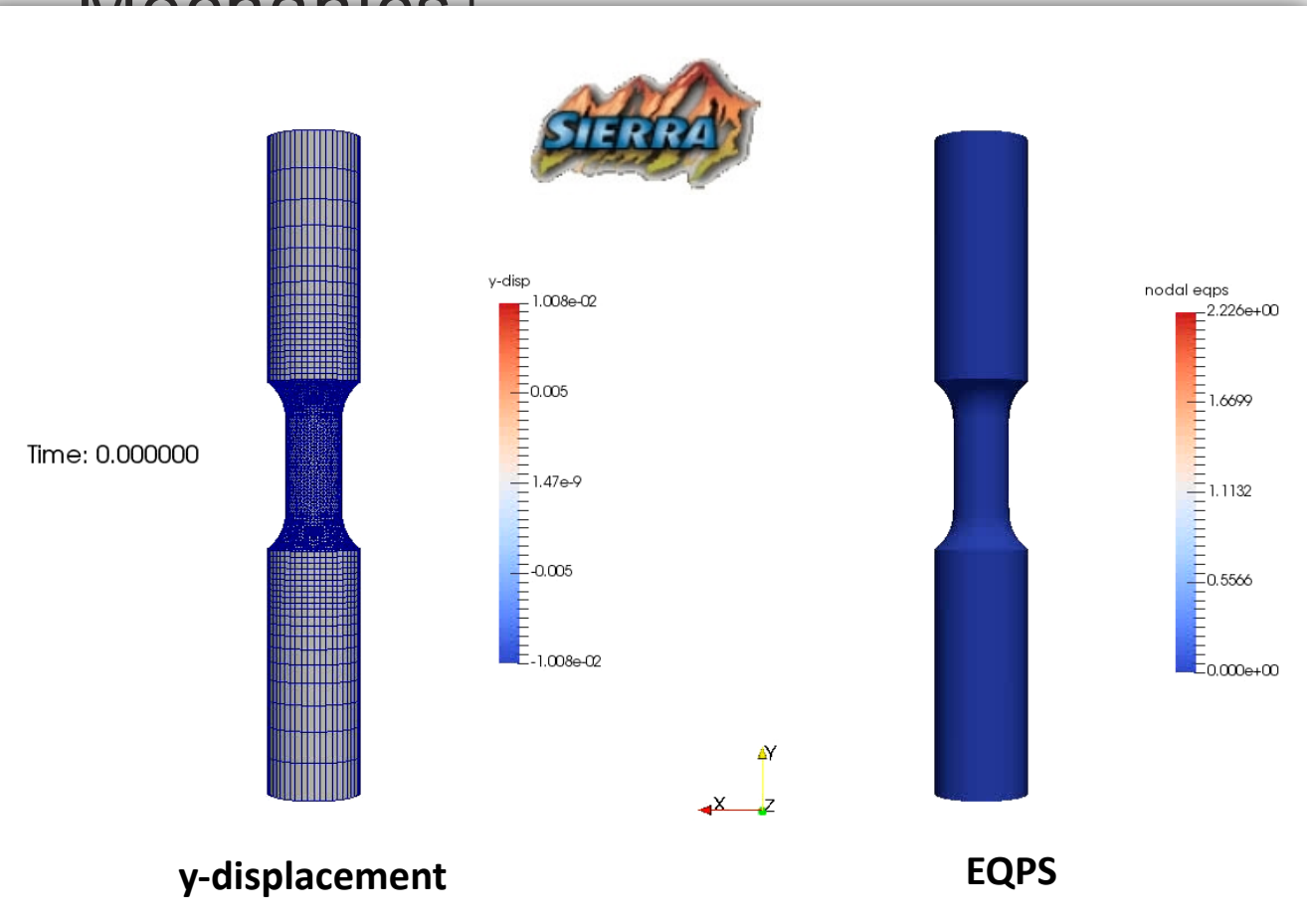
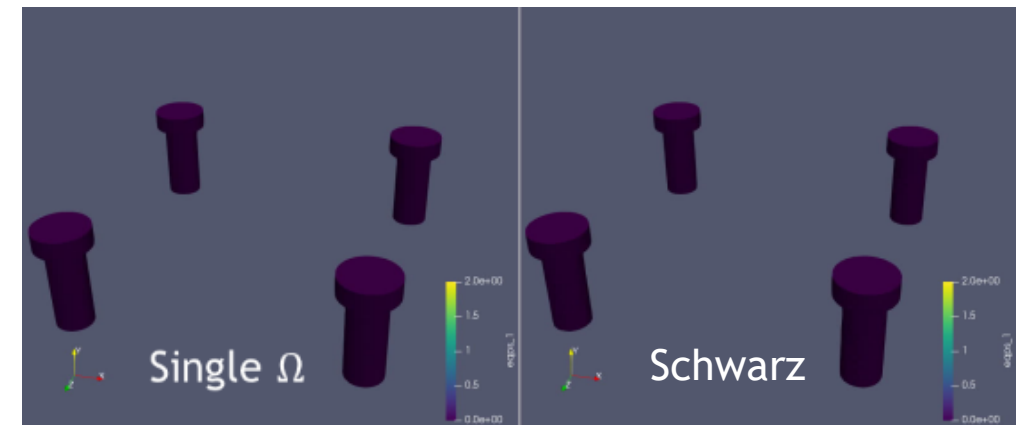
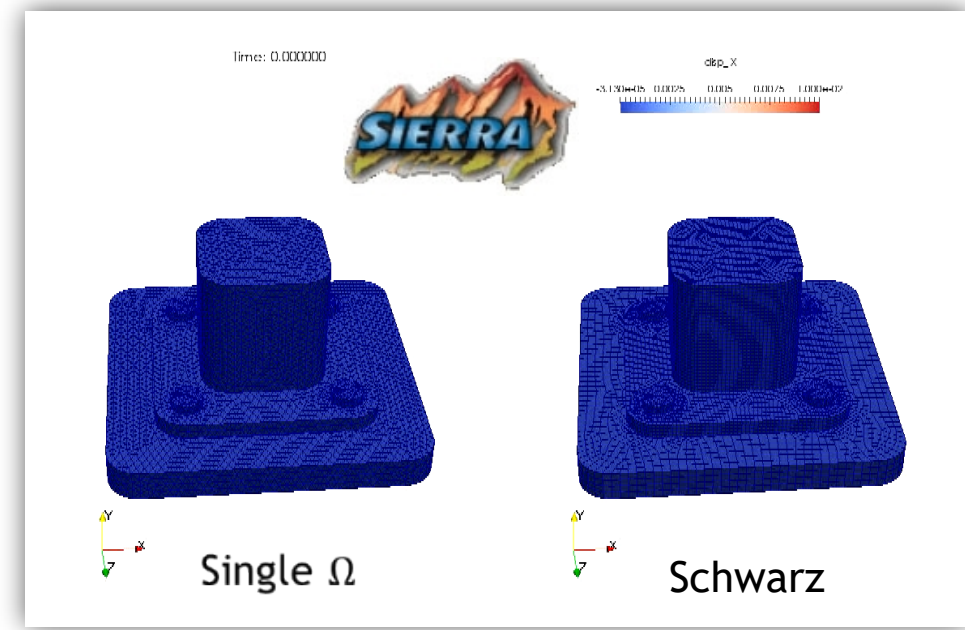


*Figure above:* tension specimen simulation coupling composite TET10 elements with HEX elements in Sierra/SM.

*Figures right:* bolted joint simulation coupling composite TET10 elements with HEX elements in Sierra/SM.

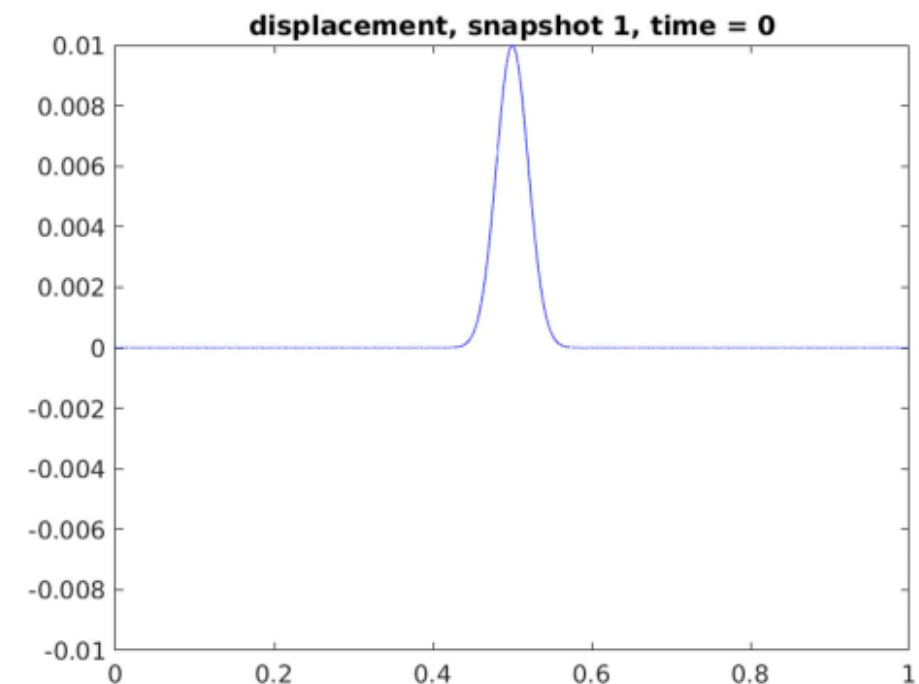


# Numerical Example: Linear Elastic Wave Propagation Problem

- Linear elastic *clamped beam* with Gaussian initial condition.
- Simple problem with analytical exact solution but very *stringent test* for discretization/coupling methods.
- *Couplings tested:* FOM-FOM, FOM-ROM, ROM-ROM, implicit-explicit, implicit-implicit, explicit-explicit.
- ROMs are *reproductive* and based on the *POD/Galerkin* method.
  - 50 POD modes capture ~100% snapshot energy



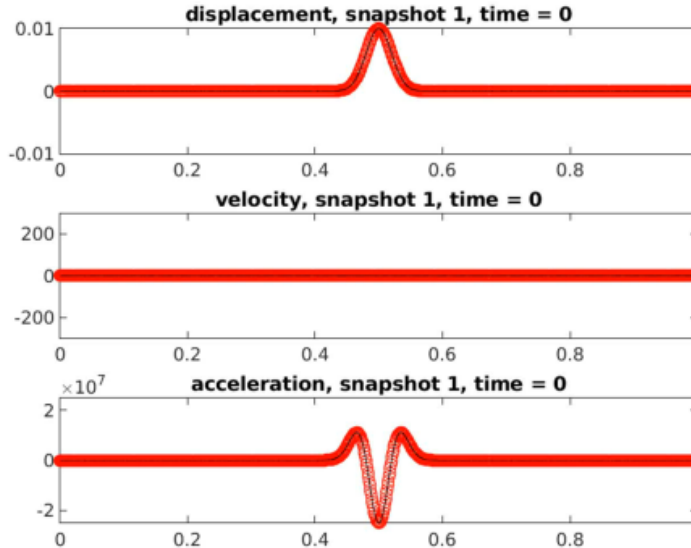
Above: 3D rendering of clamped beam with Gaussian initial condition.  
 Right: Initial condition (blue) and final solution (red). Wave profile is negative of initial profile at time  $T = 1.0e-3$ .



# Linear Elastic Wave Propagation Problem: FOM-ROM and ROM-ROM Couplings



*Coupling delivers accurate solution if each subdomain model is reasonably accurate, can couple different discretizations with different  $\Delta x$ ,  $\Delta t$  and basis sizes.*



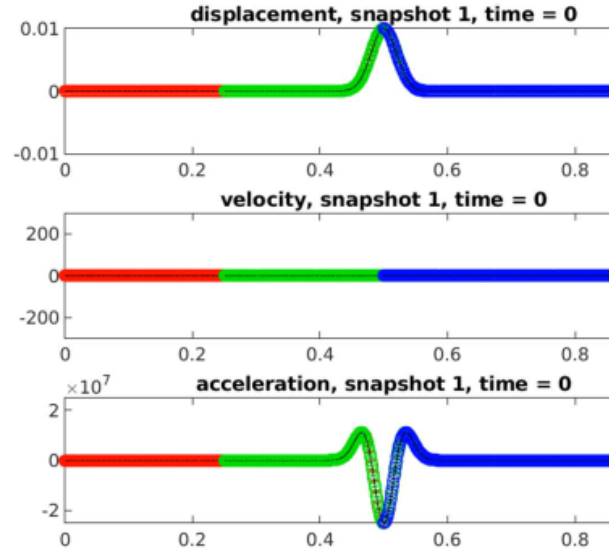
Single Domain FOM



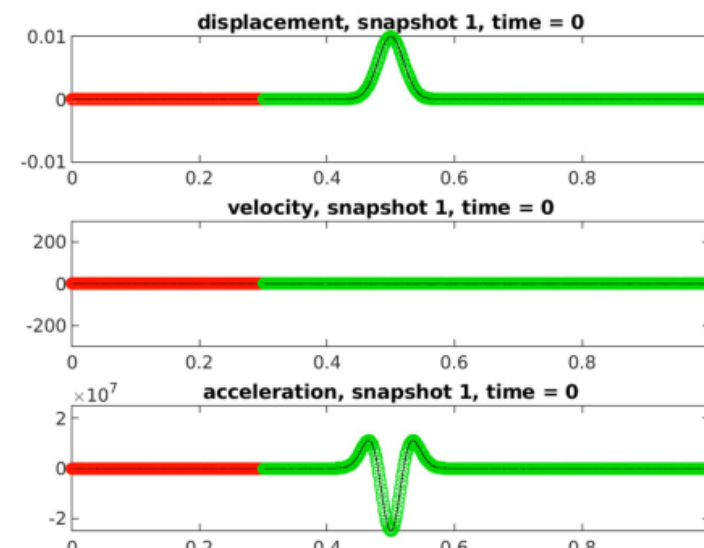
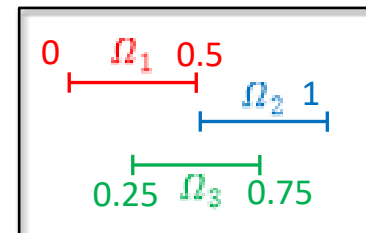
<sup>1</sup>Implicit 40 mode POD ROM,  $\Delta t=1e-6$ ,  $\Delta x=1.25e-3$

<sup>2</sup>Implicit FOM,  $\Delta t =1e-6$ ,  $\Delta x =8.33e-4$

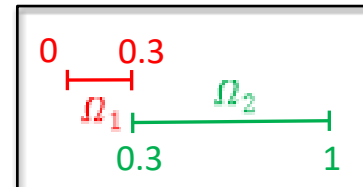
<sup>3</sup>Explicit 50 mode POD ROM,  $\Delta t =1e-7$ ,  $\Delta x =1e-3$



3 overlapping subdomain  
ROM<sup>1</sup>-FOM<sup>2</sup>-ROM<sup>3</sup>



2 non-overlapping subdomain  
FOM<sup>4</sup>-ROM<sup>5</sup> ( $\theta = 1$ )



<sup>5</sup>Implicit FOM,  $\Delta t =2.25e-7$ ,  
 $\Delta x =1e-6$

<sup>4</sup>Explicit 50 mode POD ROM,  
 $\Delta t =2.25e-7$ ,  $\Delta x =1e-6$

# Linear Elastic Wave Propagation Problem: FOM-ROM and ROM-ROM Couplings



*Coupled models are reasonably accurate w.r.t. FOM-FOM coupled analogs and convergence with respect to basis refinement for FOM-ROM and ROM-ROM coupling is observed.*

	disp MSE <sup>6</sup>	velo MSE	acce MSE
Overlapping ROM <sup>1</sup> -FOM <sup>2</sup> -ROM <sup>3</sup>	1.05e-4	1.40e-3	2.32e-2
Non-overlapping FOM <sup>4</sup> -ROM <sup>5</sup>	2.78e-5	2.20e-4	3.30e-3

<sup>1</sup>Implicit 40 mode POD ROM,  $\Delta t = 1e-6$ ,  $\Delta x = 1.25e-3$

<sup>2</sup>Implicit FOM,  $\Delta t = 1e-6$ ,  $\Delta x = 8.33e-4$

<sup>3</sup>Explicit 50 mode POD ROM,  $\Delta t = 1e-7$ ,  $\Delta x = 1e-3$

<sup>4</sup>Implicit FOM,  $\Delta t = 2.25e-7$ ,  $\Delta x = 1e-6$

<sup>5</sup>Explicit 50 mode POD ROM,  $\Delta t = 2.25e-7$ ,  $\Delta x = 1e-6$

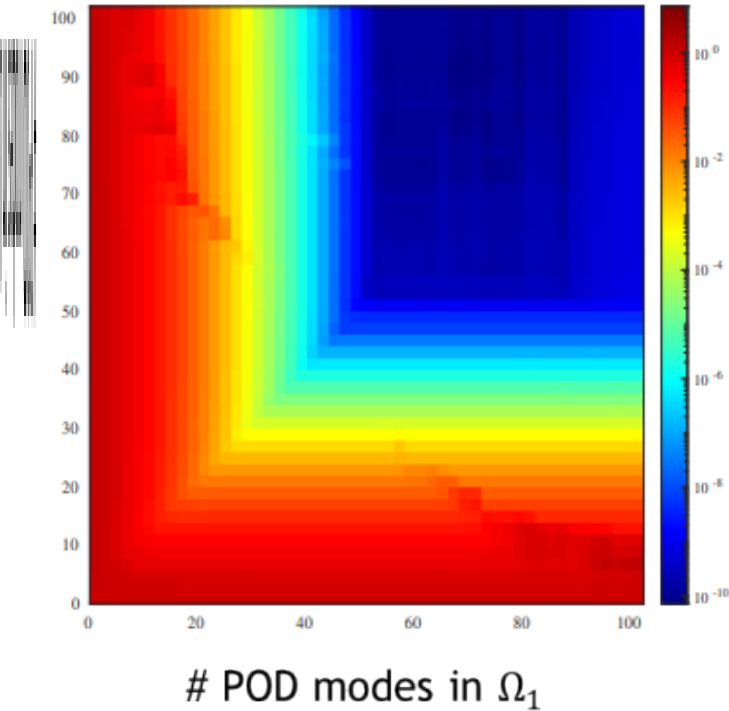
$$^6\text{MSE} = \text{mean squared error} = \sqrt{\sum_{n=1}^{N_t} \|\tilde{\mathbf{u}}^n(\boldsymbol{\mu}) - \mathbf{u}^n(\boldsymbol{\mu})\|_2^2} \Bigg/ \sqrt{\sum_{n=1}^{N_t} \|\mathbf{u}^n(\boldsymbol{\mu})\|_2^2}.$$

# Linear Elastic Wave Propagation Problem: ROM-ROM Couplings

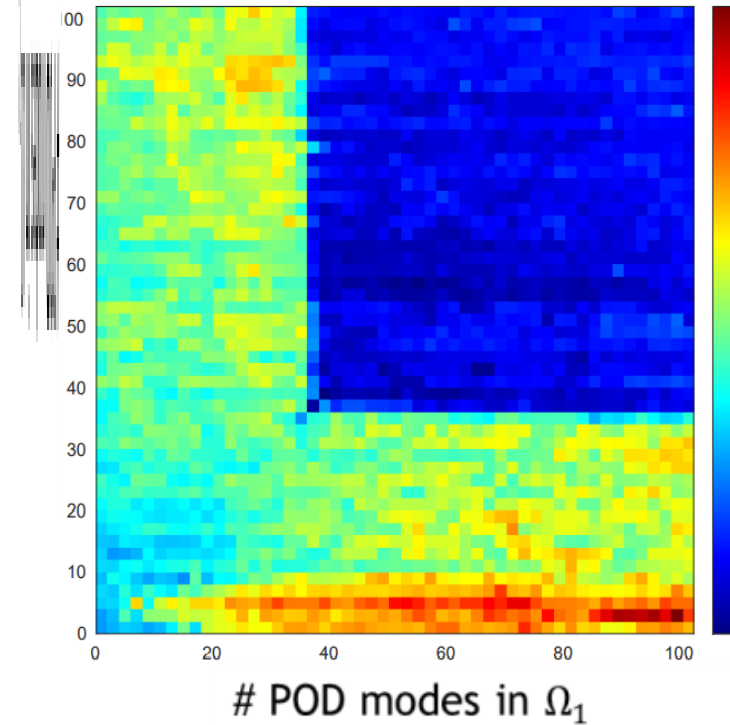


**ROM-ROM coupling gives errors  $< 0(1e-6)$  & speedups over FOM-FOM coupling for basis sizes  $> 40$ .**

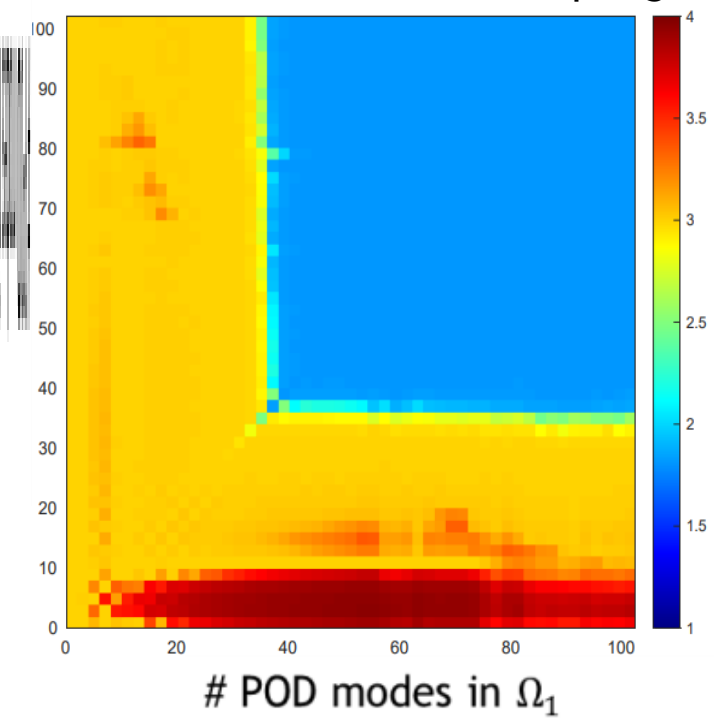
MSE in displacement for 2 subdomain ROM-ROM coupling



CPU times for 2 subdomain ROM-ROM coupling normalized by FOM-FOM CPU time



Average # Schwarz iterations for 2 subdomain ROM-ROM coupling



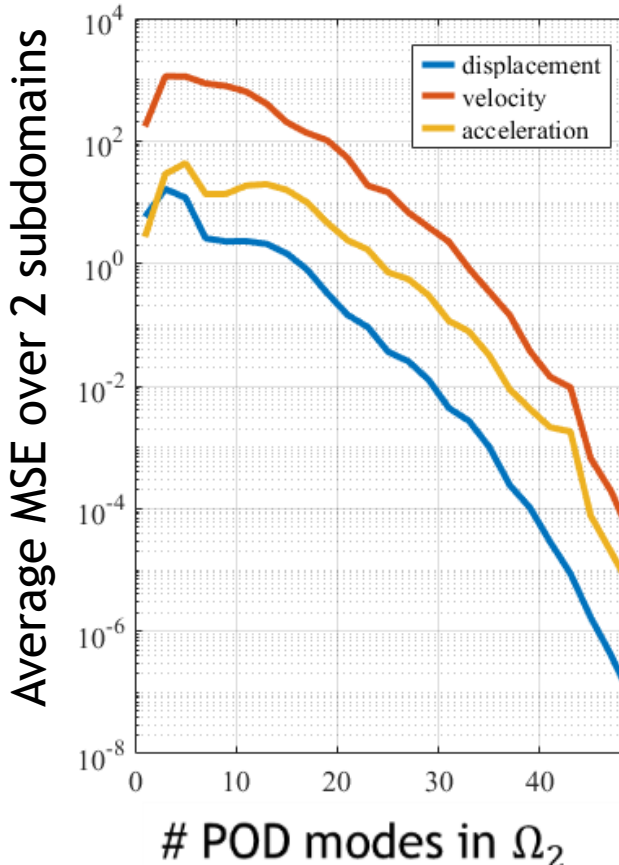
- Smaller ROMs are not the fastest: less accurate & require more Schwarz iterations to converge.
- All couplings converge in  $\leq 4$  Schwarz iterations on average (FOM-FOM coupling requires average of 2.4 Schwarz iterations).

Overlapping implicit-implicit coupling with  $\Omega_1 = [0, 0.75]$ ,  $\Omega_2 = [0.25, 1]$

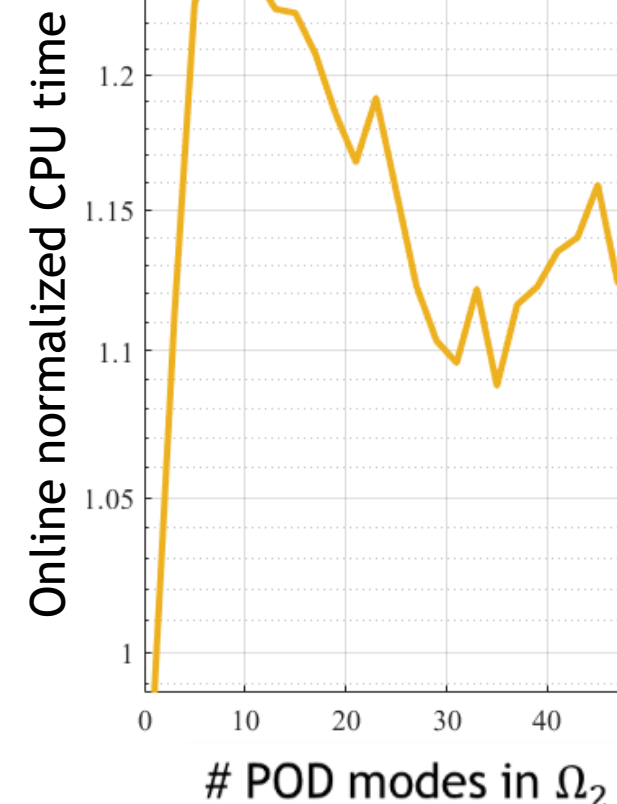
# Linear Elastic Wave Propagation Problem: FOM-ROM Couplings

*FOM-ROM coupling shows convergence with basis refinement. FOM-ROM couplings are 10-15% slower than comparable FOM-FOM coupling due to increased # Schwarz iterations.*

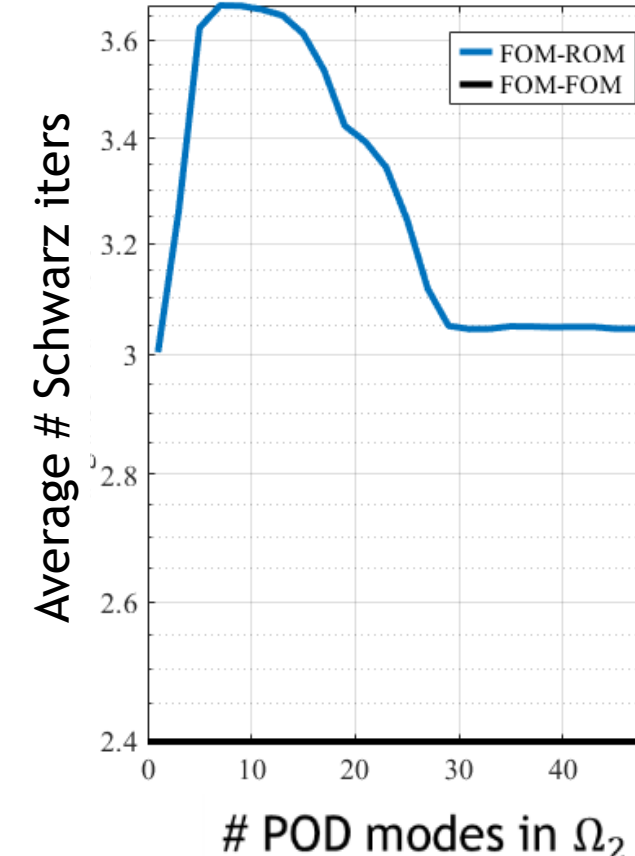
MSE for 2 subdomain FOM-ROM coupling



CPU times for 2 subdomain FOM-ROM coupling normalized by FOM-FOM CPU time



Average # Schwarz iterations for 2 subdomain couplings



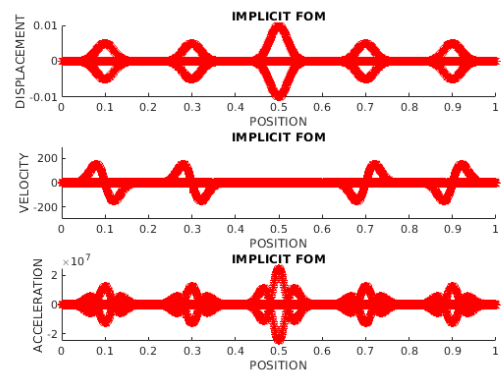
**WIP:**  
understanding & improving FOM-  
ROM coupling performance.

Overlapping implicit-  
implicit coupling with  
 $\Omega_1 = [0, 0.75]$ ,  
 $\Omega_2 = [0.25, 1]$

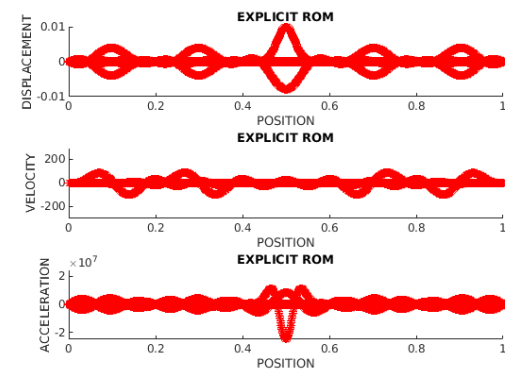
# Linear Elastic Wave Propagation Problem: FOM-ROM and ROM-ROM Couplings



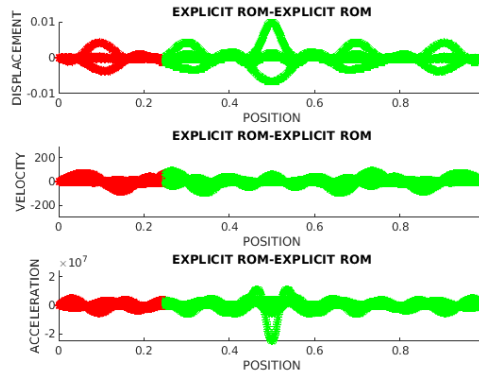
*Inaccurate model + accurate model  $\neq$  accurate model.*



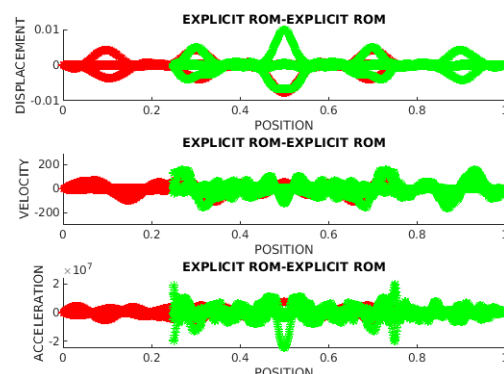
Single Domain, FOM (truth)



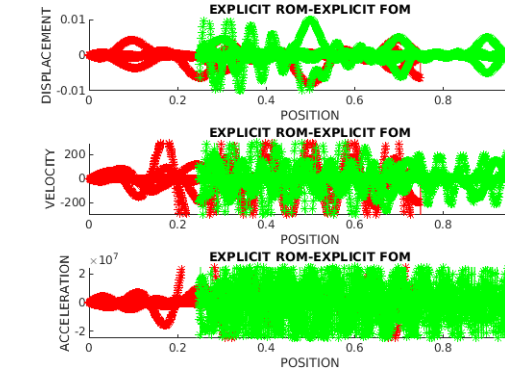
Single Domain, 10 mode POD



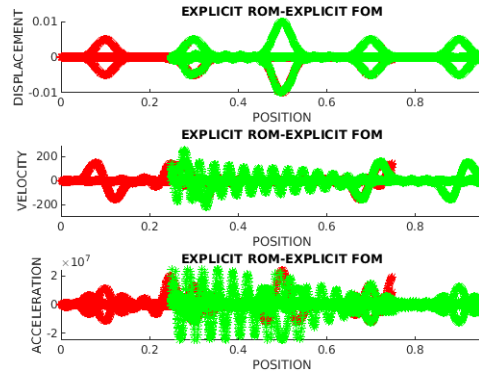
10 mode POD – 10 mode POD



10 mode POD – 50 mode POD



10 mode POD – FOM



20 mode POD - FOM

Figures above:  $\Omega_1 = [0, 0.75]$ ,  $\Omega_2 = [0.25, 1]$

Observation suggests need for “smart” domain decomposition.

Accuracy can be improved by “gluing” several smaller, spatially-local models

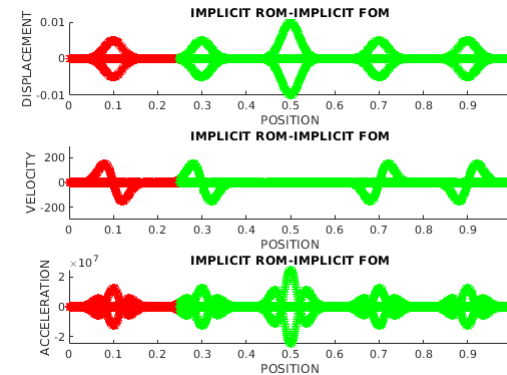
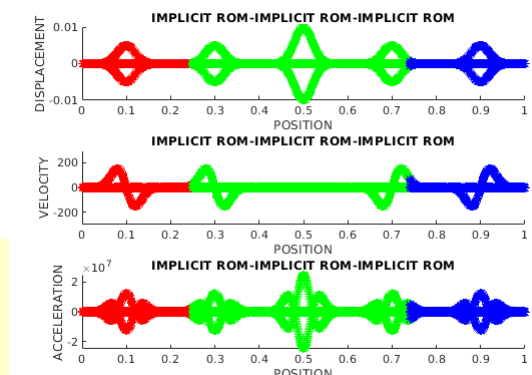


Figure above:  $\Omega_1 = [0, 0.3]$ ,  $\Omega_2 = [0.25, 1]$ , 20 mode POD - FOM

Figure below:  $\Omega_1 = [0, 0.26]$ ,  $\Omega_2 = [0.25, 0.75]$ ,  $\Omega_3 = [0.74, 1]$ , 15 mode POD - 30 mode POD - 15 mode POD



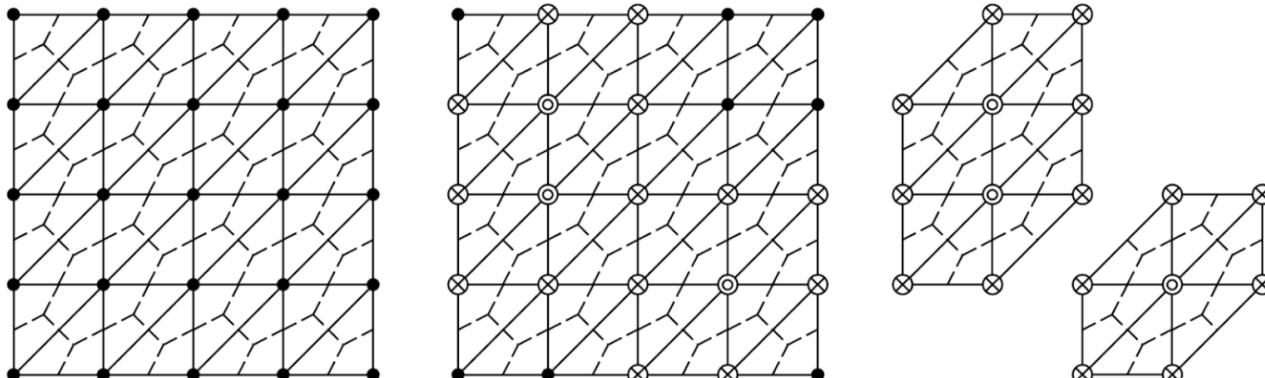
# Energy-Conserving Sampling and Weighting (ECSW)



- Project-then-approximate paradigm (as opposed to approximate-then-project)

$$\begin{aligned}
 r_k(q_k, t) &= W^T r(\tilde{u}, t) \\
 &= \sum_{e \in \mathcal{E}} W^T L_e^T r_e(L_e + \tilde{u}, t)
 \end{aligned}$$

- $L_e \in \{0,1\}^{d_e \times N}$  where  $d_e$  is the **number of degrees of freedom** associated with each mesh element (this is in the context of meshes used in first-order hyperbolic problems where there are  $N_e$  mesh elements)
- $L_e^+ \in \{0,1\}^{d_e \times N}$  selects degrees of freedom necessary for **flux reconstruction**
- Equality can be **relaxed**



Augmented reduced mesh:  $\circledcirc$  represents a selected node attached to a selected element; and  $\otimes$  represents an added node to enable the full representation of the computational stencil at the selected node/element

# ECSW: Generating the Reduced Mesh and Weights



- Using a subset of the same snapshots  $u_i, i \in 1, \dots, n_h$  used to generate the **state basis**  $V$ , we can train the reduced mesh
- Snapshots are first **projected** onto their associated basis and then **reconstructed**

$$c_{se} = W^T L_e^T r_e \left( L_e^+ \left( u_{ref} + V V^T (u_s - u_{ref}) \right), t \right) \in \mathbb{R}^n$$

$$d_s = r_k(\tilde{u}, t) \in \mathbb{R}^n, \quad s = 1, \dots, n_h$$

- We can then form the **system**

$$\mathbf{C} = \begin{pmatrix} c_{11} & \dots & c_{1N_e} \\ \vdots & \ddots & \vdots \\ c_{n_h 1} & \dots & c_{n_h N_e} \end{pmatrix}, \quad \mathbf{d} = \begin{pmatrix} d_1 \\ \vdots \\ d_{n_h} \end{pmatrix}$$

- Where  $\mathbf{C}\xi = \mathbf{d}, \xi \in \mathbb{R}^{N_e}$ ,  $\xi = \mathbf{1}$  must be the solution
- Further relax the equality to yield **non-negative least-squares problem**:

$$\xi = \arg \min_{x \in \mathbb{R}^n} \|\mathbf{C}x - \mathbf{d}\|_2 \text{ subject to } x \geq \mathbf{0}$$

- Solve the above optimization problem using a **non-negative least squares solver** with an **early termination condition** to promote **sparsity** of the vector  $\xi$

# Numerical Example: 1D Dynamic Wave Propagation Problem

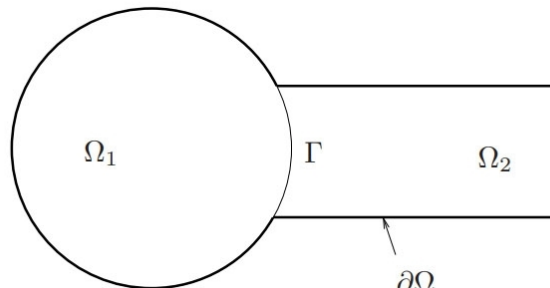


- Alternating Dirichlet-Neumann Schwarz BCs with no relaxation ( $\theta = 1$ ) on Schwarz boundary  $\Gamma$

$$\begin{cases} \operatorname{Div} \mathbf{P}_1^{(n+1)} + \rho \mathbf{B}(t_i) = \mathbf{0}, & \text{in } \Omega_1 \\ \boldsymbol{\varphi}_1^{(n+1)} = \chi, & \text{on } \partial\Omega_1 \setminus \Gamma \\ \boldsymbol{\varphi}_1^{(n+1)} = \lambda_{n+1} & \text{on } \Gamma \end{cases}$$

$$\begin{cases} \operatorname{Div} \mathbf{P}_2^{(n+1)} + \rho \mathbf{B}(t_i) = \mathbf{0}, & \text{in } \Omega_2 \\ \boldsymbol{\varphi}_2^{(n+1)} = \chi, & \text{on } \partial\Omega_2 \setminus \Gamma \\ \mathbf{P}_2^{(n+1)} \mathbf{n} = \mathbf{P}_1^{(n+1)} \mathbf{n}, & \text{on } \Gamma \end{cases}$$

$$\lambda_{n+1} = \theta \boldsymbol{\varphi}_2^{(n)} + (1 - \theta) \lambda_n, \text{ on } \Gamma, \text{ for } n \geq 1$$



$\theta$	Min # Schwarz Iters	Max # Schwarz Iters	Total # Schwarz Iters
1.10	3	9	59,258
1.00	1	4	24,630
0.99	1	5	35,384
0.95	3	6	45,302
0.90	3	8	56,114

➤ A parameter sweep study revealed  $\theta = 0$  gave best performance (min # Schwarz iterations)

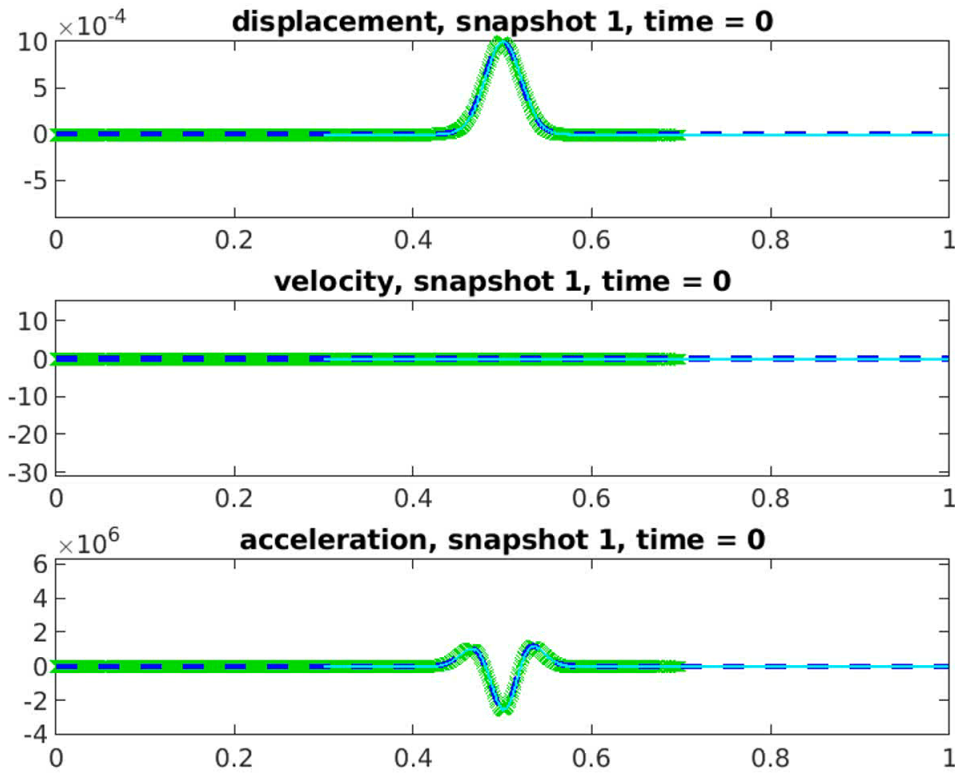
- All couplings were **implicit-implicit** with  $\Delta t_1 = \Delta t_2 = \Delta T = 10^{-7}$  and  $\Delta x_1 = \Delta x_2 = 10^{-3}$ 
  - Time-step and spatial resolution chosen to be small enough to resolve the propagating wave
- All reproductive cases run on the **same RHEL8 machine** and all predictive cases run on the **same RHEL7 machine**, in MATLAB
- Model **accuracy** evaluated w.r.t. analogous FOM-FOM coupling using **mean square error (MSE)**:

$$\varepsilon_{MSE}(\tilde{\mathbf{u}}_i) := \frac{\sqrt{\sum_{n=1}^S \|\tilde{\mathbf{u}}_i^n - \mathbf{u}_i^n\|_2^2}}{\sqrt{\sum_{n=1}^S \|\mathbf{u}_i^n\|_2^2}}$$

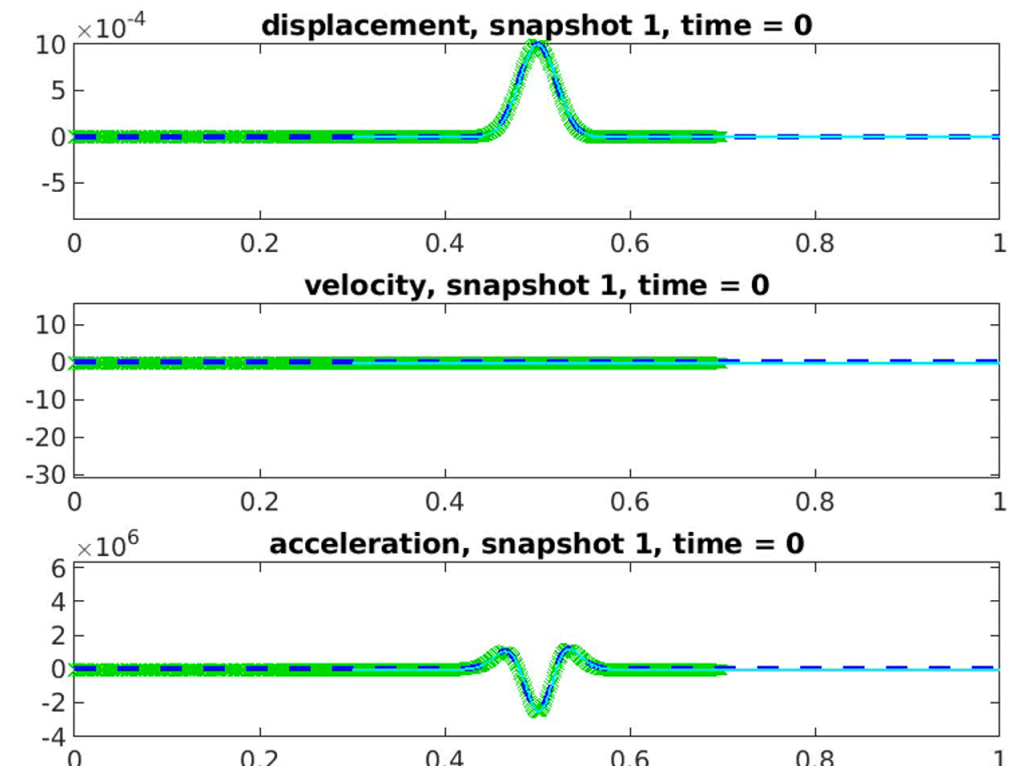
# Overlapping Coupling, Nonlinear Henky MM, 2 Subdomains



- $\Omega = [0, 0.7] \cup [0.3, 1]$ , implicit-implicit FOM-FOM coupling,  $dt = 1e-7$ ,  $dx = 1e-3$ .

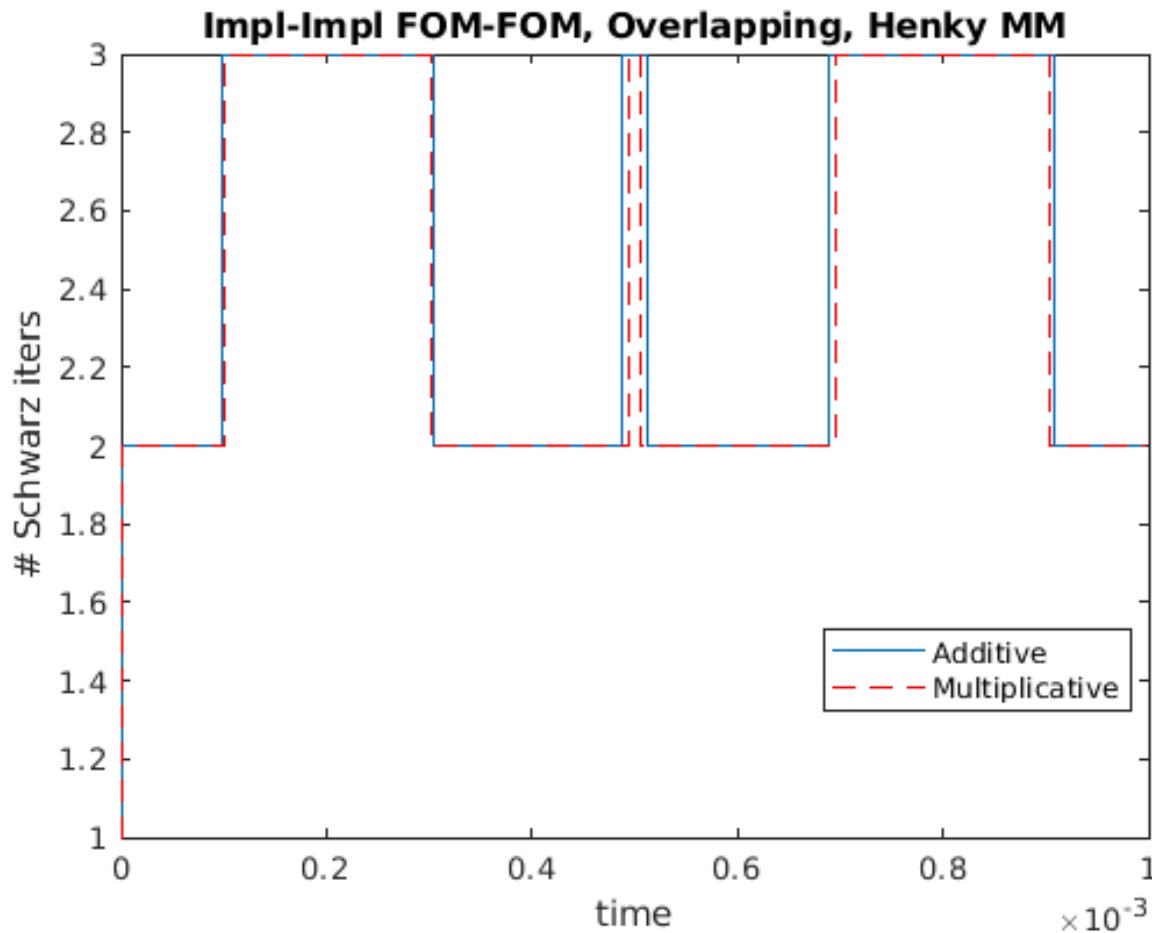


Multiplicative Schwarz



Additive Schwarz

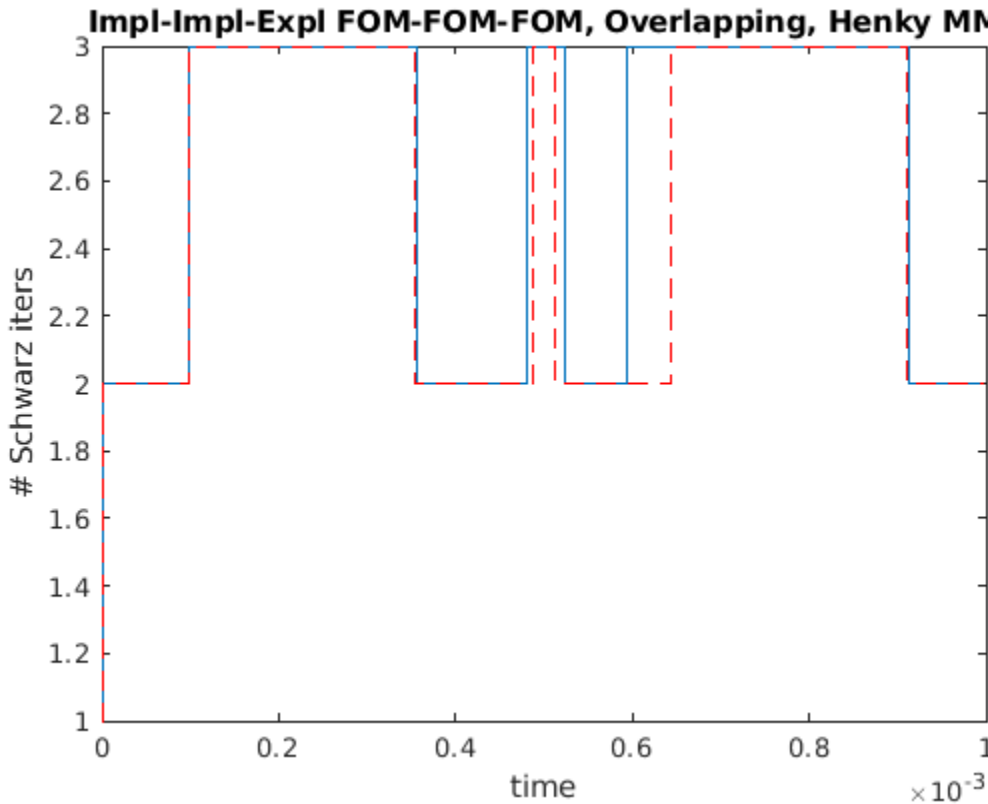
# Overlapping Coupling, Nonlinear Henky MM, 2 Subdomains



- $\Omega = [0, 0.7] \cup [0.3, 1]$ , implicit-implicit FOM-FOM coupling,  $dt = 1e-7$ ,  $dx=1e-3$ .
- Additive Schwarz requires slightly more Schwarz iterations but is actually faster.
- Solutions agree effectively to machine precision in mean square (MS) sense.

	Additive	Multiplicative
Total # Schwarz iters	24495	24211
CPU time	2.03e3s	2.16e3
MS difference in disp	6.34e-13/6.12e-13	
MS difference in velo	1.35e-11/1.86e-11	
MS difference in acce	5.92e-10/1.07e-9	

# Overlapping Coupling, Nonlinear Henky MM, 3 Subdomains

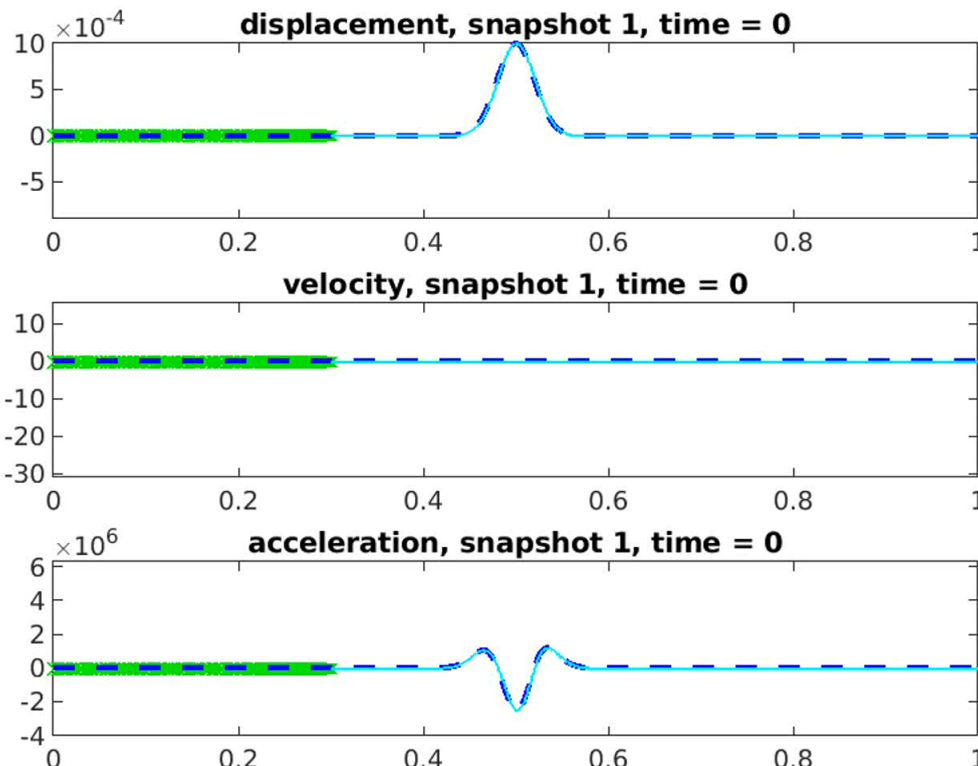


- $\Omega = [0, 0.3] \cup [0.25, 0.75] \cup [0.7, 1]$ , implicit-implicit-explicit FOM-FOM-FOM coupling,  $dt = 1e-7$ ,  $dx = 0.001$ .
- Solutions agree effectively to machine precision in mean square (MS) sense.
- Additive Schwarz has slightly more Schwarz iterations but is slightly faster than multiplicative.

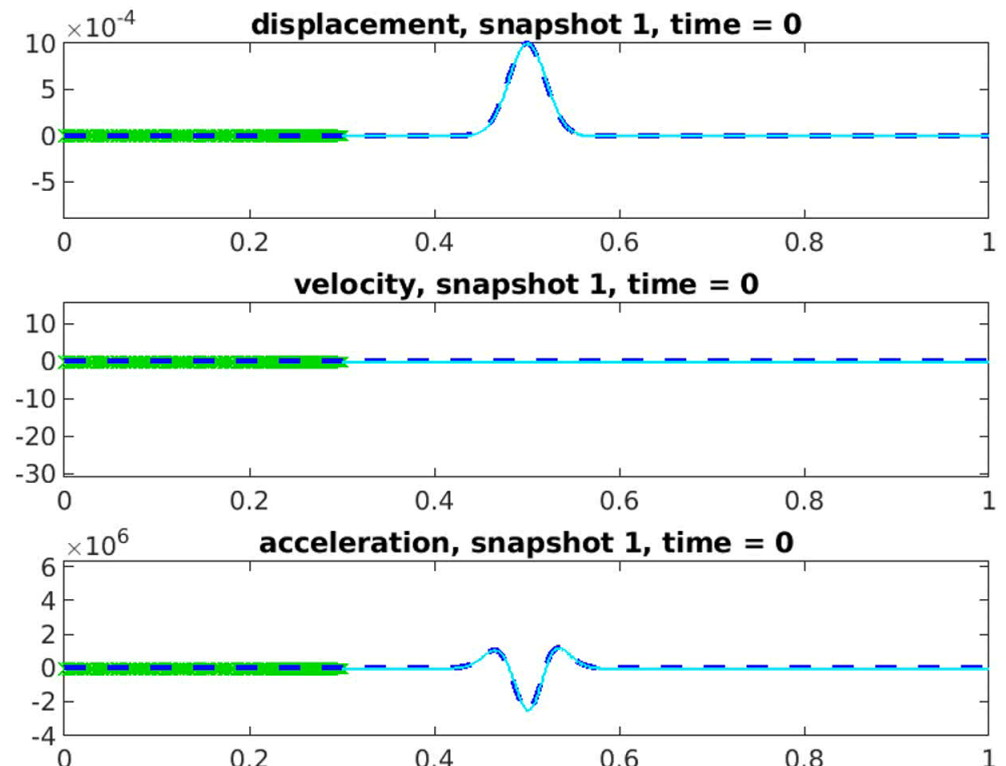
	Additive	Multiplicative
Total # Schwarz iters	26231	25459
CPU time	1.89e3s	2.05e3s
MS difference in disp	5.3052e-13/9.3724e-13/6.1911e-13	
MS difference in velo	7.2166e-12/2.2937e-11/2.4975e-11	
MS difference in acce	2.8962e-10/1.1042e-09/1.6994e-09	

# Non-overlapping Coupling, Nonlinear Henky MM, 2 Subdomains

- $\Omega = [0, 0.3] \cup [0.3, 1]$ , implicit-implicit FOM-FOM coupling,  $dt = 1e-7$ ,  $dx = 1e-3$ .

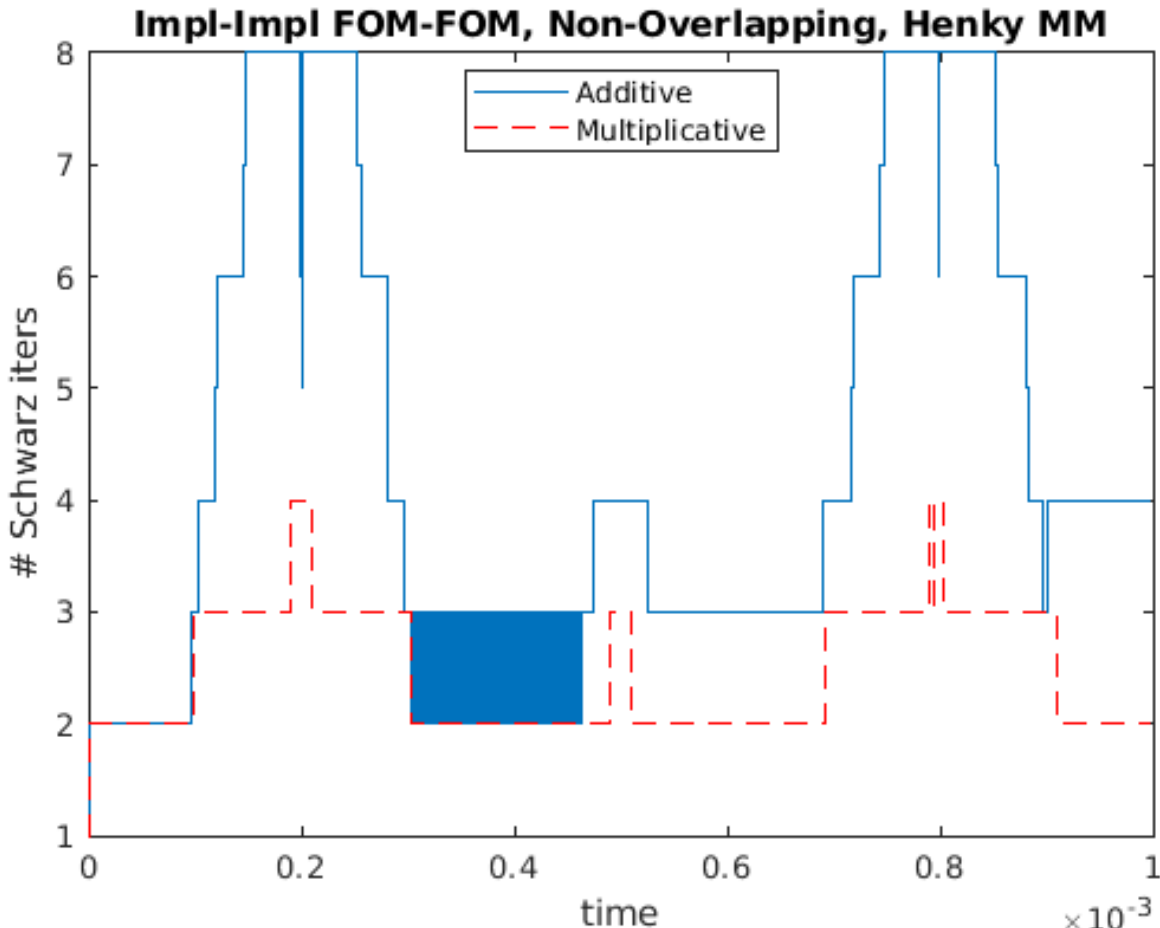


Multiplicative Schwarz



Additive Schwarz

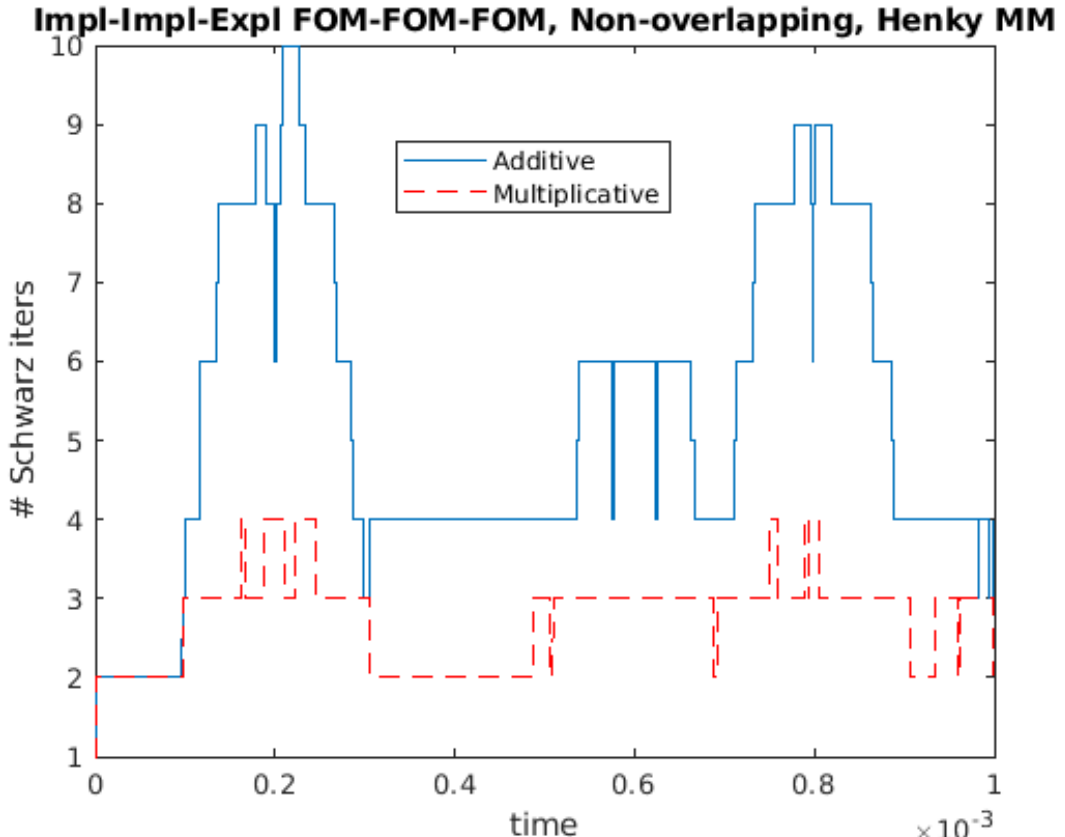
# Non-overlapping Coupling, Nonlinear Henky MM, 2 Subdomains



- $\Omega = [0, 0.3] \cup [0.3, 1]$ , implicit-implicit FOM-FOM coupling,  $dt = 1e-7$ ,  $dx = 1e-3$ .
- Additive Schwarz requires 1.81x Schwarz iterations (and 1.9x CPU time) to converge. CPU time could be reduced through added parallelism of additive Schwarz.
  - Note blue square for additive Schwarz...
- Additive and multiplicative solutions differ in mean square (MS) sense by  $O(1e-5)$ .

	Additive	Multiplicative
Total # Schwarz iters	44895	24744
CPU time	1.87e3s	982.5s
MS difference in disp	4.26e-5/2.74e-5	
MS difference in velo	1.02e-5/5.91e-6	
MS difference in acce	5.84e-5/1.21e-5	

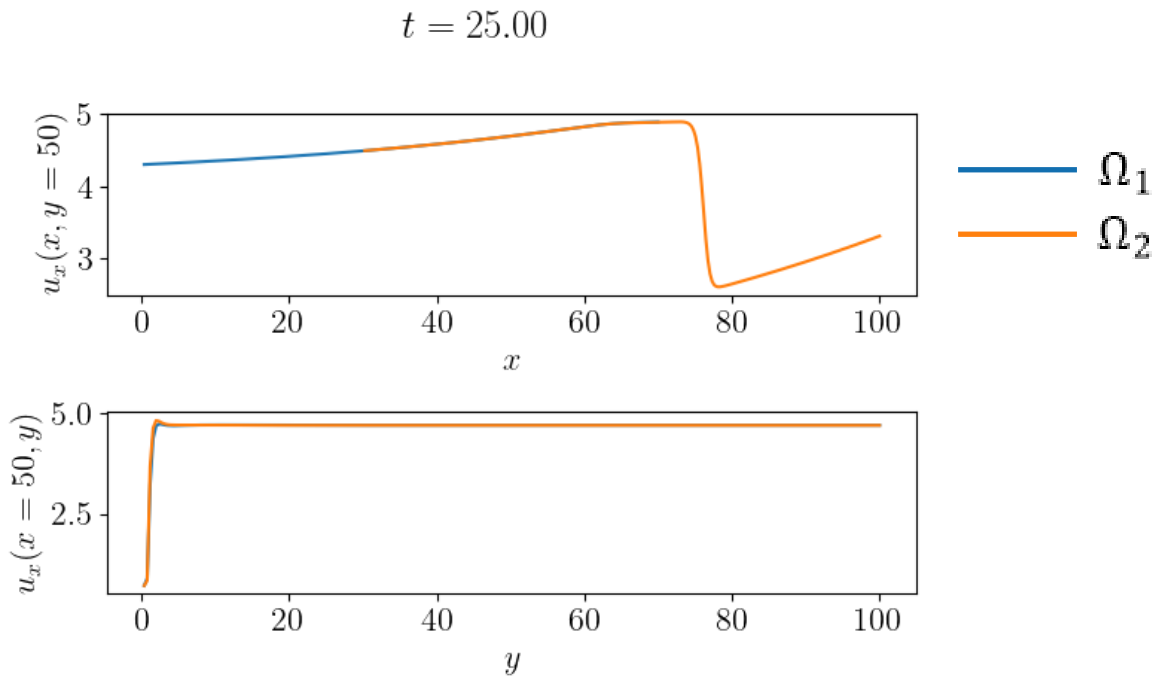
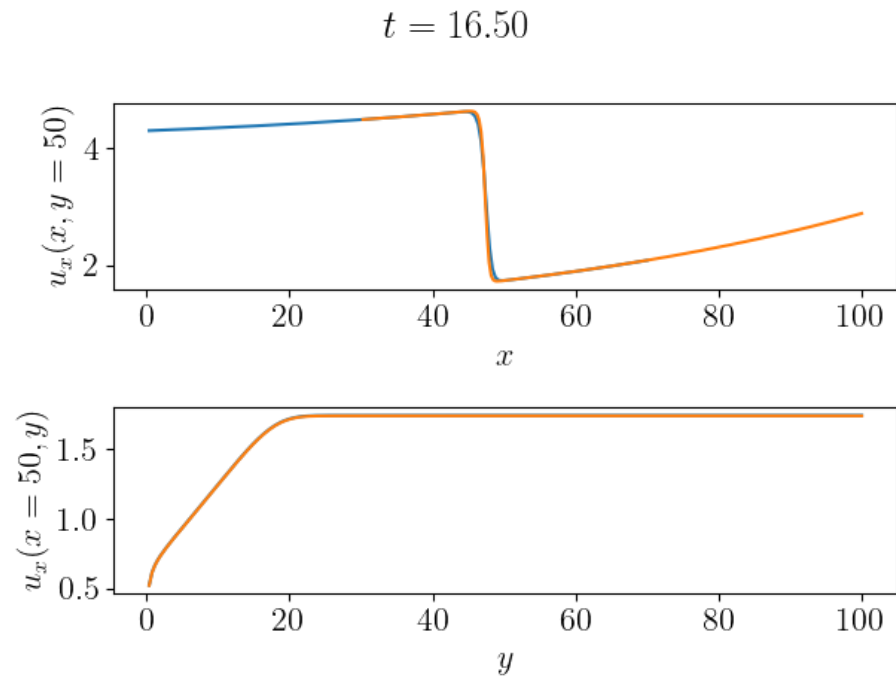
# Non-overlapping Coupling, Nonlinear Henky MM, 3 Subdomains



- $\Omega = [0, 0.3] \cup [0.3, 0.7] \cup [0.7, 1]$ , implicit-implicit-explicit FOM-FOM-FOM coupling,  $dt = 1e-7$ ,  $dx = 0.001$ .
- Additive Schwarz has about 1.94x number Schwarz iterations and is about 2.06x slower - similar to 2 subdomain variant of this problem. No “blue square”.
  - Results suggest you could win with additive Schwarz if you parallelize and use enough domains.
- Additive/multiplicative solutions differ by  $O(1e-5)$ , like for 2 subdomain variant of this problem.

	Additive	Multiplicative
Total # Schwarz iters	53413	27509
CPU time	5.91e3s	2.87e3s
MS difference in disp	2.8036e-05 / 3.1142e-05 / 8.8395e-06	
MS difference in velo	1.4077e-05 / 1.2104e-05 / 6.5771e-06	
MS difference in acce	8.7885e-05 / 3.2707e-05 / 1.3778e-05	

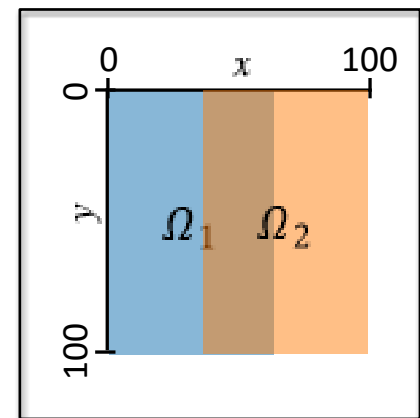
# FOM-FOM Coupling: Differing Resolution



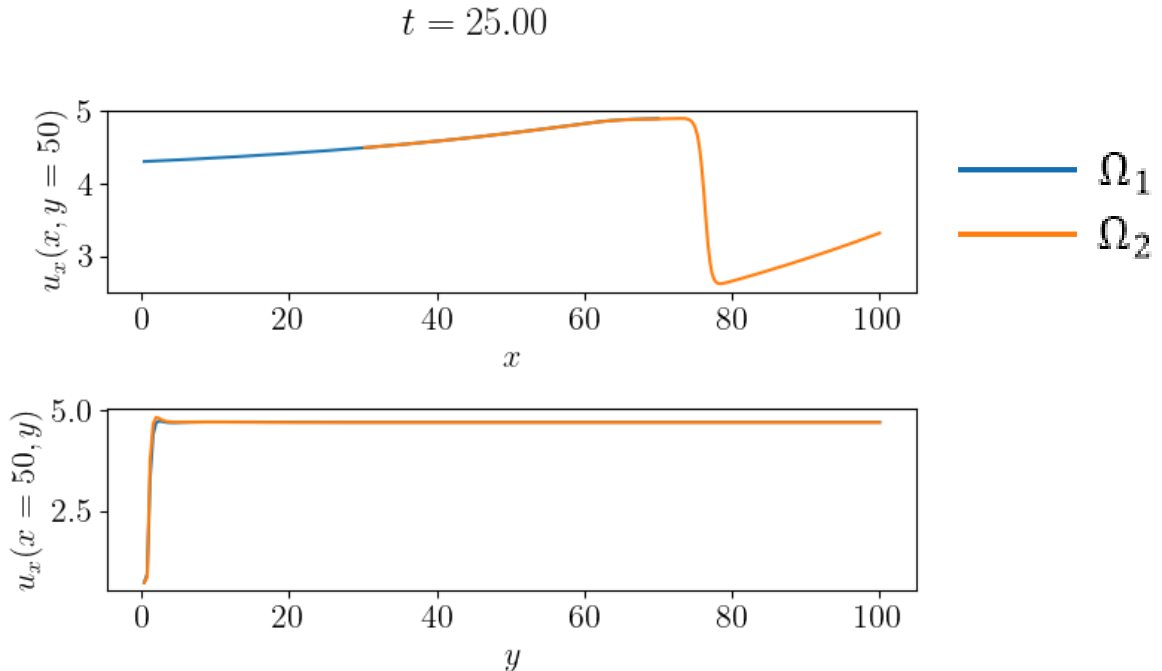
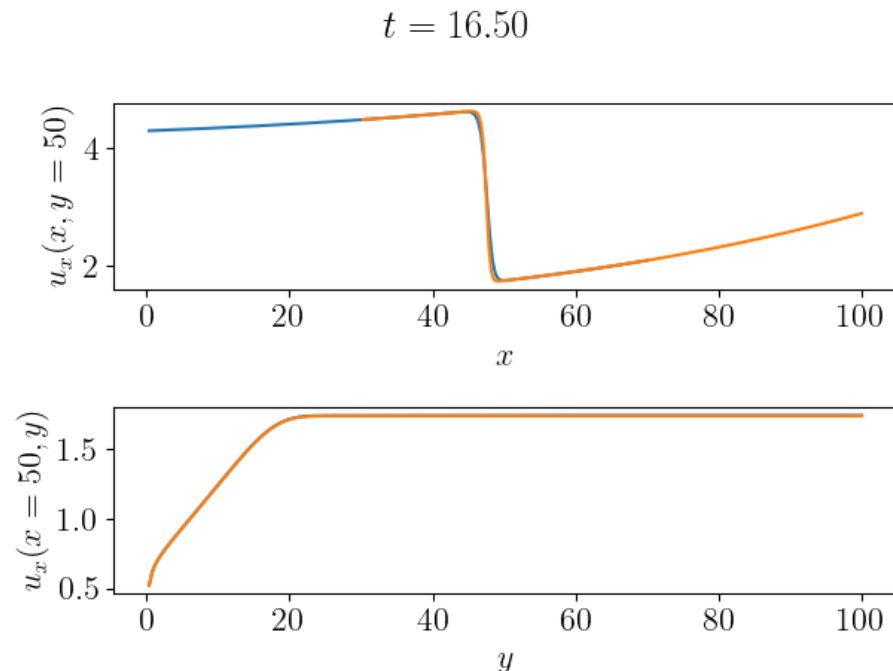
*Figures above: Two-subdomain explicit-explicit overlapping coupling in x-axis  $[0, 70] \cup [30, 100]$  where  $\mu = [4.3, 0.021]$ ,  $\Delta t = 0.005$ ,  $\Delta x_1 = 0.4$ ,  $\Delta x_2 = 0.3$*

- Figures show the mid-plane slice of the solution for  $u_x$  at various times
- The right subdomain is a finer mesh, and the difference in how the shock is resolved can be seen
- $\Omega_1 \rightarrow \Omega_2$  ordering gives 2 Schwarz iterations per global time step
- $\Omega_2 \rightarrow \Omega_1$  ordering gives 3 Schwarz iterations per global time step

Order can be important!

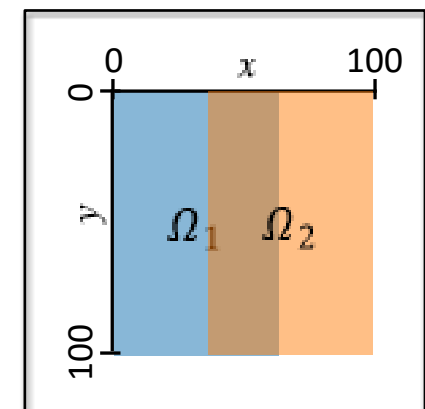


# FOM-FOM Coupling: Differing time integrators and $\Delta t$

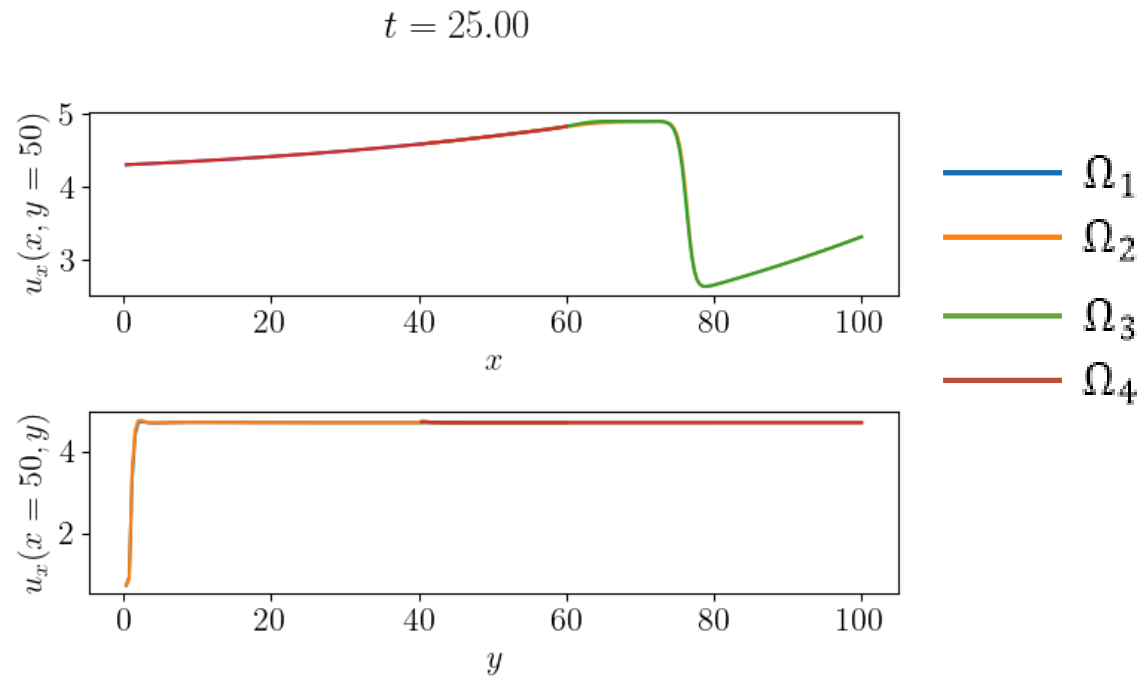
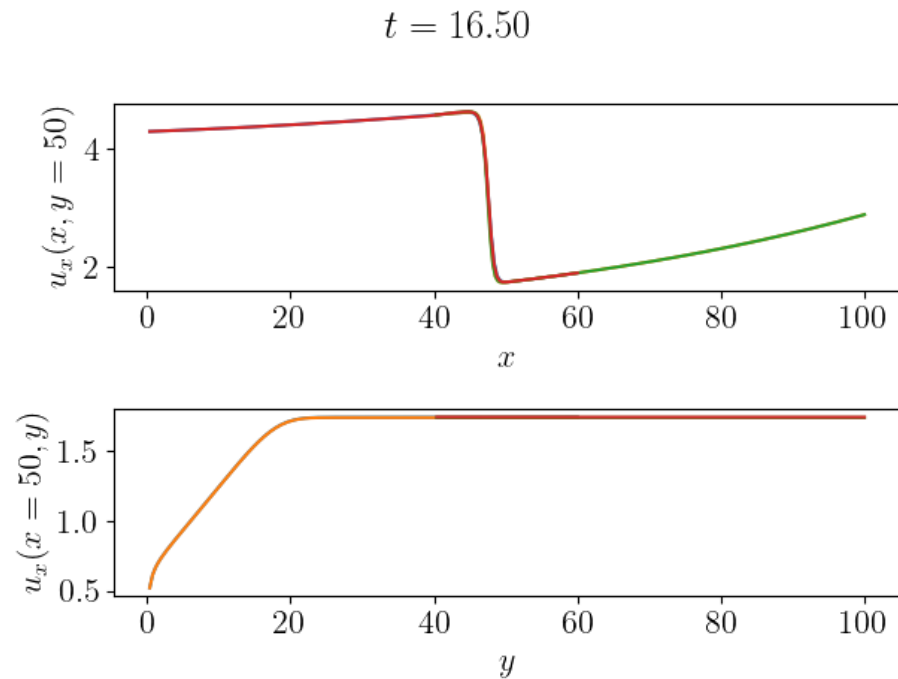


Figures above: Two-subdomain implicit-explicit overlapping coupling in  $x$ -axis  $[0, 70]$   
 $U [30, 100]$ ,  $\mu = [4.3, 0.021]$ ,  $\Delta t_1 = 0.05$ ,  $\Delta t_2 = 0.005$ ,  $\Delta x_1 = 0.4$ ,  $\Delta x_2 = 0.3$

- Introducing a different time stepper in  $\Omega_1$  has not introduced artifacts and produces visually identical solution
- Choosing  $\Omega_1 \rightarrow \Omega_2$  still only requires 2 Schwarz iterations per global time step

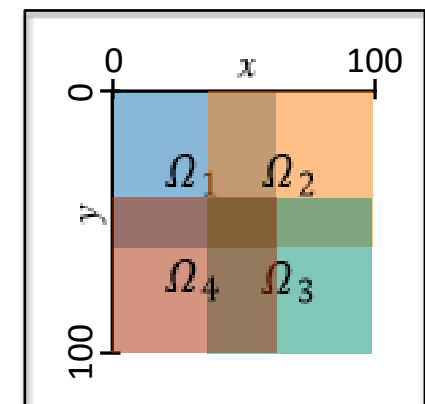


# FOM-FOM Coupling: >2 Subdomains



*Figures above: Four-subdomain implicit-explicit-implicit-explicit overlapping coupling in x-axis  $[0, 60] \cup [40, 100]$  and y-axis  $[0, 60] \cup [40, 100]$ ,  $\mu = [4.3, 0.021]$ ,  $\Delta t_1 = \Delta t_3 = 0.05$ ,  $\Delta t_2 = \Delta t_4 = 0.005$ ,  $\Delta x_1 = \Delta x_4 = 0.4$ ,  $\Delta x_2 = \Delta x_3 = 0.3$*

- Despite a heterogeneous mixture of different subdomains coupled in multiple dimensions with different solvers, resolutions, etc. the solution is still consistent
- Choosing  $\Omega_1 \rightarrow \Omega_2 \rightarrow \Omega_3 \rightarrow \Omega_4$  requires 3 Schwarz iterations per global time step

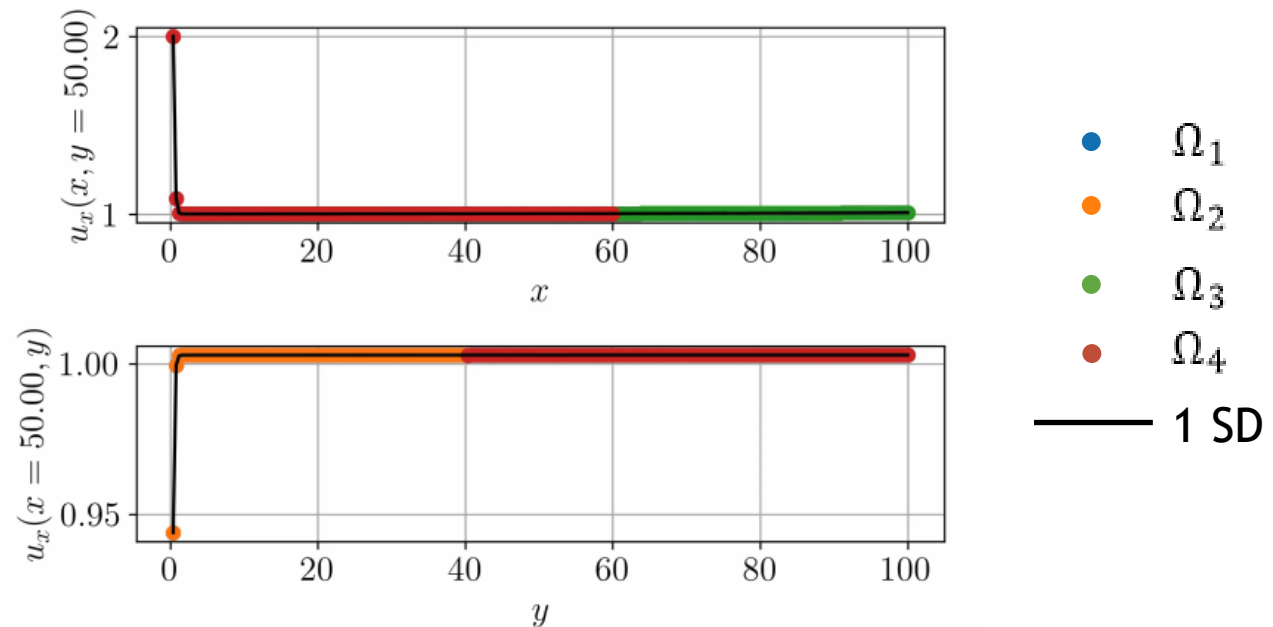


# FOM-FOM Coupling: >2 Subdomains



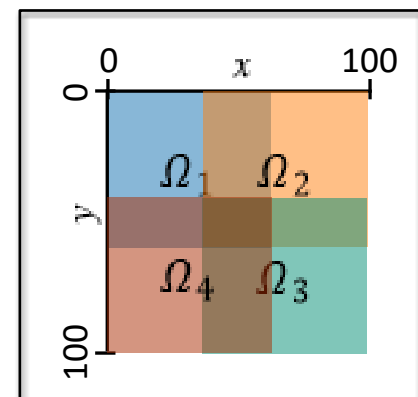
Subdomain	Wall Clock Time (s)	Total (s)
Monolithic	124	124
$\Omega_1$	75	
$\Omega_2$	62	
$\Omega_3$	62	
$\Omega_4$	77	300

$t = 0.00$

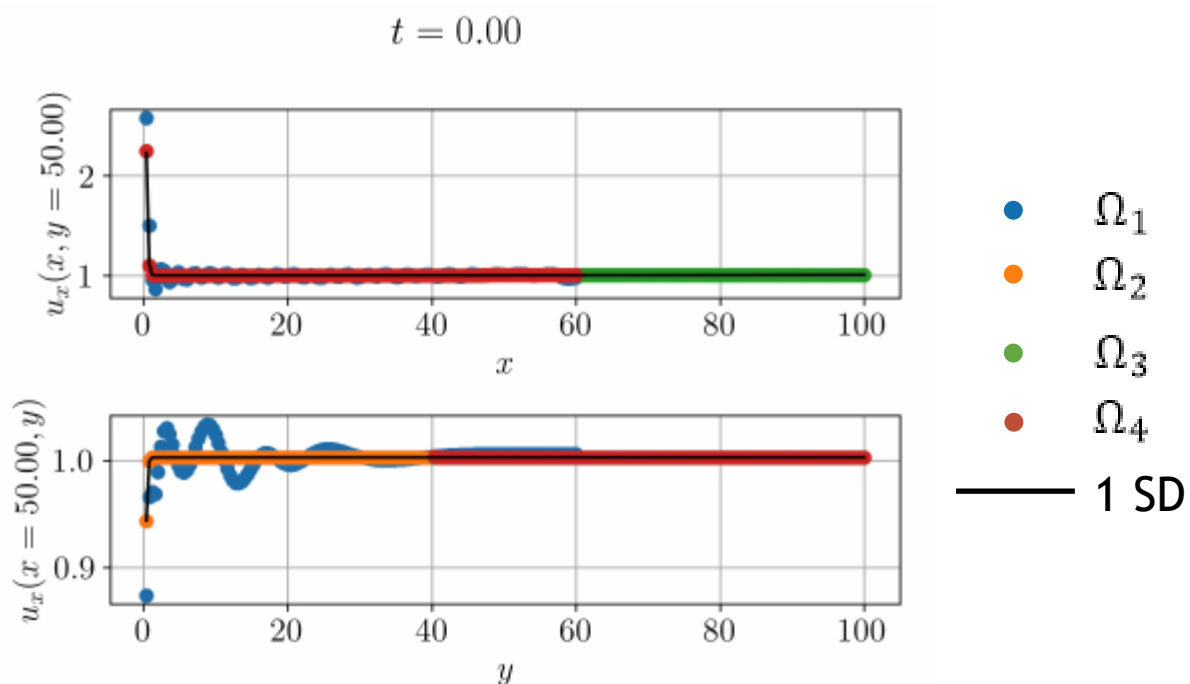


*Figures above: Four-subdomain implicit-implicit-implicit-implicit overlapping coupling in x-axis [0, 60] U [40, 100] and y-axis [0, 60] U [40, 100],  $\mu = [4.3, 0.021]$ ,  $\Delta t = 0.05$ ,  $\Delta x_1 = \Delta x_4 = 0.4$ ,  $\Delta x_2 = \Delta x_3 = 0.3$*

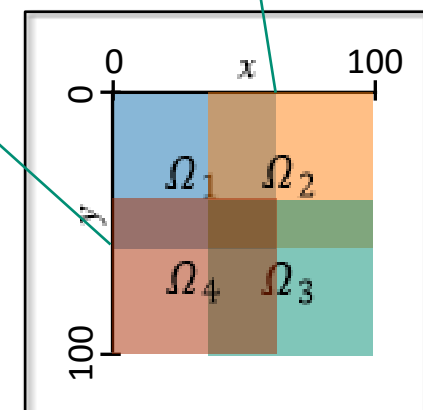
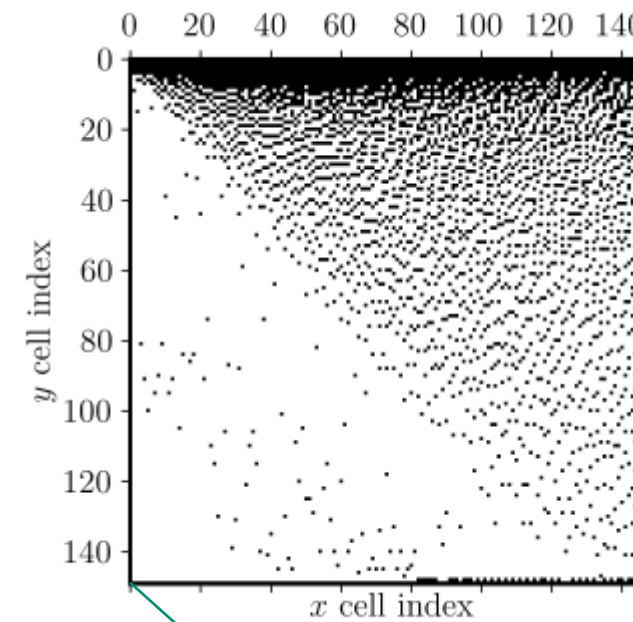
- Despite a heterogeneous mixture of different subdomains coupled in multiple dimensions with different solvers, resolutions, etc. the solution is still consistent
- Choosing  $\Omega_1 \rightarrow \Omega_2 \rightarrow \Omega_3 \rightarrow \Omega_4$  requires 3 Schwarz iterations per global time step



# HROM-FOM-FOM-FOM Coupling



Domain	$M$	MSE (%)	HROM-FOM-FOM-FOM Wall Clock Time (s)	FOM-FOM-FOM-FOM Wall Clock Time (s)	Speedup
$\Omega_1$	76	1.5	30	68	2.3
Total	—	—	276	300	1.1



- We have **computational gain** even when choosing the “worst” subdomain for HROM
- No speedup over single-domain FOM (wall clock time = 124 s)
  - **Mitigation:** additive Schwarz, which admits more parallelism



**Opinion: hybrid FOM-ROM models are the future!**

- We have developed an **iterative** coupling formulation based on the **Schwarz alternating method** and an **overlapping** or **non-overlapping** DD
- Numerical results show **promise** in using the proposed methods to create **heterogeneous coupled models** comprised of arbitrary combinations of **ROMs** and/or **FOMs**
  - Coupled models can be **computationally efficient** w.r.t analogous FOM-FOM couplings
  - Coupling introduces **no numerical artifacts** into the solution
- FOM-ROM and ROM-ROM have potential to **improve the predictive viability** of projection-based ROMs, by enabling the **spatial localization of ROMs** (via DD) and the **online integration of high-fidelity information** into these models (via FOM coupling)

# Comparison of Methods



## Alternating Schwarz-based Coupling Method

- Can do **FOM-FOM, FOM-ROM, ROM-ROM** coupling
- **Overlapping or non-overlapping DD**
- **Iterative formulation** (less intrusive but likely requires more CPU time)
- Can couple **different mesh resolutions and element types**
- Can use **different time-integrators** with **different time-steps** in different subdomains
- **No interface bases required**
- **Sequential subdomain solves** in multiplicative Schwarz variant
  - **Parallel subdomain solves** possible with **additive Schwarz** variant (not shown)
- **Extensible in straightforward way** to PINN/DMD data-driven model

## Lagrange Multiplier-Based Partitioned Coupling Method

- Can do **FOM-FOM, FOM-ROM, ROM-ROM** coupling
- **Non-overlapping DD**
- **Monolithic formulation** requiring hybrid formulation (more intrusive but more efficient)
- Can couple **different mesh resolutions and element types**
- Can use **different explicit time-integrators** with **different time-steps** in different subdomains
- **Provably convergent variant** requires **interface bases**
- **Parallel subdomain solves** if explicit or IMEX time-integrator is employed
- **Extensions to PINN/DMD data-driven models are not obvious**



- Extension/prototyping on more multi-D (2D/3D compressible flow<sup>1</sup>, 2D/3D solid mechanics<sup>2</sup>) and multi-physics problems (FSI, Air-Sea coupling)
- Implementation/testing of **additive Schwarz variant**, which admits more parallelism
- **Analysis** of method's convergence for ROM-FOM and ROM-ROM couplings
- **Learning** of “optimal” transmission conditions to ensure **structure preservation**
- Extension of coupling methods to coupling of **Physics Informed Neural Networks (PINNs)** (WIP)
- Exploration of **connections** between **iterative Schwarz** and **optimization-based coupling** [Iollo *et al.*, 2022]
- Development of **smart domain decomposition approaches** based on error indicators, to determine optimal placement of ROM and FOM in a computational domain (including **on-the-fly ROM-FOM switching**)
- Extension of couplings to POD modes built from snapshots on **independently-simulated subdomains**
- **Journal article** currently in preparation.

<sup>1</sup> <https://github.com/Pressio/pressio-demoapps>

<sup>2</sup> <https://github.com/lxmota/norma>